Mana Motuhake Ringa: The Non-Invasive Neural Interface Based Artificial Hand

A thesis

submitted in fulfilment

of the requirements for the degree

of

Doctor of Philosophy in Engineering

at

The University of Waikato

by

Mahonri William Owen

THE UNIVERSITY OF
WAIKATO
Te Whare Wānanga o Waikato

2019

“He aha te mea nui o te ao? He tāngata, he tāngata, he tāngata”

(What is the most important thing in this world? It is people, it is people, it is people).

Abstract

Ten million people on the earth at any given time suffer from the loss or lack of a limb. Three million of these are upper extremity amputees. No matter the cause or reason for amputation the amputees' life is never the same again. Independence can be lost and never regained. The loss of a limb can be an overpowering event that effects the mental, social, and physical well-being of a person. Although there has been many attempts to restore hand function through neural prosthetics there is little to no credible solutions to regain it. This thesis presents methods to restore hand function based on the human grasping system and addresses key challenges in the practical application of those methods. The contribution of this work lies in improving artificial hand function by mimicking the human grasping system. The human grasping system consists of the brain, the nervous system and the hand. The methods used investigate: biomechanical design principles for artificial hands, the limitations of machine learning in non-invasive neural interfaces (NI's) and the development of an autonomous hand control framework for artificial hand control.

The application of the Support Vector Machine (SVM) to a non-invasive neural interface is principally limited to binary applications in the real world. In order to overcome this limitation an autonomous approach is developed to achieve better response and accuracy from NI control frameworks. In binary applications the SVM performed well with a classification accuracy of around 80% accompanied by a response time of just under 5 seconds. When applied to multiple classifications the SVM decreased in accuracy and response dramatically. The accuracy of the autonomous hand control framework had a classification accuracy of 95% with a response time comparable to that of the SVM. This outcome has the potential to

move non-invasive NI research into the real world and to restore hand function in an intuitive and meaningful way. A key learning of this research is that machine learning methods for non-invasive neural interfaces are not the best way to restore hand function for amputees. Hand function is best restored through the combining of machine learning and machine vision into a single NI based control framework. Additionally, this work is based in Mātauranga Māori with a western science approach. By so doing, amputees will be empowered, have increased independence and enjoy a better quality of life.

The scope of this work is limited to the consideration of hand function restoration for upper extremity amputees. In particular trans-radial amputees. Focus is given to non-invasive methods of control, therefore, investigations are limited to the electroencephalography (EEG) signal. Mimicking the human grasping system is a complex and difficult process, therefore, the attempts in this work to restore hand function only consider mechanisms and processes related directly to the motor control of the human hand.

Acknowledgements

There is no way I can express my full appreciation to everyone that has influenced me over this academic journey in the few pages I have to do so. I was always told growing up that it takes a village to nurture and raise a child. In this sense I have been raised and nurtured through my doctoral journey by many. Firstly, I must acknowledge and thank God, who without, this work would not have been accomplished. I would also like to thank my wife Ruby for her support and strength throughout the challenges of doctoral studies. There were many times she looked after our children and kept everything in order while I worked. After long days my children Alma, Iris and Aaria would greet me with warm smiles, something I will not forget. I would like to thank my siblings and especially my mother for stressing the importance of education and making wise decisions.

Thanks to my supervisors especially Dr Chi Kit Au, who was always supportive and mindful of my work. I am thankful that he took me under his wing and accepted me with all my weaknesses. His extended interest in my studies shaped my research and gave valuable opportunities of which I will always be grateful. There are so many staff members and academics with whom I would conduct business with that are deserving of acknowledgement. To Mary Dalbeth, Hine Ioane, Carol Robinson, Cheryl Ward and Gwenda Pennington thank you for the lovely temperament I was always greeted with and for the support I felt every time I needed to bother you with something.

I must also thank the Wotherspoon and Verry families for all the support and love I and my family received from them throughout my studies. There were many times

they made the journey more bearable. I especially would like to thank the Wotherspoons for appreciating the position I was in and providing a home where my family were fed, protected and safe. I will always be thankful for the influence, understanding and guidance given by Paul throughout the years.

I would like to thank the Health Research Council of New Zealand for the Māori Career development scholarship which allowed me to undertake this endeavour. The scholarship provided food, shelter and warmth for my family of which I will forever be grateful. I was able to realise my potential because I knew my wife and children were financially supported. I would also like to thank the Māori education trust and the Hellaby whanau for considering me as a recipient of the Rose Hellaby postgraduate scholarship. I will continue to strive to be my best and to make Rose proud. Thank you to my Iwi Ngapuhi and Ngati Tuwharetoa for their support. Thank you to the New Zealand Artificial Limb Service and the Knowledge Engineering Development Research Institute for your collaborative efforts and for the uplifting work we all engaged in.

A huge thank you to my friends for all the times we have spent where I was able to take my mind off the stresses and worries of doctoral studies and for the influence you have been in my life.

Contributing Works

This thesis is supported by the following works which are published in international peer reviewed journals, conference proceedings or under review. A considerable portion of chapter 3 is supported by [1] and backed by the master's thesis [3]. [3] is a preliminary work and not a repetition of information to be published. The end portion of chapter 3 is supported by [5] which is currently under review. Chapter 4 will be published in the International Journal of Biomedical Engineering and Technology [4]. The results and content of chapter 5 are currently under review to be published in the Journal of Bionic Engineering [6]. [2] is considered for future work and represents a novel NI for prosthetic control. Research comprising this thesis has been presented at several conferences, television and radio interviews.

[1] **Owen, M**., Au, C. and Fowke, A. (2018). Development of a Dexterous Prosthetic Hand. Journal of Computing and Information Science in Engineering. **18**: 1-7.

[2] Kumarasinghe. K., **Owen. M**., Taylor, D., Kasabov, N. and Au, C. (2018). FaNeuRobot: A Framework for Robot and Prosthetics Control Using the NeuCube Spiking Neural Network Architecture and Finite Automata Theory. IEEE International Conference on Robotics and Automation. Brisbane. Australia. 4465-4472.

[3] **Owen, M**. (2015). The Development of a Brain Controlled Robotic Prosthetic Hand. Thesis, Master of Engineering. University of Waikato, Hamilton, New Zealand. Retrieved from https://hdl.handle.net/10289/9522

Accepted for publication

[4] **Owen, M**. and Au, C. (2018). The development of a Brain Controlled Interface Employing Electroencephalography to Control a Hand Prostheses. International Journal of Biomedical Engineering and Technology.

In the process of review

[5] **Owen, M**. (2019). Tendon Displacement and Excursion: A Design Approach to the Optimisation of Tendon Driven Artificial Electro-mechanical hands. International Journal of Biomechatronics and Biomedical Robotics.

[6] **Owen, M**., Au, C. and Dredge, D. (2019). An Autonomous Anthropomorphic Prosthetic Hand for Grasping Tasks. Journal of Bionic Engineering.

Table of Contents

List of Figures

List of Tables

Nomenclature

I_B	Base insertion	**VL**	Very large
I_H	Head Insertion	d_{max}	Maximum object size
C	Centroid/ Penalty weight	O	A set of grasping rectangles
L_H	Head Length	G	A finite set of grasps
L_B	Base Length	φ_o^k	Grasp type with the initial values of φ_i^k
L_{BC}	Distance from base to centroid	T_i	Tension of the tendon
L_{HC}	Distance from head to centroid	T_i^m	Servomotor torque
L_{BI}	Percentage of total phalanx length	τ_i	Torque acting on the fingertip
L_{HI}	Percentage of total phalanx length	f_i	Fingertip force
L_P	Phalanx length	R	Servomotor horn length/ Ring finger
S1-S4	Servomotor angles	θ	Joint angles/ Thumb orientation angle
N	Number of samples	e_i	Tendon extension
ω	Wrist angle	r_{ij}	Radius of the pulley at the j^{th} joint
$w_{(n)}$	Discrete-time symmetrical window Function	φ_i	Servomotor horn angle
n	Current sample/ Dimension measured in pixels	δ	Correction factor of finger base positions
K	Frequency/ Pixel per metric/ Kernel	B	Base position of a digit
X_n	Value of the signal	**T**	Thumb
X_k	The amount of frequency K in the sample	**M**	Middle finger
d	Minimum dimension/ Displacement	**I**	Index finger

r	Aspect ratio	F_c	Characteristic frequency
h	Dimension of the grasping region of the object	A	Amplitude
C	Webcam pixel size/ Penalty weight	A_t	Threshold amplitude
$\vec{x}_h$	Horizontal axis of the artificial hand	A_{base}	Base signal
$\vec{y}_h$	Vertical axis of the artificial hand	A_{act}	Activated signal
$\vec{z}_h$	Cross product of $\vec{y}_h . \vec{x}_h$	y_i	Class labels
$\vec{x}_{obj}$	Horizontal axis of the object	m	Training Signals
$\vec{y}_{obj}$	Vertical axis of the object	ϕ	Non-linear mapping
Obj	Object	λ_i	Lagrange multiplier
α	Orientation of object	$S_{\alpha,\beta}$	Set of training signals
u	Distance between the hand and the object	$f_{\alpha,\beta(x)}$	Decision function
ψ	Grasp mapping	$W_{(z)}$	Window function
l	Characteristic hand length/ Phalanx length	$Y_{(z)}$	Output
VS	Very small	$X_{(z)}$	Input
S	Small	**L**	Large/ Little finger
M	Medium/ Middle finger	n_g	grasp types
x_i	An element of real space	$\bar{C}$	Confidence
L_D	Lagrangian	C_T	Threshold confidence
b	Bias	t	Time
e	Event within the signal	C_{SVM}	Confidence of the SVM

(Note: Symbol definitions separated by a '/' indicate the specified symbol has two or more meanings)

Abbreviations

NI	Neural Interface	**PIP**	Proximal interphalangeal
SVM	Support Vector Machine	**IP**	Interphalangeal
GLM	Generalised Linear Model	**DIP**	Distal Interphalangeal
FA	Finite Automata	**CAD**	Computer Aided Design
LDA	Linear Discriminant Analysis	**AI**	Anthropomorphism Index
EEG	Electroencephalography	**FDP**	Flexor Digitorum Profundus
CNS	Central Nervous System	**FPL**	Flexor Pollicis Longus
PNS	Peripheral Nervous System	**APL**	Abductor Pollicis Longus
FFT	Fast Fourier Transform	**EPB**	Extensor Pollicis Brevis
DFT	Discrete Fourier Transform	**EPL**	Extensor Pollicis Brevis
QR	Quick Response	**ANN**	Artificial Neural Network
DoF	Degrees of Freedom	**MRCP**	Extensor Pollicis Longus
CMC	Carpometacarpal	**SNN**	Spiking Neural Network
MCP	Metacarpophalangeal	**EMG**	Electromyography
BCI	Brain Controlled Interface	**GPRM**	Gaussian Process Regression Model

Chapter 1

Introduction

1.1 Background

There is no question that the loss of a limb has more than just a physical effect on individuals. The mental, social and spiritual well-being of those affected by limb loss is altered for the remainder of their lives (Elder and Kersten 2015). Around three million of the ten million amputees on the earth at any given time suffer from the loss of an upper limb (Maurice 2011). This type of amputation is particularly limiting in an environment engineered to suit the movement and capabilities of the hand. In such environments, hand amputation leads to the amputee becoming dependent on others for their quality of life. The loss of independence and freedom can be testing for amputees. Accepting these facts is the current reality for most amputees. Therefore, this research attempts to restore independence for amputees by developing artificial hand control frameworks that restore lost hand function.

To this point in time, the human hand remains unparalleled in its function and dexterity as proven by the many attempts to artificially recreate it (Belter, Segil et al. 2013). Although the goal to mimic the human hand is lofty and hard to realise, we are closer to achieving it than ever before. The technological climate and environment to reproduce or mimic the human hand has never existed as it does today, therefore, this research is exciting and highly valued. Accompanying this field of research are the methods used to control the artificial hands. A main contributor to the field of artificial hand control is the EEG signal. EEG is attractive because of its natural and intuitive nature of control. It also provides a non-muscle

based option of control for electromechanical devices. The advancements of EEG based control schemes for artificial hands are based on the fact that non-invasive EEG acquisition technology is becoming more accessible and affordable. As a result, NI control frameworks for electromechanical devices have become more popular (Abiri, Borhani et al. 2019). Although the field is progressing, there are limiting factors that halt the non-invasive EEG based NI's from entering the market. These limitations include signal acquisition, pre-processing, signal processing and artefact/noise removal. Potential solutions to these limitations are provided through reviews like Bashashati, Fatourechi et al. (2007) who assess the best approaches for NI based control systems. Alternate solutions to these limitations can be found by the implementation of autonomous robotic principles. Autonomous robotics has great potential to improve the functional outcomes of these control frameworks (Iris 2014, Fajardo, Ferman et al. 2018).

This thesis is exploratory and holistic, it seeks to find viable avenues through which hand function can be restored to upper limb amputees by the combining of western science and Te Ao Māori (Hikuroa, Morgan et al. 2011). The unique and holistic view given through Te Ao Māori considers how all living things and processes are connected. Information relating to this work stems from diverse research fields including but not limited to anatomy, biomechanics, electronic engineering, mechanical engineering, computer science, and neuroscience. The combination of these fields in conjunction with the aims of this work has the potential to unlock important information regarding the restoration of independence and quality of life for amputees.

1.2 Motivation

Throughout my life, I have had great experiences that have taught me the importance of making wise decisions. I have come to realise that true value lies in helping people. Although I live in a small part of the world, I feel lucky to have the opportunity to help others through whatever means I can. My heritage as a Māori from a small island in the south pacific has given me a unique view of the world in which we live. My perspective is conveyed in the overarching research idea expressed in the following section. I begin with my Pēpeha and explain its significance to this work.

1.3 Overarching Research Idea

1.3.1 Ko Wai Au? Who Am I?

PĒPEHA

Tīhei Mauri Ora!

Ko Rāhiri te tangata

Ko Hikurangi me Mōtatau ngā maunga

Ko Kaikou te awa

Ko Pipiwai, Kaikou, Matawāia, Mōtatau, me Waiōmio ngā marae

Ko Mātaatua me Ngātokimatawhaorua ngā waka

Ko Ngāpuhi te iwi

Ko Ngāti Hine te hapū

E kīia nei ko Ngāti Hine Pukepuke Rau

Ki te taha e pā ana ki Tūwharetoa

Ko Te Heuheu te tangata

Ko Tongariro te maunga

Ko Roto-a-Ira te moana

Ko Pāpākai, Ōtūkou, me Te Rena ngā marae

Ko Te Arawa te waka

Ko Tūwharetoa te iwi

Ko Hikairoa te hapū

He uri ahau nā rātou katoa

Ko Shane William Owen tōku matua

Ko Lorne Catherine Kydd tōku Whaea

Ko Mahonri Owen tōku ingoa

Tēnei te mihi ki a koutou katoa

Nō reira, tēnā koutou, tēnā koutou, tēnā tātou katoa

1.3.2 Te Ao Māori: The Māori Worldview

Takitoru, or the three vital questions 'ko wai au?', 'nā wai au?' and "i ahu mai au i hea?" are defining in every culture. Translated these questions are 'who am I?' "who are my ancestors?" and 'where do I belong?' Within my pēpeha lie the names, places and events that define me, representing who I am, and where I come from. Common features of a pēpeha include ancestors, names, mountains, rivers, tribes and areas. A pēpeha is a grounding and a foothold in an ever-changing world that gives identity and belonging. Important to me and of particular significance to this work is the importance of whenua (land), tāngata (people) and maunga (mountains). Maunga are sacred and in many cases named after ancestors. As such, they have the same respect and reverence as living elders. Mountain peaks represent the head of ancestors. The ūpoko (head) is the most sacred part of the human body representing the pathway to knowledge. From the mountains flow the awa (rivers) which gives life and vibrancy to the whenua and its tāngata whenua (people of the land).

The grandeur and astonishing beauty of the mountains in Aotearoa (New Zealand) are inspiring and closely related to the history of my people. Mōtatau maunga, also named 'Tū te ao, tū te pō' meaning 'standing day and night' references the ongoing strength and stability of the natural environment. Mōtatau is the Maunga with which my family relates. Standing at the feet of Mōtatau water flows through the valley towards Ōpahi, through Waingārara, Pokapū, Waiharakeke, Ōpua and finally exiting at Te Moana nui a Kiwa (The Pacific Ocean). From the water comes life. Mōtatau protects and provides for the people of the land through its natural systems. The people respect the land and take guardianship responsibility over it as custodians of its Mauri (life force) so it remains healthy and vibrant.

In respect to and in consideration of my heritage, a holistic approach that encapsulates the overarching research idea of this work is justified. Holistic in this context refers to the connection and interrelationship between all living things. The maunga, awa and whenua represent three distinct but interconnected processes that are part of the human body. The maunga are representative of the human head, being the source of information and the foundation upon which this work stands. The awa represents the flow of information through the nervous system of the body. The land represents the life, the movement and the power of the limbs of the body.

The human body is remarkable; it is full of processes and systems that are complex and hard to comprehend. The aim of many researchers is to understand then mimic the human body and its many intricacies. Even the simplest of tasks that the human body is capable of are not trivial to duplicate and reproduce. In most cases, mimicking any part of the human body necessitates simplification. Although there are obvious limitations to replicating the human grasping system, there is this exciting prospect: that the current technological climate brings us closer than ever before to the replicating of the human body. The potential contribution of this and similar research work is applicable to an enormous range of applications and fields.

This work focuses on replicating the biological processes involved with the movement and manipulation of limbs. Conveyed in a succinct manner: every physical movement experienced by the human body is a result of muscle innervation motivated by signals communicated through the nervous system originating at the brain. Simply described, there are three distinct areas of limb control: The brain, the nervous system and the limb. The brain interprets sensory

information and generates signals to actuate limbs. The brain signals travel through the nervous system and innervate muscles. Muscle innervation converts the signals into physical forces that move and manipulate limbs. From an engineering perspective, the brain is a control unit responsible for signal production, the nervous system is a communication pathway responsible for transferring information and the limb is any electro-mechanical device appropriate for application. If any degree of the human grasping process is lacking, not functional or absent we have the opportunity to recognise and replace function in any of the three areas. The idea of replacing any part of these biological processes is daunting and unreasonable to address within the limited time of doctoral studies, therefore, this work is limited to the control of artificial hands by non-invasive signals emitted from the brain.

1.4 Thesis Aim

The aim of this research is to restore hand function for amputees by mimicking the human grasping system through an artificial non-invasive based neural interface. The scope of the research includes the replication of the human grasping system. Focus in the research is given to the artificial replication of some of the functions of the human brain, nervous system and hand. This work is limited to the control of artificial hands by non-invasive signals emitted from the brain. The physiological signal considered is the non-invasive electroencephalography (EEG) signal. To achieve the overall aim, neural interface based methodologies for artificial hand control are investigated. Strategies for improving classification accuracy and response time are developed. Methodology for an autonomous artificial machine vision based hand is designed. The roles of machine vision, machine learning and artificial hand design are defined within the artificial human grasping system.

1.5 Thesis Outline

To achieve this aim chapter 2 methodically reviews the key literature relating to the human grasping system. It gives a brief background of human limb control by describing the anatomy of the human brain, nervous system and hand. It highlights artificial hand design and the current state-of-the-art in artificial hand control by NI's. Autonomy and its relationship with the control of artificial devices is expressed. The interactions between western science and Mātauranga Māori is acknowledged and its effect on this research is stated. Chapter 2 concludes with a description of the methodology used throughout the work. Chapters 3, 4 and 5 are descriptive of the contributions of this work and represent the bulk of the numerical and experimental results. Chapter 3 accounts for a biomechanically inspired artificial hand that is used as the artificial testbed for chapters 4 and 5. Chapter 4 deals with the control of the artificial hand by the development and incorporation of a SVM for a NI. The NI developed in chapter 4 is advanced in chapter 5 where an autonomous machine vision approach is employed to extend the capabilities of the SVM based NI. Chapter 6 discusses the contributions of chapters 3, 4 and 5 that meet the aim of this thesis. Finally, chapter 7 completes the thesis by drawing conclusions and providing recommendations for further work.

Chapter 2

Literature Review

2.1 Background

As stated in the introductory chapter the overarching research idea of this work is that three distinct but interconnected components make up the human grasping system. The brain, the nervous system and the hand. Each component directly influences hand function. The aim of this chapter is to review literature relating to the mimicry of the human grasping system and to form methodology for meeting the overall thesis aim. By understanding the mechanisms and processes of the human grasping system, we can mimic and replace these processes with artificial substitutes in the attempt to restore the function and quality of life of those who have limited or no hand functionality. In order to understand the nature and function of the human grasping system it is important to describe its anatomy. After establishing the anatomy of the brain, nervous system and hand the review looks at the current state of artificial electro-mechanical hands. The development of NI's for artificial hand control is reviewed and the potential of autonomous approaches towards the mimicking of the human grasping system are reviewed. Grounding is given to how this research is implemented within the realms of Mātauranga Māori and western science. This review is split into six sections: The human grasping system with its anatomy, artificial electro-mechanical hands, neural interfaces, autonomy, Mātauranga Māori and finally the methodology employed to meet the aim of the research.

2.2 The Human Grasping System

The human grasping system consists of three main areas the brain, the nervous system and the hand. The following section addresses the anatomy, function and role of these areas with respect to a human's ability to grasp.

2.2.1 The Human Brain

The human brain is a central organ of the human body. It is complex in its function and responsible for controlling the body and its limbs. The brain consists of three parts: the cerebrum, the brainstem and the cerebellum (Lewis 2019). The cerebrum consists of the left and right hemispheres. These hemispheres consist of four lobes (Damasio 1995). These are the frontal lobe, temporal lobe, parietal lobe and the occipital lobe. Each section of the brain is important and integral to the functioning of the human body (Cherry 2018). Neurons are the basic unit of the brain and carry electrical impulses throughout the nervous system (Mai and Paxinal 2012). Neurons (Figure 1) consist of a cell body (soma) containing a nucleus, dendrites and axons.

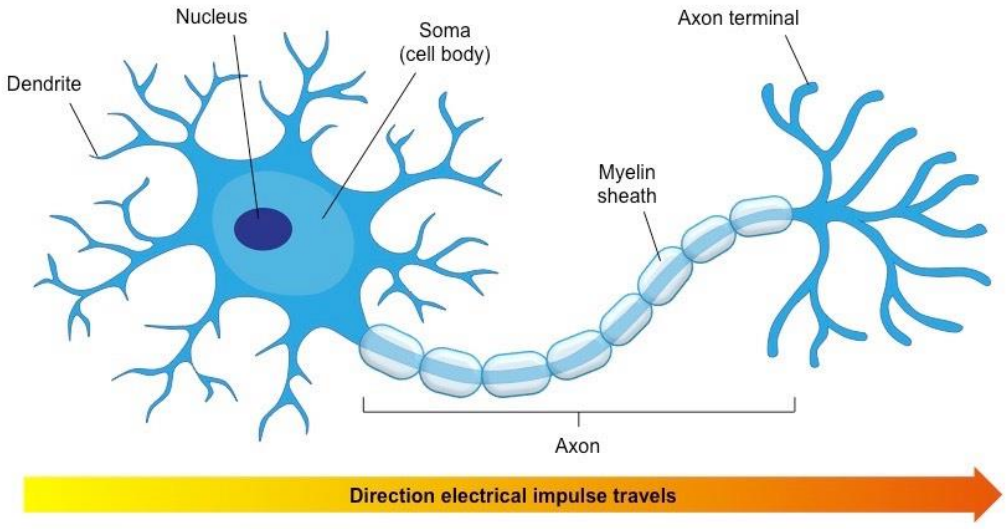

Figure 1: Neuron Anatomy (Aleksandra 2018).

There are many classes of neurons found in the nervous system. These can be sensory neurons, motor neurons or interneurons (Szymik. B 2011). Neurons in the

brain connect through synapses with their interactions constituting brain activity (Marquard 2012). Action potentials are the result of neurons in an excited state. When the neuron membrane becomes excited it produces an electrical impulse called an action potential (Devices 2019). Understanding and decoding action potentials is at the heart of brain signal interpretation technology.

2.2.2 The Nervous system

The nervous system coordinates sensory and motor information (Mai and Paxinal 2012). The Central Nervous System (CNS) and the peripheral nervous system (PNS) constitute the nervous system. The CNS consists of the brain and the spinal cord. It is responsible for integrating and coordinating all the parts of the human body. (Cherry 2018). The PNS connects the CNS to the organs of the body. It functions as a relay between the brain and the body. Within the nervous system there are motor nerves and sensory nerves (Westfall and Westfall 2011). Motor nerves carry action potentials to muscles (Hunt and Kuffler 1954). The motor nerves communicate with muscles through the neuromuscular junction (Dodge and Rahamimoff 1967). The neuromuscular junction forms by the contact of a motor neuron with a muscle fibre (Hall and Sanes 1993). The sliding filament theory by Huxley (2004) and the cross-bridge theory by Fitts (2008) compliment and support each other as to how muscles provide limbs with movement.

2.2.3 The Hand

Thirty-four muscles activate the human hand. Over half of these muscles are extrinsic, located in the forearm. The other muscles are intrinsic and located within the palm of the hand (McMinn and Hutchings 1977). Actuation and movement of the human hand originates from the contraction of muscles, which displaces tendons attached to the bones of the hand. The linear motion provided from the muscle creates torque at the joints of the hand. Ligaments and pulleys support the

tendons of the hand, which create structures and networks throughout the hand and forearm. There are twenty seven bones in the hand including the carpals of the wrist.

2.2.4 Relevance

Traditional approaches to NI development tend to simplify and ignore the full complexity of the human grasping system. A human based approach serves as a unique and foundational setting for the development of human-like NI's for prosthetic hand control. Understanding the basic anatomy and function of the human body is integral to this work. The human grasping system relies on the synergy and interaction of the brain, the nervous system and the hand. To continue this review artificial hands are examined with the intent to address the chasm between artificial hand design and the human hand. The following section addresses the state-of-the-art in prosthetic and artificial hand design.

2.3 Artificial Electro-Mechanical Hands

The mechanical design of artificial hands is often limited to the specialty of the designer. For example, a mechanical engineer will create a hand based on mechanical principles, however, this approach has the possibility of omitting organic features of bones and joints that are essential from a biological and biomechanical point of view. It is important to note that novel and effective artificial hand design in the current technological climate arise from multidisciplinary viewpoints that consider more than just traditional mechanical principles. As such, the important aspects of artificial hand design are considered throughout this section.

The design of artificial hands involves a number of mechanical considerations. The mechanical design at an introductory level involves decisions focussed on the digits of the hand. Commonly, fingers have three phalanx or sections representing the bones of the human hand skeleton. The configuration and actuation of these fingers can be complex or simple depending on the level of dexterity and anthropomorphism required. The number of digits in artificial hands depends on the purpose of its existence. In cases where anthropomorphism, dexterity, aesthetics and biomimicry are important mimicking the human hand becomes the goal, therefore, four fingers and one thumb is the common design approach. There is however, a big challenge in orienting the digits in a manner that is aesthetic and functional. In most cases, thumb simplification accommodates control methods and increases design feasibility at the cost of function and dexterity. Thumbs are complex in nature accounting for up to fifty percent of hand function. The design of an effective thumb is one of the greatest challenges in current hand design and is described aptly by Ladd, C.A-P. et al. (2013) who state the thumbs function as ‘articulation by reciprocal reception’. In cases where precise and accurate

movements are required, it is common for artificial hands to employ planar manipulators, for their digits. In these cases, the hand resembles a factory robot and is unnatural looking. The increased popularity of electromechanical prosthetic hands has given rise to the judgment and scrutiny of such devices. There are five defining areas of what good artificial hands possess. The review by Owen. M (2015) describes some of the available electromechanical hands. The review defines the DoF (Degrees of Freedom), drive mechanism and actuator type of fourteen electromechanical hands (Table 1).

Table 1: Current electromechanical and artificial hands.

Hand	DoF	Actuators	Under-actuated	Self-contained	Drive Mechanism
I-limb	6	DC motor	yes	Yes	Rigid Link
Bebionic	5	DC motor	yes	yes	Rigid Link
Dextrous	6	DC motor	yes	yes	Tendon Driven
Robonaut	12	DC motor	yes	yes	Tendon Driven
Shadow	20	Air muscle	no	no	Tendon Driven
Utah/MIT	15	pneumatic	no	no	Tendon Driven
Hitachi	12	Shape Memory Alloy	no	no	Tendon Driven
Biomimetic hand	21	DC motor	yes	no	Tendon Driven
Belgrade	4	DC motor	yes	no	Rigid Link
Stanford/Salisbury	9	DC motor	yes	no	Tendon Driven
NTU	17	Micro-motor	no	yes	Tendon Driven
DLR	13	DC motor	no	yes	Gears
Michaelangelo	17	DC motor	yes	yes	Gears and Rigid Link
Azzurra	11	DC motor	yes	yes	Tendon Driven

This review is backed by Deshpande, Xu et al. (2011) who also review artificial hands and identify important features towards their design. In general the lower the DoF of the hand the simpler the design of the hand. The ability of an artificial hand to function in an unmodified human environment directly relates to its capacity to function like the human hand. The DoF of a system is the number of independent parameters that define its configuration. In the attempt to design anthropomorphic artificial hands, its DoF is a good measure of its functionality. Put simply, the closer the artificial hands DoF to the human hand the greater its potential is. Research into modelling the human hand claim that twenty-four DoF accurately represents the posture and movement of the human hand (including the wrist) (Cobos, Ferre et al. 2010) This claim is trivial with most literature agreeing that the human hand has twenty-one DoF (excluding the wrist). Others assert similar DoF with their research claiming between twenty-one and twenty-six DoF (Gustus, Stillfried et al. 2012).

Current state-of-the-art shows definite trends in the design of artificial electro-mechanical hands. In the past, rigid couplings tended to dominate artificial hand design, however, tendon based driving mechanisms are becoming more popular and effective. A tendon based driving mechanism represents an anthropomorphic approach that is functional and aesthetically pleasing. As artificial hands develop, tendon driven mechanisms are likely to be the dominant mode of actuating artificial hands. Tendon driven hands maximize design space within the hand and tend to ease the mechanical design process. The benefits of tendon driven hands are obvious, however, a tendon driven approach dictates that the actuators need extrinsic placement. In many cases, this is not a feasible solution.

2.3.1 Biomimetic Artificial Hands

The latest attempts at hand design employ a human inspired approach. The focus of these types of hands are on the tendinous structures actuating the hand and their synergies with ligaments, joints and actuators. Deshpande, Xu et al. (2011) approached the design of an artificial hand using human like bones and joints. Of considerable note to the study, was the natural look and movement of the prosthetic. A bulky unnatural looking wrist was implemented in the design and is pinpointed as requiring improvement. Xu and Todorov (2016) developed further the idea of anthropomorphic biomimetic hands by developing human like tendinous structures and improving the design of artificial thumbs. Their approach was unheralded and provided an aesthetically pleasing artificial hand that functioned well. Their approach was aided by replacing traditional mechanical joints with natural human like joints and joint capsules. Further studies in the same year by Hockings (2016) presented attempts at artificially emulating the human hand by the mimicry of the mechanics and material properties possessed by the human hand.

The biomimetic approaches of these hands give rise to design concepts in the development of synergistic tendon networks, bone configuration, bone orientation and joint development. These ideas are worthy of further investigation if hand function is to be restored to amputees through biomechanical hand design approaches. It is expected that these types of approaches will increase in popularity and improve as the research climate and time allows. The development of artificial anthropomorphic hands is exciting and progressive.

2.3.2 Grasp Taxonomy

Understanding the way humans grasp objects is important in many research fields. Many study the tasks of grasping, gripping and holding. One of the earliest reviews of grasp taxonomy was developed in 1989 where everyday tasks were identified and labelled (Cutkosky 1989). In review of later literature Feix, Pawlik et al. (2011) suggested that all grasps can be categorized into seventeen grasp types. Feix, Romero et al. (2016) supports this idea by arranging literature in a systematic way where all grasps can be reduced into a number of manageable categories.

2.3.3 Relevance

The aim to restore hand function directly relates to the ability of an artificial hand to mimic the human hand. Boundless attempts are made to mimic the human hand, however, there is still no man-made hand that is on par with the human hand. The consideration of mechanical hand design in conjunction with NI control has the potential to restore hand function for amputees by mimicking the human grasping process. The following section describes the history and development of neural interfaces for artificial hand control

2.4 Neural Interfaces

A Neural Interface (NI) is a device that interprets neurological information for controlling external devices. The first instance of a NI in application was the use of neural oscillations to play musical instruments. Alvin Lucier produced a NI that played music based on the production of alpha waves (Straebel and Thoben 2014). Since the discovery of EEG in 1924, the development of NI's has accelerated. Although Lucier produced a NI in 1965 the term 'BCI' (brain computer interface) was not coined until 1977, where a visually evoked potential was used to control a cursor for maze guidance in a computer system (Vidal 1977). (As a preliminary investigation to this work an example of an artificial hand controlled by neural oscillations is presented in the appendix section A1). It is common in today's technological climate for NI to employ complex signal processing and machine learning (Samuel 1967, McFarland, Lefkowicz et al. 1997, Srinivasan, Eden et al. 2007, Muller, Tangermann et al. 2008, Carvalho and Suleman 2009, Taghva, Song et al. 2012, Liao, Xiao et al. 2014, Stewart, Nuthmann et al. 2014, Uriguen and Garcia-Zapirain 2015, Agilent Technologies 2018). In general, NI's consist of signal acquisition, machine learning and device incorporation. According to Nicolas-Alonso (2012) some of the common features of NI's are: signal acquisition, pre-processing, signal enhancement, feature extraction, classification and control interface. This claim is verified earlier by Lotte (2008) who separates the control interface feature into translation, command and feedback. From all attempts to create NI's for device control there remains one major challenge. That challenge is performance in accuracy and response (Nooh, Yunus et al. 2011).

2.4.1 Electroencephalography (EEG)

The monitoring and recording of action potentials originating from the brain is fundamental to NI technology. EEG is the recording of electrophysiological activity of the brain and is a main contributor to the field of neural prosthetics; it gives access to the action potentials present along the scalp produced by neurons in the brain. This method involves the placing of electrodes along the scalp to measure voltage fluctuations over populations of neurons. As acknowledged, the first recording of EEG in a human subject occurred in 1924 where Hans Berger a German psychiatrist discovered the electroencephalogram (David 2001). Since then EEG has been developed to a point where it is at the heart of many modern medical practices. There are two types of neural interfaces: synchronous and asynchronous. Synchronous NI's are restricted to predefined time frames while asynchronous NI's operate independently (Nooh, Yunus et al. 2011). EEG supports research in the fields of neurology, cognitive science, psychology and neuro-prosthetics to name a few.

2.4.1.1 Equipment

Non-invasive Electroencephalography (EEG) equipment is easily accessible due to its affordability and mobility over other acquisition methods. Its non-invasive nature makes it the most common of all the acquisition techniques for neural prosthetic control. In most cases, the equipment is mobile but does require shielding and or accessory equipment. Typical EEG recording techniques should give consideration to electrode choice and configuration (Teplan 2002).

2.4.1.2 Signal Processing

Much of the NI technology used today relies on signal processing. The connection of signal processing and machine learning has unlocked the doorway to many of

today's NI technological breakthroughs. Applications of machine learning utilising signal processing has great potential to improve the technological climate and push the capacities of what we are currently capable. Machine learning and signal processing has great potential to improve NI outcomes. One of the critical steps in designing NI's is the processing and analysis of brain signals in real time. Signal processing is the analysis, synthesis and modification of signals. There are two domains used to process EEG signals. The time and frequency domains. The time domain records raw EEG data and contains a wealth of information that is not accessible without viewing in the frequency domain. For this reason, signal processing of EEG data is a 'matter of perspective'(Agilent Technologies 2018). The Fast Fourier Transform (FFT) is used to traverse between the time and frequency domains (Instruments 2019). The FFT is a Discrete Fourier Transform (DFT) that transforms a signal or waveform into discrete values that the FFT processes. Viewing a waveform (signal) in the frequency domain adds perspective to the construction of the waveform. Preliminary to signal processing is Pre-processing. Pre-processing is sufficiently described in the next sections by filtering and windowing.

2.4.1.3 Filtering

Filtering is the removal of artefacts and noise in the raw EEG signal. According to Roberts, Gruber et al. (1999) artefacts are "any potential difference due to an extra cerebral source". There are three main sources of artefacts in the EEG signal: ocular, muscular and cardiac (Uriguen and Garcia-Zapirain 2015). Filters eliminate artefacts that effect the reliability of the EEG signal and are required in all non-invasive EEG signal processing. Signal filters have a very specific function to reject unwanted artefacts and ignore interference. There are four basic filter types: low-pass filters, high-pass filters, band-pass filters and notch filters (OpenEdition 2019).

Successful filtering is an integral part of developing NI technology and important in signal processing.

2.4.1.4 The Window function

In order to acknowledge the need for window functions there is the requirement of understanding the effect of the FFT on wave forms. The application of FFT to EEG data often creates the output of a phenomenon called 'spectral leakage'. Spectral leakage occurs whenever there is a sharp discontinuity in the sampled signal and is a result of power spreading through the frequencies of the signal. The discontinuities occur from the assumption of the FFT, that the dataset is finite and that the endpoints of the waveform are connected and continuous. When this assumption is not met, spectral leakage is introduced to the signal. The effect of spectral leakage is limited by windowing. A window function is a function that is zero outside a chosen interval. Multiplying another function by a window function produces an overlap of the two functions with everything outside of the interval equating to zero. In essence, windowing allows the management of spectral leakage. The application of windowing to a dataset essentially changes the properties of the dataset. Consider the following definition of a system involving $H(z)$.

$$Y(z) = X(z)H(z) \tag{1}$$

Where, $Y(z)$ is the output and $X(z)$ is the input. By multiplying the window function $W(z)$ by the input $X(z)$ we get

$$X'(z) = X(z)W(z) \tag{2}$$

Applied to the original system yielding,

$$Y'(z) = X'(z)H(z) \tag{3}$$

Different window functions have different characteristics and are suitable to different applications.

2.4.2 Machine Learning

After pre-processing and signal processing the data can be applied to any desired machine learning method. In 1959, Arthur Samuel introduced the term machine learning (Samuel 1967). Machine learning is a field of artificial intelligence where a machine can learn, identify patterns and make decisions on its own. This property is incredibly valuable to NI technology and is integral to meeting the aim of this work. By the implementation of machine learning we can better understand the functions of the brain and interpret its resulting EEG signals. The application of machine learning is wide-ranging and ongoing. In the context of NI technology, machine learning identifies patterns and classifies data. Pattern identification and classification occurs in four ways (Varone 2019): supervised, unsupervised, semi-supervised, active and reinforced. Of particular importance to this work is supervised learning. Supervised machine learning is comparable to concept learning in the human being and involves the comparing of new data to example data (Kotsiantis, Zaharakis et al. 2006) .The aim of supervised learning is to create a function from known input and output data that predicts the output of a set of unknown input data.

2.4.3 Neural Interfaces: State of the Art

A state of the art review of NI was conducted by Nicolas-Alonso (2012) from the perspective that NI technology is underpinned by its potential to restore function to the disabled. A later review by Lotte, Bougrain et al. (2018) recognized the need to include the progression and status of classification algorithms within NI technology. Earlier reviews addressed the importance and significance of non-invasive EEG-based NI's where the contribution of EEG to the fields of robotics, neuroscience and computer science is recognized (Carpi and De Rossi 2014). Between each study, there remains five concepts that envelop the development and progression of NI technology: The identification of useable signals, the development of training methods, data handling, signal processing, artefact elimination and machine learning.

The development of the NI is an exciting field with great potential. The most recent review of NI technology by Abiri, Borhani et al. (2019) recognizes that the development of NI over the past ten years is founded upon technological advances. The review highlights the importance of linking the design paradigm of NI to the specific application of the NI. The climate and accessibility to NI technology has advanced and increased giving way to new and novel NI design paradigms and frameworks. The application of NI is wide-ranging and diverse. Another recent study of NI development by Nishimoto, Kawakami et al. (2018) investigates the feasibility of developing a NI that is not limited to clinical applications. Their results suggest NI's have the potential to succeed in real world applications in a safe and accurate manner, there is however, limited proof and evidence of this being the case. Other recent studies investigate the implications of disease on NI performance and

the recognition of mental states for machine actuation (Bird, Manso et al. 2018, Bridges, Meyers et al. 2018).

2.4.3.1 Application of NI

The investigation by McFarland, Lefkowicz et al. (1997) of an EEG based NI produced a preliminary framework for an alternate communication pathway for paralyzed people. Their result claimed that NI's require three features: Signal analysis in real time, real time data conversion and training. Most studies agree with this claim, however, as technology and signal processing has progressed the frameworks and approaches toward NI have as well. In 2001, oscillatory EEG components served as the control signal for a NI used to recognize hand movement. Although considered basic in today's climate, this and other works served as a foundation for most NI based frameworks to recognize hand movement in the EEG signal. In 2006, the development of NI's for prosthetics gained more traction. The continuance of such traction at the time was thought to depend on performance, safety and cost (Schwartz, Cui et al. 2006). A secondary idea suggested that development of the NI would relate directly to the progress of extraction algorithms. This notion is indeed true and will continue to be the case as NI's develop into the future.

Until 2007, there was no comprehensive review of signal processing techniques used in NI technology (Bashashati, Fatourechi et al. 2007). This review defined the most common processing algorithms used before 2006. Of the one hundred and thirty two NI studies, the Support Vector Machine (SVM) and Linear Discriminant Analysis (LDA) were the prevalent machine learning methods used in NI applications. The SVM presented the most reliable and robust of all the machine-learning methods. These claims are backed by the more recent studies of (Alomari,

Samaha et al. 2013, Elstob and Secco 2016, Lotte, Bougrain et al. 2018). In 2010, attempts to move NI into the real world continued with a focus on training optimisation (Hazrati and Erfanion 2010). Classification accuracies of seventy percent and above were claimed at this time. From 2010 until the recent times, NI research has focused on pattern recognition and biologically inspired approaches. Today, focus is given to classification accuracy and response time.

Classification accuracy is how well a machine learning classifier differentiates between different EEG signals acquired from the user. Between 2010 and 2018 multiple studies have claimed classification accuracy of around seventy to ninety percent (Guger, Harkam et al. 2001, Hazrati and Erfanion 2010, Li, Zhao et al. 2012, Alomari, Samaha et al. 2013, Pattnaik and Sarraf 2018). In most cases these studies are theoretical and without application in the real world. In cases where the NI is applied for prosthetic control classification accuracy reduces by ten to twenty percent. This suggests there are elements of design related to NI application that diminish its potential in real world applications. These principles must be addressed. Response is the time taken for the NI to recognize and actuate a physical electromechanical device. A NI applied for prosthetic control is subject to the scrutiny of the user. If the NI framework does not respond within a reasonable period, the NI will not be useful in application. The study by Li, Zhao et al. (2012) claims eighty five percent classification accuracy with a response time of thirteen seconds . In application this is not an incredible result, however, in terms of the state-of-the-art it is a significant advancement.

Although the progression of NI is exciting Elstob and Secco (2016) convey that there is no use for an NI that does not have consistent control. This suggests that

further work and development is required in the field for NI's to be successful in real world applications. The state-of-the-art in NI technology for prosthetic hand control is a relatively new field when considering its application in the real world. In theory, there is no reason to suggest that a non-invasive EEG based prosthetic control framework is not possible in real world application. The classification accuracy and response time are the main areas of NI performance that, limit the progression of NI's into the market.

2.4.4 Relevance

NI's are responsible for the interpretation of physiological signals. These signals hold critical information relating to hand function and, therefore, are integral to the aim of this work to restore hand function. The correct application of NI's creates a sense of belonging between an amputee and their prosthetic device. At the heart of NI design, lies signal processing and machine learning. There are two critical areas of interest in applying NI's in the real world: Classification accuracy and response time. The investigation of NI's leaves the following questions unanswered. Why are non-invasive NI's limited to research and not the real world? What is the full potential of NI's in the current technological climate? What is the current limit of non-invasive EEG based NI's for hand control? Further investigation is required to answer these important questions. By answering these questions a response to the aim of this work can be given.

This section has described the underlying science, reviewed existing theories for mimicking the human grasping system and provided preliminary investigations that give relevance to the approaches presented in chapters 4 and 5 of this work. The following section describes the potential of restoring hand function by mimicking the human grasping system through autonomous robotics principles.

2.5 Autonomy

The history and development of autonomous robots is involved and exciting. Perhaps, the most widely known application of autonomous robots is self-driving cars (Pendleton, Andersen et al. 2017). The idea for self-driving cars emerged in 1988 and real world applications started developing in 2005. Since 2005 attention to self-driving autonomous cars has increased dramatically. Autonomous vacuum cleaners represent another application of robots that have been successful with the earliest autonomous vacuum cleaners emerging in 2001 (Prassler, Ritter et al. 2000). Autonomous robots are self-reliant, they make decisions based on the information gained from the surrounding environment. Sensors help robots to perform their tasks without human intervention. These robots have the tasks of object avoidance and navigation. Infrared, ultrasound and Lidar are common sensors for object detection in autonomous mobile robots, which allow them to navigate around known and unknown working environments. The ability of gathering environmental information provides a high degree of autonomy to a robot. The intelligence of a robots response depends on the richness of information gained from the environment. Perception, planning and control are the three core processes of autonomous robotics (Krotkov and Simmons 1996, Pendleton, Andersen et al. 2017). Figure 2 depicts the interactions among these processes and the environment for an autonomous robot.

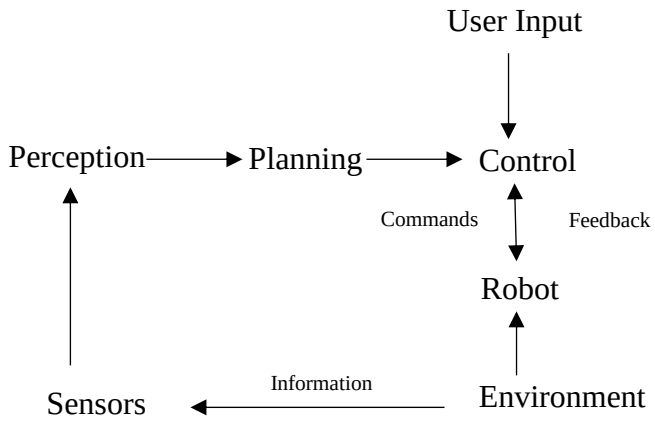

Figure 2: The interactions of autonomous robots with the environment.

Perception of the autonomous robotic system is how well it is able to acquire information from the surrounding environment. This process involves collecting information through sensors and extracting relevant environmental knowledge. An autonomous system develops an environmental model it can use to determine future actions. Planning is the decision making process. The environmental model dictates this process. Control is the competency of an autonomous robot to execute planned actions. Actions are converted into a set of commands that actuate the robot. The attributes of autonomous robots are human like and fitted for mimicking the human grasping system. The application of autonomous robot principles to artificial hand control frameworks is reviewed in the following section.

2.5.1 Autonomous Artificial Hands

Autonomous robots are common in industrial settings and automation processes. As a result, autonomous artificial hands are linked into the same category. The autonomous principles of both are the same, however; the control scheme is different and, therefore, alternate approaches are required. Prosthetic hands need to adapt to different objects and require the ability to handle the intervention of human interaction. For these reasons, a relatively new field of autonomous artificial hands is gaining traction. Several claims to autonomous control schemes for artificial

hands have been made. Iris (2014) presented an approach to artificial hand grasping that employed QR codes as the classifier of objects within a known environment. Fajardo, Ferman et al. (2018) use a webcam for object classification. A Neural Network classifies objects according to a stored dataset and hand operation depends on classification output. In 2017, a Convolutional Neural Network approach to an autonomous vision based hand produced a control system that classed objects into grasp categories that can be used to assign grasp poses to an artificial hand (Ghazaei, Alameer et al. 2017). A single camera requiring the object to be a fixed distance from the object limited the studies application. Weiner, Starke et al. (2017) produced a vision-based framework that had the ability to classify six objects by a Convolutional Neural Network. The most recent claim comes from Ficuciello (2019) who uses a machine learning based approach to mimic the human decision making process of grasping three different objects within a given volumetric space. Dosen and Popovic (2011) presented an artificial vision framework for grasping. The goal of the work was to test a concept, therefore, a methodology was not developed for their system. The results were encouraging, however, the following reasons limited their work: The work did not consider pre-shaping and the work assumed an artificial hand with an articulated wrist which is not common to acquire.

Perhaps the biggest limiting factor of all the autonomous hand approaches spoken of is the applicability of their methodologies. Although the theories are sound, there are multiple limiting factors that arise from the physical implementation of their ideas. Each method is good but does not seem to fully appreciate the complete complexity of the whole challenge of an artificial hand and its grasping system. Until now existing theories to develop autonomous hands are found lacking and represent a gap in knowledge in the field. It is expected that by unifying NI's with

autonomous principles the potential of mimicking the human grasping system will be improved immensely.

2.5.2 Relevance

The application of autonomous principles to artificial hand control is exciting. By sensing the surrounding environment, control schemes and strategies can be employed to grasp objects effectively. Autonomous approaches reduce the cognitive demand of amputees in non-invasive neural control applications. This type of approach is valuable for its potential to reinforce a natural sense of belonging between amputees and their prosthetic devices. Autonomous hands potentially represent a great improvement in the field of neural prosthetics. The following section departs from the technology based review of this chapter and delves into the possibility of unifying Mātauranga Māori and western science to provide outcomes to restoring the quality of life of amputees.

2.6 Mātauranga Māori and Western Science

Stemming from the strained historical relationship between the Māori and European colonisers, the value of Mātauranga Māori has been consistently overlooked as a reliable source of information. For many researchers the information regarding Māori knowledge is presented through two perspectives. The first is that of the western world and the second is that of the Māori. As stated by Bristowe (2017) researchers are subjected to the view that was speaking the loudest at the time. In this case the Māori perspective was not given ear to and somehow, the history of Aotearoa/New Zealand became the history of Europeans and not the Māori. This and many other injustices have made the combination of Mātauranga Māori and western science difficult.

In speaking of the differences between the two knowledge bases, it is important to state that there is a fundamental difference in the epistemology (way of learning) between western science and Mātauranga Māori (Crawford 2009). Māori knowledge is transferred orally and in many instances cannot be shared through the classical research methods of hypothesis and testing. For this reason avenues through which indigenous knowledge is researched is not shared in the light it was given, therefore, there is limitation at the outset of producing Māori based works in professional and academic engineering settings. These epistemology differences lead to great insights but do not always converge seamlessly. An example of this is given by Newman and Moller (2005). Their study recognised that western science and Mātauranga could agree on observed patterns in seabirds, but, would disagree on reasons as to why these patterns occurred. This idea is developed and given justification by Hikuroa, Morgan et al. (2011) where it is stated that “Indigenous knowledge cannot be verified by scientific criteria nor can science be adequately

assessed according to the tenets of indigenous knowledge." The study goes on to define the origin of indigenous knowledge and describes it as holistic being unified with the environment.

In recognition of this holistic approach it is important to introduce the concept of Mauri. Mauri is the life force and essence of every living thing. As such it is important within any research based on Mātauranga Māori to take responsibility of observing Mauri. Lapsley, Waimarie et al. (2002) state that at the base of Māori health is the consideration of Mauri across all aspects of a person's life. In addition to this Mātauranga Māori acknowledges additional ideas that are not always considered in western science. For example, the Wairua theory introduced by Elder and Kersten (2015) acknowledges a spiritual injury accompanying all physical injuries and use it as a cultural assessment tool. In response to the aims of this work when amputees are affected physically from limb loss, it is important to have tools to overcome the accompanying spiritual, and mental injuries that occur. This and other ideas are relevant to this work and require consideration. There is great potential in linking the ideas of western science and Mātauranga Māori because what one lacks the other does not. This type of approach is applicable to many fields and requires further investigation.

2.7 Research Objectives

The literature review has identified areas in need of additional research for NI's through non-invasive EEG based autonomous hand design. It is well recognised that the field of non-invasive EEG based NI's is a difficult area to work in. While there have been examples of EEG controlled machines and devices in conference publications there are not any real world or marketable cases of artificial hand control through non-invasive EEG that can perform beyond open and close tasks. The following areas have been identified as requiring additional research:

1- The application of machine learning approaches for NI's in artificial hand control.
2- The application of machine vision for an autonomous hand.
3- The combination of a NI's with autonomous principles for artificial hand control.

The purpose of the research can be summarised by the following research questions:

1- Does the non-invasive EEG signal provide sufficient information to control artificial electromechanical hands beyond binary (open and close) tasks?
2- What methods have the greatest potential to improve and restore hand function in NI based grasping systems?
3- What value is there in basing this research in Mātauranga Māori but maintaining a western academic approach?

The research questions can be broken down into four areas where hand function restoration can be realised.

1- Hand function restoration through mechanical design and the mimicry of the human hand.
2- Hand function restoration through machine learning in NI's.

3- Hand function restoration through a vision based autonomous hand.
4- Hand function restoration through the acknowledgement of Mātauranga Māori and western science.

With these ideas in mind, the objectives of the research are:

1- To investigate the effect of artificial hand design on hand anthropomorphism and function,
2- To investigate the machine learning methods that can obtain the highest accuracy and response for classification tasks,
3- To evaluate the SVM for NI based grasping applications,
4- To investigate and evaluate the value of autonomous vision in hand grasping applications, and
5- To integrate NI technology and autonomous robotics into one holistic design.

Achieving these objectives will maximize the restoration of hand function for amputees.

2.8 Methodology

Of particular importance to the methodology of this work is Mātauranga Māori. Mātauranga Māori is the understanding, comprehension or knowledge of everything whether visible or not that exists in the universe. The unique perspective given in this work comes from the unifying of Mātauranga Māori with western science approaches. Throughout this work whare kōrero (overarching philosophies) are presented as ideas on which the contributions of this work is based. The aim of this research is to restore hand function for amputees by creating an autonomous, artificial, non-invasive NI based grasping system. The research is applied and experimental. An artificial hand testbed needed to be developed to meet the

requirements of the grasping system and answer the research questions. NI development and autonomous machine vision is necessary to determine if the quality of life of an amputee can be improved through the restoration of hand function. The methodology of this work is presented in two sections, a NI for artificial hand control and a NI based autonomous hand. Each section specifically relates to hand function and, therefore, contributes vitally to the aim of the research to restore hand function. The methodology used relies on the development of an artificial hand as a physical testbed. Therefore, the physical design methodology of the artificial hand is described. Following this, the methodology of the autonomous NI for artificial hand control is given.

2.8.1 Biomechanical Hand Design Approach

The contribution of a biomechanical approach toward artificial hand design is justified by the requirement of the research to have a physical testbed to accomplish testing with. The current state of artificial prosthetic hands is such that cost, patents, rights or insufficient hand function limits the availability of such devices. The design of a hand makes up less than a third of the work presented herein but is vital to this works completion. In light of this, particular design choices and basic design principles are excluded in the description of the hand because it is only a means to an end and not the focus of the thesis. Standard engineering design processes were used in conjunction with the idea to biomechanically replicate the human hand. The artificial biomechanical hand was designed on the principle of biomimicry and incorporates the following concepts within its design:

1- the stabilization of joints through supporting ligaments,

2- the optimization of thumb orientation, and

3- a solution to tendon excursion

Each concept is justified and its importance in the overall work is stated below.

The Stabilization of Joints through Supporting Ligaments

Ligament insertions are tested by the investigation of bone to bone interactions and how the collateral ligaments of the hand affect those interactions. The actual geometry and size of the human hand skeleton used in testing proves the value of such an approach. These interactions elucidate the importance of bone geometry on hand function and contribute to the hands overall anthropomorphism.

The Optimization of Thumb Orientation

This approach is chosen for its influence on the restoration of hand function for amputees. The thumb is responsible for more than half of the hands function. It cannot be ignored. Therefore, quantifying its effect on hand function is approached through comparing the anthropomorphism of artificial hands to the human hand (Gustus, Stillfried et al. 2012) based on common grasp taxonomies (Feix, Pawlik et al. 2011). Kinematic equations are used to model an artificial hand which is then compared to the human hand. Action manifolds are developed to quantify the level of anthropomorphism of artificial hands. These action manifolds are then compared to the human hand and an anthropomorphism index (AI) is used to describe how closely the artificial hand mimics the function of the human hand.

Tendon Excursion

The effect of tendon excursion is investigated through the physical adjustment of tendons to measure the excursion induced on other tendons within the artificial hand. In many instances this excursion completely eliminates useful hand function. Therefore, excursion cannot be ignored in artificial hands with articulated wrist movement. Movement induced tendon excursion is measured by isolating individual tendons of the artificial hand and iteratively actuating the associated joint. As movement in the joint occurs, displacement of the other tendons in the hand are measured. A reverse engineering approach is then applied to counter the unwanted

tendon excursion through servomotor actuation and microprocessor control. This approach allows articulated wrist motion in tendon driven artificial hands and maximizes the functional range of artificial hands.

2.8.2 A NI for Artificial Hand Control

This approach is focussed on restoring hand function by investigating the limitations of non-invasive NI's. The approach investigates whether more robust approaches to machine learning methods for NI based artificial hand control can be developed in the current technological climate. Machine learning methods for the analysis of non-invasive EEG signal is investigated through the application of a SVM based NI. Standard pre-processing and conventional machine learning methods are employed to test the response and accuracy of the SVM approach. EEG data is provided through publicly available data sets. The approach employs MATLAB and EMOTIV software with C++ and Python computer languages. EEG acquisition is achieved through the EPOC+ EEG acquisition headset and servomotor actuation is controlled by the Arduino Uno. The servomotors are Hitec HS-645MG. The choice of the SVM is justified through analysis. Finding the limits of this approach is required to meet the thesis aim and answer the research questions. This approach is important because it identifies the best way to maximise hand function restoration. This work uses asynchronous methods so that all the frameworks and methods involved in this work can be applied in real time and in the real world.

2.8.3 The NI Based Autonomous Hand

An environmental/object interaction approach was used to develop an autonomous hand with the intent to restore hand function. This approach has great potential to improve the performance of current non-invasive NI's. Machine vision and

autonomous robotic principles are applied to increase the accuracy and response of the NI. The potential of this approach is too great to ignore. The approach employs LABVIEW software in conjunction with the Logitech c5255 webcam, SharpGP2Y0A21YK infra-red sensor, myRIO microcontroller, Arduino and multiple Hitec HS-645MG servomotors. Image processing occurs in the visual studio of LABVIEW provided by National Instruments. After image processing a landscape of grasp mapping is developed. Pre-shaping and object manipulation complete the process. The approach is justified by mimicking the human grasping system and reducing the unnecessary human involvement required by the NI. This approach implements a harmonious relationship between robot and human to maximize hand function restoration.

2.9 Summary

The overarching research idea is now supported by relevant literature stemming from multiple fields and disciplines. The chapter aim to detail the mechanisms and processes of the human grasping system is achieved and methodology to meet the overall thesis aim has been formed. The three areas of interest are the brain, the nervous system and the hand. It is expected that as attempts to mimic the human grasping system are popularized the potential to restore hand function will improve. There are many attempts to decipher the raw non-invasive physiological signals emitted from the brain. These attempts are focussed on the development of machine learning methods. Research into machine learning for artificial hand control requires further investigation, particularly in how reliable and responsive they can become. In addition to investigating the effect of machine learning in NI's there is great potential to be found in the collaboration of machine learning and autonomous machine vision. The review recognised the key design principles and approaches present in the field for developing artificial hands. The following chapter

investigates artificial hand design with the intent to provide a physical testbed for the development of the NI of chapter 4 and the autonomous NI framework of chapter 5.

Chapter 3

The Biomechanical Design of an Artificial Hand

3.1 Background

Three distinct but interconnected processes constitute the overarching idea of this work as shown throughout the entirety of chapter 2. The biomechanical design of an artificial hand represents one third of this idea and is integral to the aim of restoring hand function. It is possible to begin investigations without an artificial hand for testing, however, the control frameworks described later in the thesis (chapters 4 and 5) require an artificial hand prototype for experimental and application purposes. Current electromechanical artificial hands are either in the research stage, expensive, have patents, lack severely in function and or are driven by robotic/mechanical principles which tend to ignore the biological requirements of such designs. Therefore, a biomechanical hand addressing gaps of knowledge in the literature is presented as the starting point for this work. In response to the thesis aim, the purpose of this chapter is to investigate how hand function can be restored to amputees through biomechanical artificial hand design. The following hypothesis is formed: Through investigating the effect of biomechanical design concepts on hand function we can contribute to the optimisation of artificial hand design and thus restore hand function to amputees in a more meaningful way. The aim of this chapter is achieved by the improvement of artificial hand design through joint stabilization, thumb orientation and tendon excursion.

3.2 Biomechanical Approach

In general, traditional engineering and robotics are the foundation for artificial hand design, however, a purely robotic or engineering approach lacks the consideration of the physiological and biological requirements for such systems. Therefore, prominent features of hand design that directly influence hand function are considered. The following concepts explore artificial hand design ideas eluded to in the literature review that are worth following up.

1- Joint Stabilization,

2- Thumb orientation, and

3- Tendon excursion.

The resulting hand (Figure 3) incorporates these concepts with the intent to improve artificial hand grasping functionality.

Figure 3: Biomechanical approach towards artificial hand design.

Preliminary to investigation is the need to consider the unquantifiable nature of human anatomy. The nature of anatomy presents a unique challenge in the replication of the human hand. Mechanical engineering approaches rest on the expectation that the design approach is quantifiable. The following reasons provided by Hockings (2016) provide insight as to why mimicking the human body is not always quantifiable.

1- The boundaries of ligaments, tendons and muscles are not easily definable.
2- Ligament, tendon and muscle insertions differ from person to person.
3- Some tendons and ligaments possess non-linear characteristics that make measurement inaccurate.
4- Some human tissues have no measurable resting position.

The reality of working in this space of design is that there are some challenges that cannot be quantified and are subject to engineer/designer best knowledge or experience.

3.3 Joint Stabilization

This particular approach links hand function to artificial ligament design. The bones on which hand ligaments are inserted provide pathways on which joint stabilization relies. In order to understand the contribution of mimicking the ligament structures of the hand it is important to comprehend the interaction between them and bone geometry. The bones of the human hand are essential to hand function. The way in which these bones interact and connect with each other is of utmost importance. The bones of a joint are the stabilising base on which all digit movement occurs, therefore, each joint of the hand has a series of ligaments that limit undesirable movement and protect the hand against excessive force and unwanted movement.

The incorrect placement of any ligament severely effects the movement of these bones. For this reason joint stabilization is integral to hand function. Three of the main ligaments responsible for finger stabilization and movement are: The collateral ligament, the volar plate, and the annular ligament. This section describes the joint stabilization of the artificial hand by firstly establishing collateral ligament insertion locations and then applying them to fully stabilised finger joints.

3.3.1 Establishing Collateral Ligament Insertion locations.

The purpose of this section is to define collateral ligament insertion locations for each phalanx of the hand that optimises the movement between bones. The collateral ligaments of the hand are the primary stabilisers that connect adjacent bones. Each bone of the hand has a head and a base. The head of one phalanx is connected to the base of the next and so on as shown in figure 4 below where the four bones of the fingers are named and oriented.

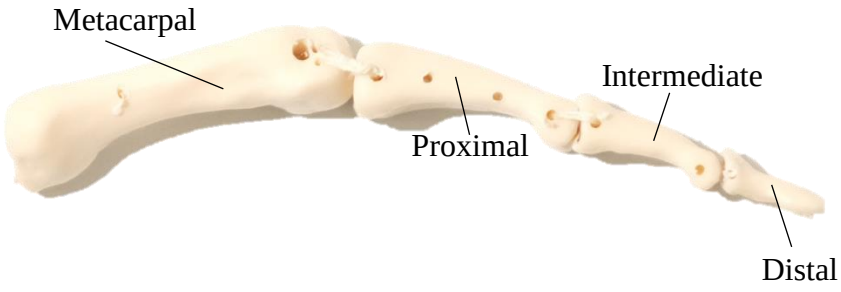

Figure 4: Index finger bone names and configuration.

In order to define insertion locations for each combination of bones the proximal phalanx of the index finger is used as an example. The proximal phalanx (Figure 5) has two defining features that help describe insertion locations: The Phalanx Length and the Centroid. The phalanx length, L_P is the summation of L_{BC} and L_{HC} and the centroid is found using the mass property evaluation in SOLIDWORKS (Results found in the appendix, section A2).

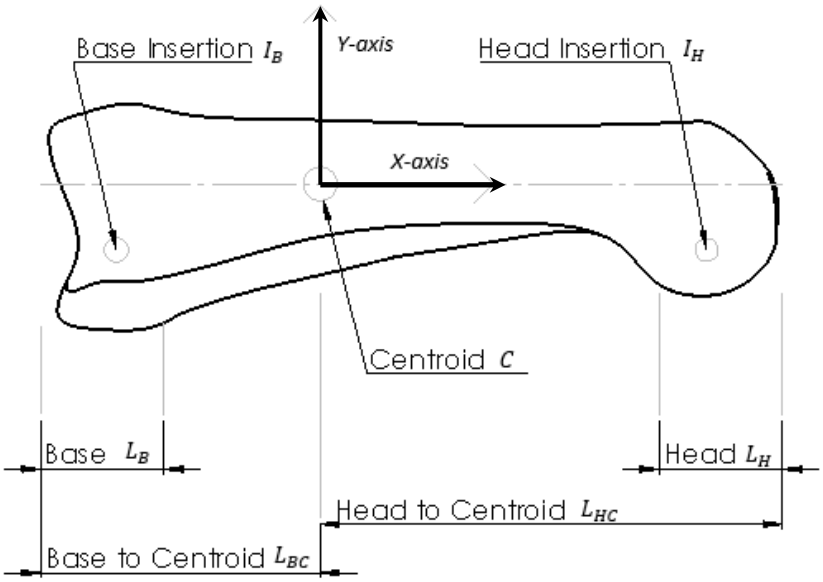

Figure 5: Collateral ligament insertion points.

The coordinate system is established on the centroid of the phalanx. The phalanx length and the location of the centroid determine the ligament insertion locations I_H and I_B. L_B and L_H define the limits that bound the insertion locations. The coordinates of the head insertion I_H and base insertion I_B are given by

$$I_H = (x, y) = ((L_{HC} - L_{HI}), (y < 0)) \quad (4)$$

And

$$I_B = (x, y) = ((-L_{BC} + L_{BI}), (y < 0)) \quad (5)$$

Where L_{BI} and L_{HI} are a percentage of the total phalanx length, L_P, that is still acceptable for correct bone interaction between each phalanx. The values for L_{BI} and L_{HI} are determined by a joint motion test. Insertion points are designed and modelled at distances between 3mm and 8mm from each end of the involved phalanx. Joint motion is quantified by a rating between one and three. Where one

represents a good range of motion and three represents a poor or severely lacking range of motion. Any insertions below 3mm or above 8mm do not provide any range of motion and do not add any value to the investigation. (Values for L_{BI} and L_{HI} are found in section A3 of the appendix and are found by dividing the insertion distance by the phalanx length). As shown in equations (4) and (5) the location of the insertion in the vertical direction is governed by the variable, y. If, $y = 0$ the insertion is located along the x-axis. If $y < 0$ the insertion is located below the y-axis. If the insertion is governed by $(\pm y)$ then it has two insertion points either side of the y-axis. The three insertion location conditions are expressed by the following equations:

Condition 1 is expressed by

$$(x, y) = ((L_{HC} - L_{HI}), (y = 0)) \tag{6}$$

Condition 2 is expressed by

$$(x, y) = ((L_{HC} - L_{HI}), (\pm y)) \tag{7}$$

Condition 3 is expressed by

$$(x, y) = ((-L_{BC} + L_{BI}), (y < 0)) \tag{8}$$

Table 2 below shows what condition is to be used at either the head or the base of each phalanx. For example, condition 1 is applied to the head of the proximal phalanx whereas, condition 3 is applied at its base.

Table 2: Insertion location conditions assigned to each phalanx.

	Metacarpal		Proximal		Intermediate		Distal	
	Head	**Base**	**Head**	**Base**	**Head**	**Base**	**Head**	**Base**
Condition 1			x		x			
Condition 2	x							
Condition 3				x		x		x

Any major variance from the values and conditions listed in this table are detrimental to the joints range of motion and its stabilization. Through this method collateral ligament insertion is generalized for all artificial hand design. The geometry of the bones in the hand compliment the collateral ligaments at each bone-ligament interface. Collateral ligament placement determines joint function and, therefore, hand function. Bone surfaces are congruent and possess depressions or protuberances that give clues to ligament insertion locations. The bone surfaces also permit human like range of motion at each joint. Figure 6 shows the resulting range of motion, μ for the MCP and PIP joints.

Figure 6: The resulting range of motion at the MCP and PIP joints.

The MCP joint commonly allows a ninety degree range of motion while the PIP joint is found to have around one hundred degrees in its range of motion. The resulting range of motion of the artificial MCP and PIP joints fit within two degrees of these ranges. The correct interaction of bones and ligaments is rarely realised in artificial hand design. Digit function, range of motion and dexterity are maximised

through correct design and implementation of artificial collateral ligaments. The collateral ligaments are vitally important to hand function, however, as recognised at the beginning of this section there are three main ligaments responsible for joint stabilization. Therefore, an approach towards the complete design of digit joints is presented in the following sections.

3.3.2 Digit Joints

The collateral ligament insertion locations have been established in the previous section. The collateral ligament represents one of the three stabilising ligaments of the joints of the fingers. This section will describe the implementation of these ligaments towards a stabilised finger joint design. Take as an example the metacarpophalangeal (MCP) joint shown in figure 7. The collateral ligament provides lateral stability. The insertion points of the collateral ligament (black box figure 7) are realised via an extruded cut through the proximal phalanx of the artificial finger according to the condition described by equation (7). The volar plate protects the fingers against hyperextension. Insertion points on the palmar sides of the metacarpal head and proximal phalanx base combine to prevent hyperextension (red boxes figure 7).

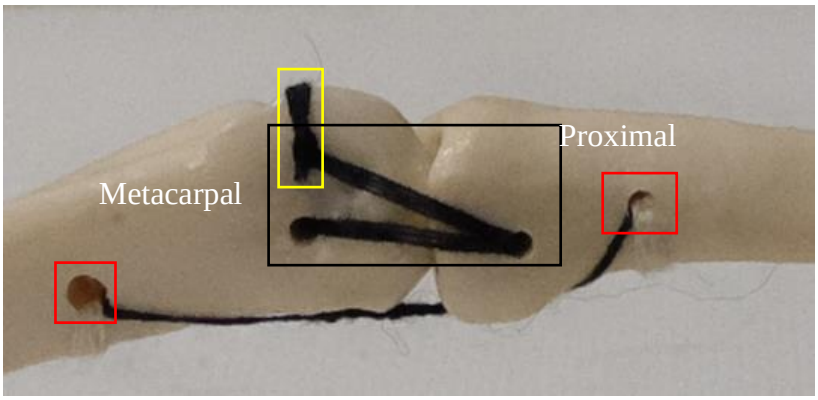

Figure 7: Lateral view of the Metacarpophalangeal joint and its stabilising ligaments.

Artificial wound ligaments distribute force evenly around each joint. A sagittal band (yellow box of figure 7) is responsible for housing the extensor tendon and minimises the chance of transverse tendon slippage. The sagittal band shares insertions with the collateral ligament. Annular ligaments share insertions with the volar plate. The MCP joint allows two movements: Abduction/adduction, flexion/extension. Lateral movement is limited through the placement and angle of the collateral ligaments. The bone ends are complimentary allowing smooth rotation through the flexion and extension movements of the joint. The concave/convex relationship between the bones allows abduction and adduction. The Proximal interphalangeal (PIP) joint shown below in figure 8 connects the intermediate phalanx to the proximal phalanx. The PIP joint has one DoF capable of only flexion and extension.

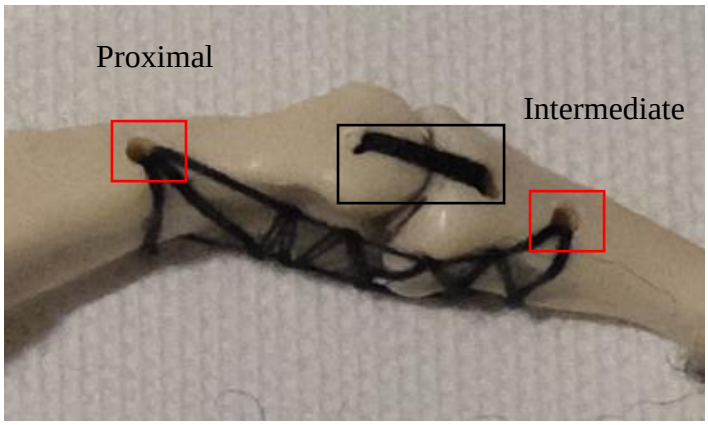

Figure 8: The proximal interphalangeal joint and its stabilising ligaments.

The primary stabiliser of the PIP joint is the collateral ligament (black box figure 8). On the palmar side of the joint is the volar ligament (red boxes in figure 8 indicate insertion points for the volar ligament) that protects the joint from hyperextension. The volar ligament shares an insertion with the annular pulleys. These auxiliary joints provide simple planar movement that provide the hand with the ability to grasp and manipulate objects with precision and force. Bone geometry constructively limits/allows motion inherent in the joint, thus making the joint more anthropomorphic. The Distal interphalangeal (DIP) joint connects the intermediate phalanx to the distal phalanx. The DIP joint is stabilised in the same manner as the PIP joint. Of the two joints the PIP provides around ninety degrees of motion while the DIP joint provides a significantly smaller amount.

3.3.3 The Carpometacarpal Thumb Joint

The thumb is responsible for more than half of the hands total function, therefore, a biomechanical approach to its replication is required. The carpometacarpal (CMC) joint of the thumb is complex and hard to replicate. Of any bone in the hand the trapezium bone is the largest contributor to hand function. Its geometry allows the complex multi-axial movement possessed by the thumb. Five artificial ligaments provide stabilization for the CMC joint of the thumb. The five artificial ligaments

are described below. The first artificial ligament (Figure 9) mimics the function of the Anterior Oblique ligament. T1 and M1 locate the trapezium bone and the metacarpal bone of the thumb respectively. The anterior oblique ligament connects the metacarpal bone to the trapezium bone and prevents the thumb from dislocating while allowing wide ranging motion. The insertions are highlighted in red.

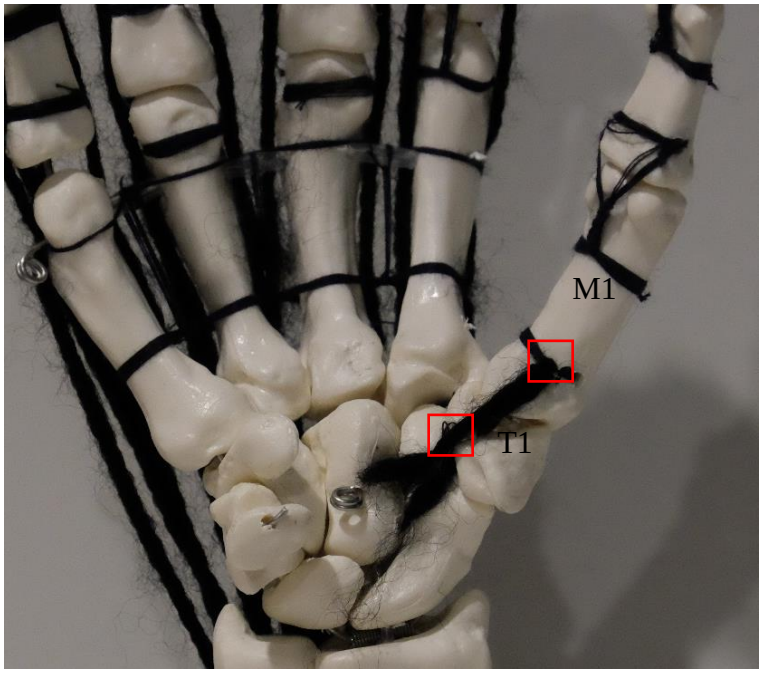

Figure 9: A palmar view of the carpometacarpal joint and the artificial anterior oblique ligament.

The second artificial ligament (Figure 10) has the function of limiting movement of the thumb away from the hand, acting as a stabiliser of the joint. This ligament connects the metacarpals of the thumb and index finger. The insertions are highlighted in red.

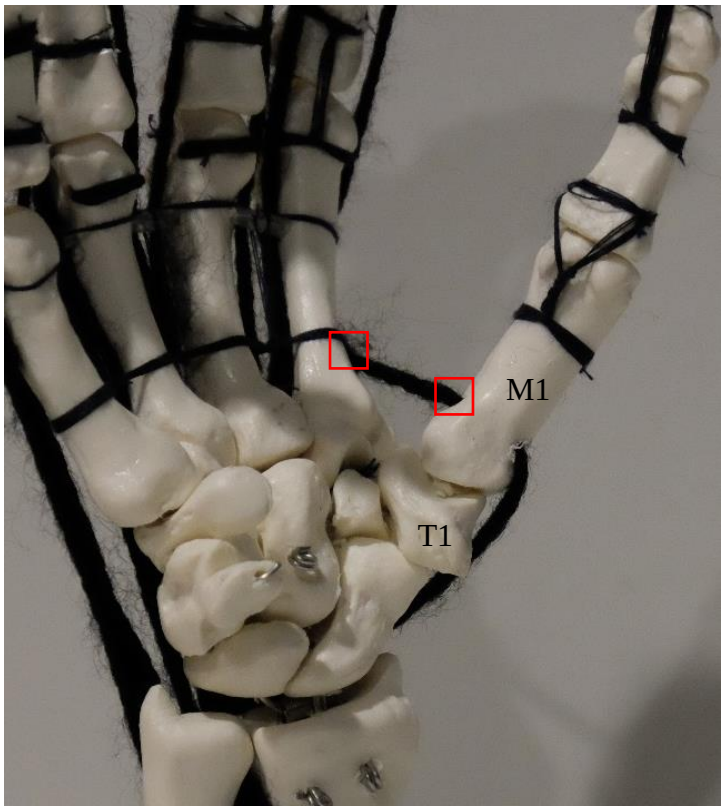

Figure 10: The dorsal view of the carpometacarpal joint and the stabilising ligaments.

The third, fourth and fifth ligaments replicate the function of the Dorsal Deltoid Shaped Ligaments. These are stabilising ligaments named: the dorsal radial ligament, the dorsal central ligament and the posterior oblique ligament. The ligaments originate at the trapezium and insert at different points along the dorsal surface of the metacarpal. All three ligaments allow and limit movement in varying degrees to support and/or limit movement in different planes. These three ligaments are visible in figure 11. The insertions are highlighted in red.

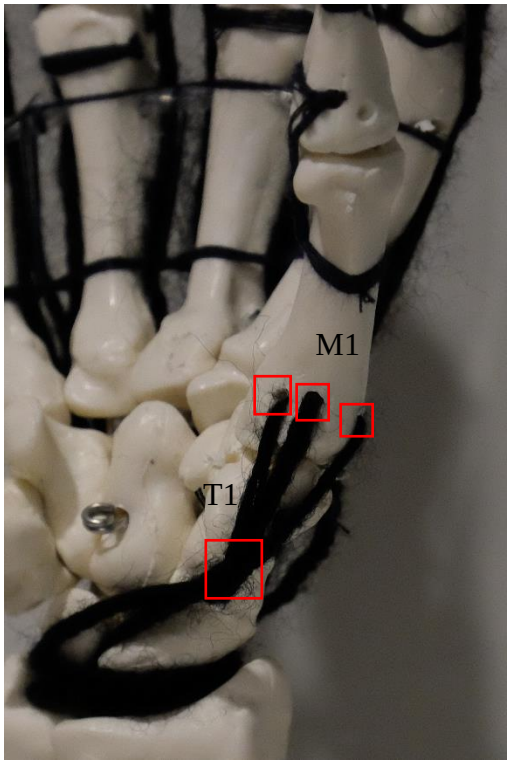

Figure 11: Palmar/Lateral aspect of the carpometacarpal joint showing the dorsal deltoid shaped stabilising ligaments.

The five thumb ligaments in total make up the stabilization of the thumb at the CMC joint. These ligaments define the thumbs orientation and movement. Therefore, an investigation into the effect of these ligaments on hand function is required.

3.4 The Effect of Thumb Orientation on Hand Function

As stated the thumb accounts for a majority of the hands total function. Poor thumb design simply means poor artificial hand design. Thumb function is reliant upon the bone geometry of the trapezium bone and the thumbs metacarpal. The geometry of these bones allow complex multi-axial ranges of movement that are not possible through traditional mechanical joints. The interaction between thumb bones and its orientation with respect to the fingers of the hand is critical to hand function. This section investigates the effect of thumb orientation on hand function by comparing the thumbs orientation against hand anthropomorphism. This is accomplished by

establishing kinematic structures that can represent the artificial hand, employing a comparative analysis to evaluate it and finally, comparing it to the human hand.

3.4.1 Defining the Artificial Hand by Kinematic Structures

The human hand is made up of twenty seven bones connected by joints that possess a number of Degrees of Freedom (DoF). Kinematics can be used to define the assembly and configuration of a hand. A kinematic chain is a series of rigid objects connected by joints that limit/allow motion. The artificial digit can be modelled as a kinematic chain as shown in figure 12, therefore, the artificial hand can be perceived as a series of these kinematic chains fixed on the palm of the hand.

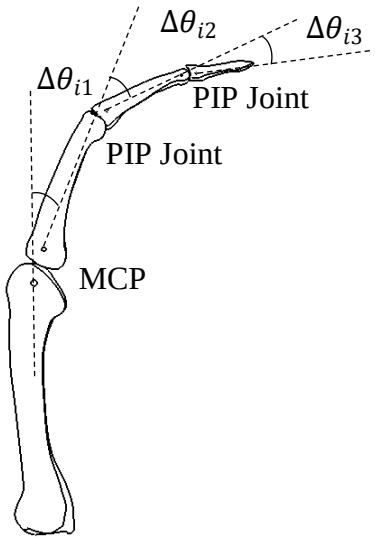

Figure 12: Prosthetic finger kinematic chain and associated movement.

The following kinematic equations can be used to describe the fingertip location of the artificial digit in two dimensions.

$$x = l_1 cos(\Delta\theta_{i1}) + l_2 \cos(\Delta\theta_{i1} + \Delta\theta_{i2}) + l_3 \cos(\Delta\theta_{i1} + \Delta\theta_{i2} + \Delta\theta_{i3}) \quad (9)$$

$$y = l_1 sin(\Delta\theta_{i1}) + l_2 \sin(\Delta\theta_{i1} + \Delta\theta_{i2}) + l_3 \sin(\Delta\theta_{i1} + \Delta\theta_{i2} + \Delta\theta_{i3}) \quad (10)$$

Where, l is representative of the phalanx length and $\Delta\theta_i$ is the angle of rotation at each joint. By adding a DoF at the MCP joint of each finger and modelling the artificial hand within a CAD environment, the fingertip trajectories can be demonstrated in real space (Figure 13). (Appendix, section A4 presents the data containing the 3D workspace of the hand)

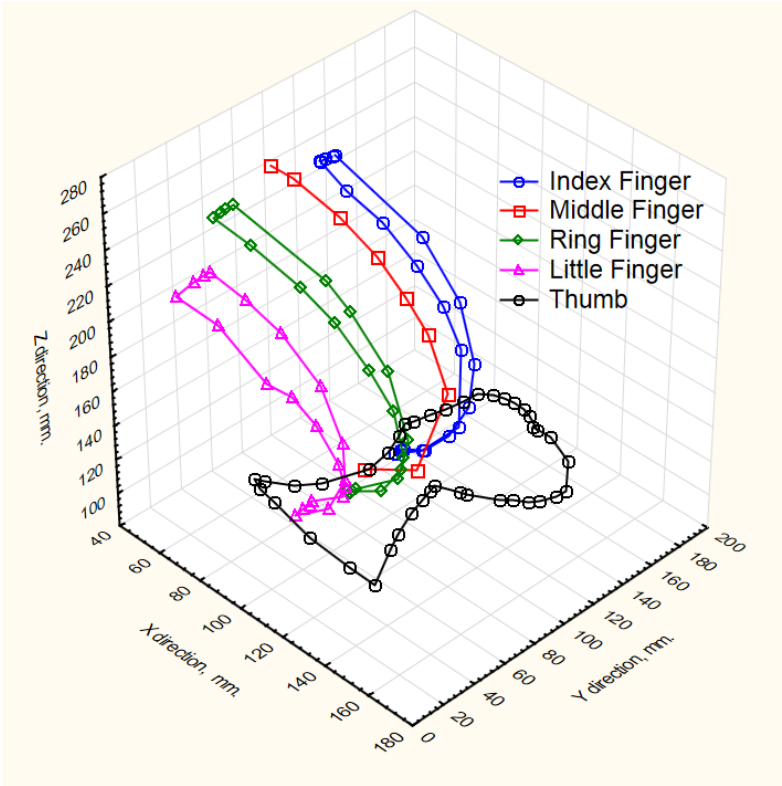

Figure 13: Workspace of the artificial hand conveyed in three dimensions.

Extending this idea, we can model the artificial hand in the MATLAB environment by establishing a coordinate frame at the MCP joint of the middle finger (Figure 14).

Figure 14: Establishment of the coordinate frame based at the MCP joint of the artificial hand.

The base position of the kinematic chain of each digit is defined by

$$\begin{bmatrix} x \\ y \\ z \end{bmatrix} - \delta = B \tag{11}$$

Where, B, is the base position of the digit and x, y and z are the coordinates of that base position for any given finger. δ, is used to translate the original positions of each finger to a useable condition within the environment.

The base position of each finger in the artificial hand (Figure 14) is given below based on the positioning given in figure 15. (All distances are given in cm).

Thumb	Index Finger	Middle Finger	Ring Finger	Little Finger
$\begin{bmatrix} 2.7 \\ -2.6 \\ 4.2 \end{bmatrix} = B_T$	$\begin{bmatrix} 1.7 \\ 0 \\ 0 \end{bmatrix} = B_I$	$\begin{bmatrix} 0 \\ 0 \\ 0 \end{bmatrix} = B_M$	$\begin{bmatrix} -1.3 \\ -0.5 \\ 0 \end{bmatrix} = B_R$	$\begin{bmatrix} -2.6 \\ -1.9 \\ 0 \end{bmatrix} = B_L$

Where the subscripts $T, I, M, R\ and\ L$ represent the thumb, index, middle, ring and little fingers respectively.

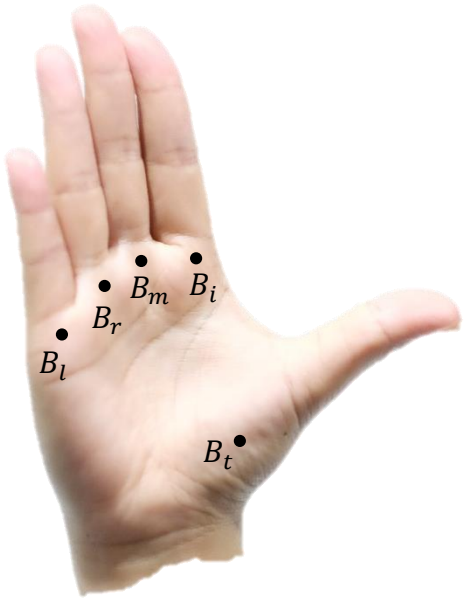

Figure 15: Base positions for each digit of the hand.

By establishing the base position of each finger a 6x5 base matrix is used to define the position and orientation of the digits. Where the columns 1-3 are the base positions $B_t^T, B_i^T, B_m^T, B_r^T$ and B_l^T and the columns 4-6 represent rotations around the x, y and z axis respectively. (The base matrix is defined in the appendix section A5)

The main characteristics of the artificial hand are reduced to a series of phalanx lengths and base orientations. The kinematic structure and phalanx lengths are used to develop the model below (Figure 16).

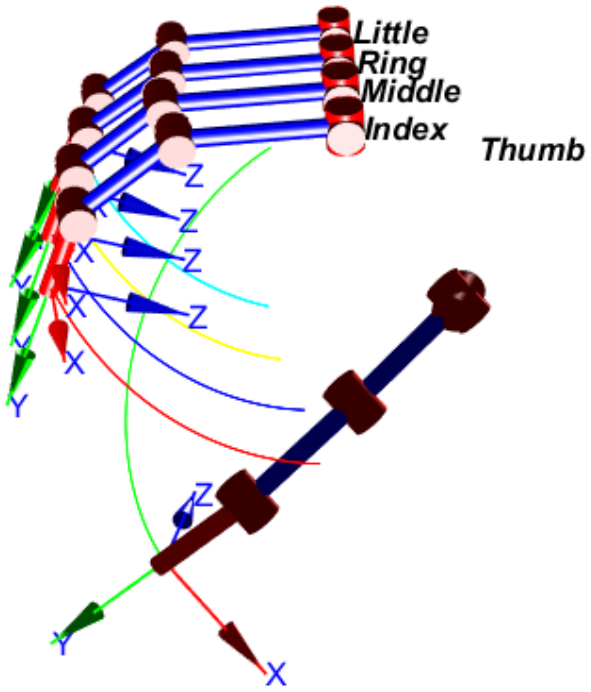

Figure 16: Full kinematic structure of the artificial hand in the MATLAB environment.

(The definition for the model above can be found in the appendix section A5)

3.4.2 Comparative Analysis

The artificial hand model is compared to the human hand using the action manifold description given by Feix, Romero et al. (2013). This process consists of four steps.

1- The fingertip poses of the artificial hand are calculated by use of the kinematic equations.

2- The fingertip poses are scaled to fit the human hand.

3- The data is projected in two dimensions by linear dimensionality reduction.

4- The overlap of the action manifolds are calculated to produce a value called the Anthropomorphism Index (AI).

The comparative analysis is based on a set of poses that are performed by the human hand. Hand position is measured through a series of sensors fixed to a glove worn by the hand. Using the human hand as the standard to which every other hand is measured. The AI is a measure of how well an artificial hand compares to the human hand. The method used has not been applied to quantify the effect of thumb orientation parameters before, therefore, it is a new approach. The following section quantifies the effect thumb orientation on hand function.

3.4.3 Quantifying the Effect of Thumb Orientation on Hand Function

The idea of quantifying thumb orientation is that if one angle, θ, is changed in the artificial hand model the optimal thumb orientation can be established. By creating an axis through the CMC joint of the thumb we can control the direction of the thumb face normal (since the thumb becomes a planar manipulator after the CMC joint). The thumb orientation, θ, will be defined as the angle between the direction normal to the thumb face as shown in figure 17. The orientation and position of the MCP, CMC and Thumb face normal are given in the form $[x, y, z, x_{rot}, y_{rot}, z_{rot}]$ where the subscript '*rot*' represents an angular rotation about an axis and the subscript 't' represents the position of the distal phalange of the thumb. By fixing the CMC joint of the thumb the values of x_t, y_t and z_t can be determined using kinematics.

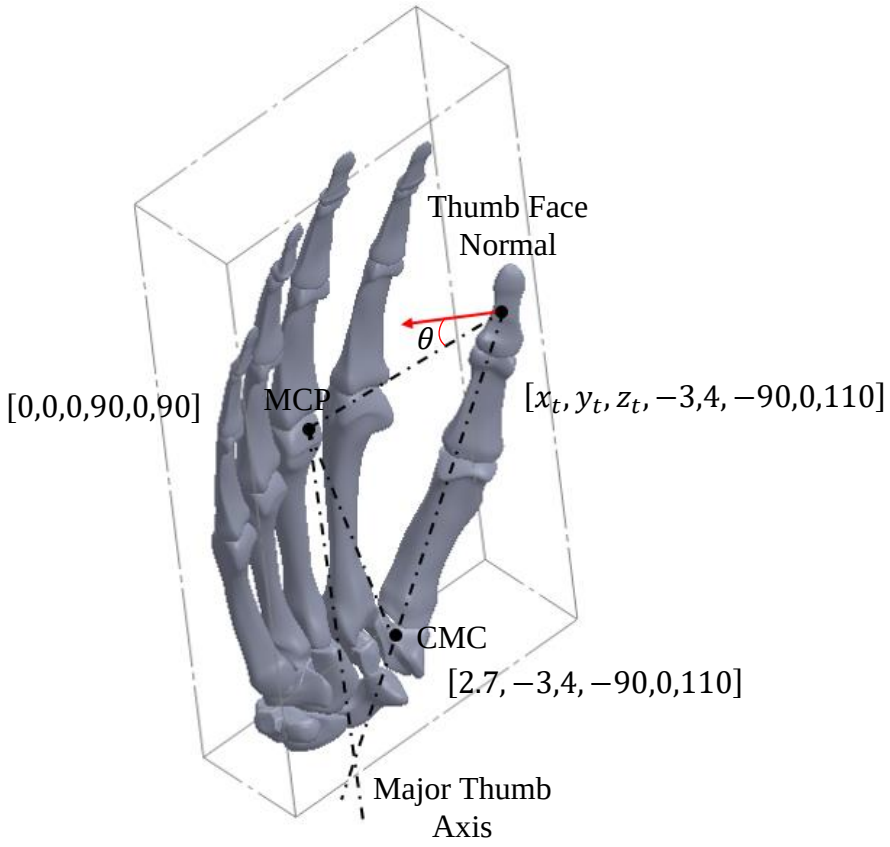

Figure 17: Description of the thumb orientation angle, $\boldsymbol{\theta}$.

Mapping the thumb orientation against the AI distinguishes optimal thumb orientations for artificial hand design. The description of the artificial hand in the MATLAB environment is centred on the MCP joint of the middle finger. Testing is accomplished by comparing twenty one iterations of the modelled hand against the human hand. Each iteration differs by a five degree angle which changes the thumb face normal angle incrementally between 0 and 160 degrees. (Results and explanation of the offset angle can be found in the appendix section A6). The results are shown in figure 18.

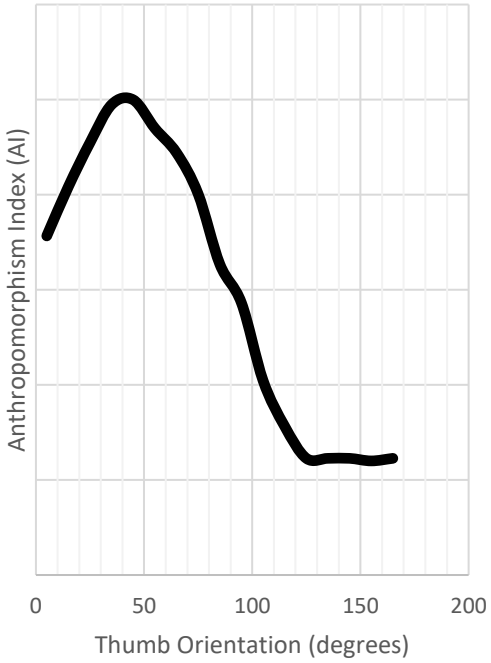

Figure 18: Thumb orientation angle optimisation.

These results show that an angle between thirty-five and forty-five degrees yields the maximum AI value. This implies that as the thumb orientation of a prosthetic hand approaches forty degrees the more it functions like a human hand.

As a result, the thumb is capable of interacting with and opposing each finger of the hand (Figure 19).

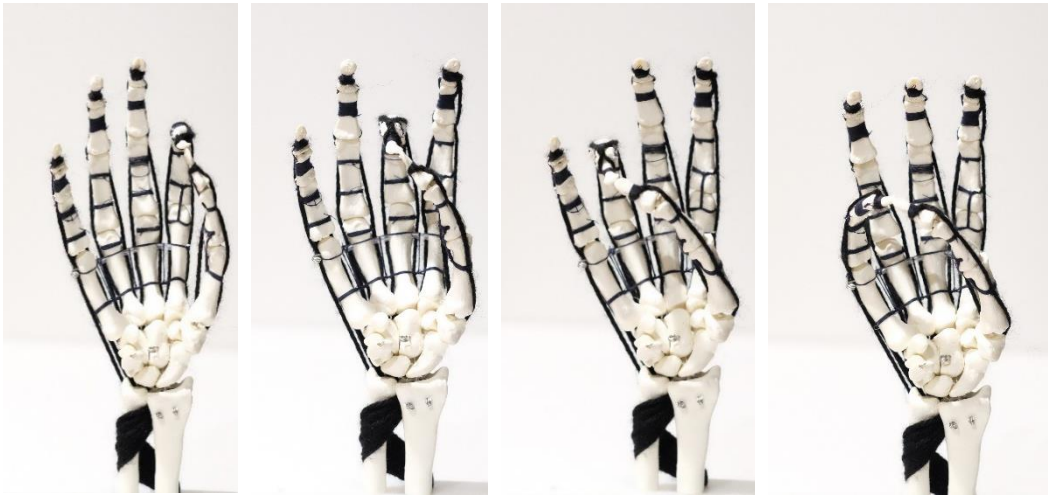

Figure 19: Finger opposition in result to correct thumb orientation.

The interaction between the thumb and the fingers is the gateway to improving human grasping function. Improving thumb orientation increases hand functionality through the improvement of its ability to interact with the fingers of the hand. Application of the correct thumb orientation produces improved function that is capable of multiple grasps, grips and gestures. Thumb orientation represents one of the dominant challenges in realising human-like hand function. The effect of thumb design on overall hand function is acknowledged in literature, however, there is no quantifiable and reliable evidence proving its importance. This approach quantifies and stresses the critical value of thumb design and proves it by quantification.

3.5 Tendon Structures

The human body uses tendons to transfer forces produced at muscles to the bones of the human skeleton. To describe the structures responsible for movement in the hand it is logical to separate the information into two sections: The tendons that

control the fingers and the tendons that control the thumb. The pathway of each tendon is specific to its function. The biomechanical approach used in this section describes the design of the tendon networks of the hand and the associated effect of tendon excursion.

3.5.1 Tendons of the Finger

The extensor tendon is responsible for extension, abduction and adduction in the fingers. There are two insertions for the extensor tendon: one on the distal phalanx and another on the intermediate phalanx (Red boxes in figure 20). At the second insertion the extensor splits. The main extensor is responsible for finger extension while the branches of the tendon provide abduction and adduction.

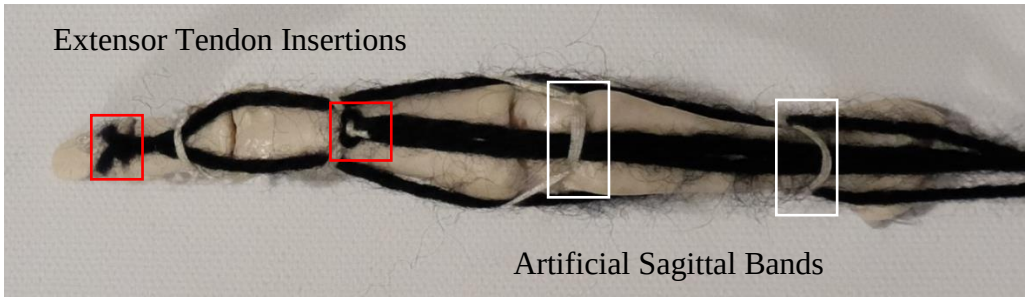

Figure 20: Dorsal view of the finger conveying the pathway and insertion points of the extensor tendons.

Artificial sagittal bands control the extensor tendon pathway (Figure 20, white boxes) and prevent transverse slipping of the tendon. The flexion of the fingers in the hand are actuated by the Flexor Digitorum Profundus (FDP) tendons. These tendons traverse the palmar side of the hand and insert at the distal phalanx of each finger. A pathway and supporting structure for each FDP are the annular ligaments (described in section 3.3.2) that are found at the head and base of each phalanx.

3.5.2 Tendons of the Thumb

The thumb is unique and complex in its movement, as such, it is essential to understand the basic anatomy and function of it in order to replicate it. There are four thumb tendons: The Abductor Pollicis Longus (APL), the Flexor Pollicis Longus (FPL), the Extensor Pollicis Brevis (EPB) and the Extensor Pollicis Longus (EPL). The following section describes the design and function of these tendons. The artificial FPL shown on the left hand side of figure 21 makes a path through the carpal tunnel towards the base of the distal phalanx of the thumb where it inserts. The APL shown on the right hand side of figure 21 inserts into the radial side of the base of the thumbs metacarpal via a second insertion located on the trapezium bone. The movement induced by this tendon is abduction of the thumb at the CMC joint.

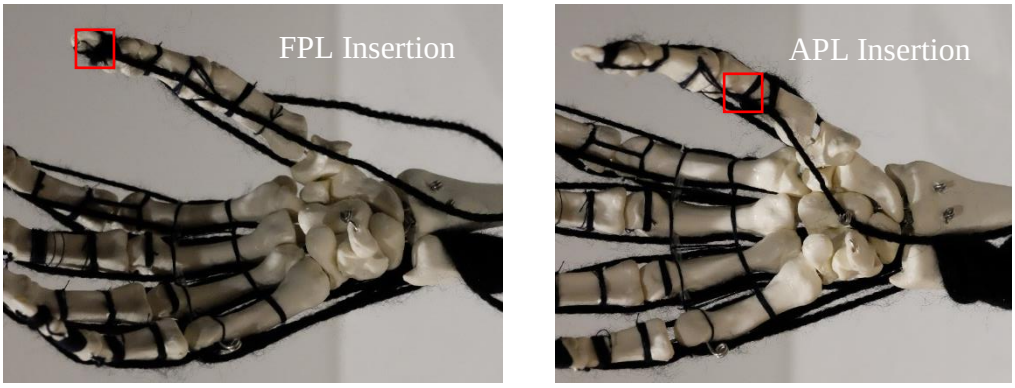

Figure 21: Palmar view of thumb with its artificial FPL and APL insertions.

The insertion points of the EPB and the EPL are shown in the red boxes of figure 22. The EPB inserts into the base of the first phalanx of the thumb. Displacement of the EPB generates extension and abduction of the thumb at the CMC joint. The EPL inserts at the distal phalanx of thumb. The EPL extends the thumb from the distal phalanx and is the only means whereby the thumb can fully extend.

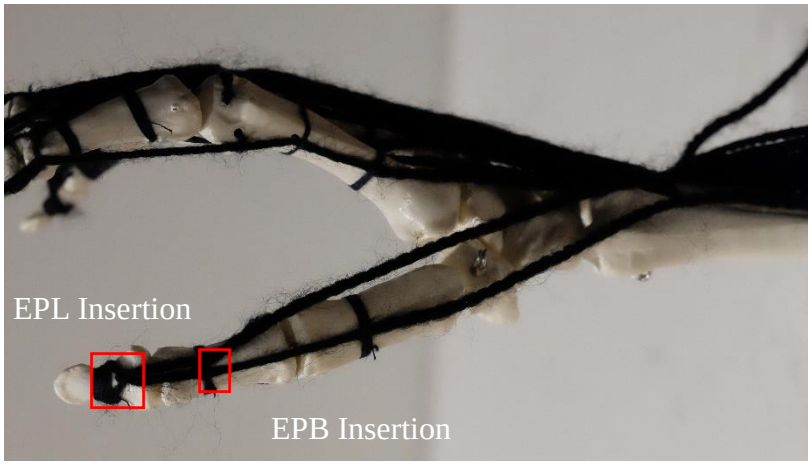

Figure 22: Rear view of thumb with its artificial EPL and EPB insertions.

A synergy between the tendons of the thumb provides complex movement including flexion, extension and circumduction.

3.5.3 Tendon Excursion

The use of tendons in artificial mechanical hands is a widely used approach, however, throughout literature there is little acknowledgement of the effect of tendon excursion on hand function. This section introduces the concept of tendon excursion. Tendon excursion is the displacement a tendon experiences when the associated muscle contracts and induces tensile forces on it. Tendon excursion is directly related to joint movement and in some cases, the excursion of one tendon effects neighbouring tendons.

For example, wrist movement induces tendon excursion on all the FDP tendons of the fingers. This can be seen in the natural flexion of the fingers during wrist extension and their natural extension during wrist flexion (Figure 23).

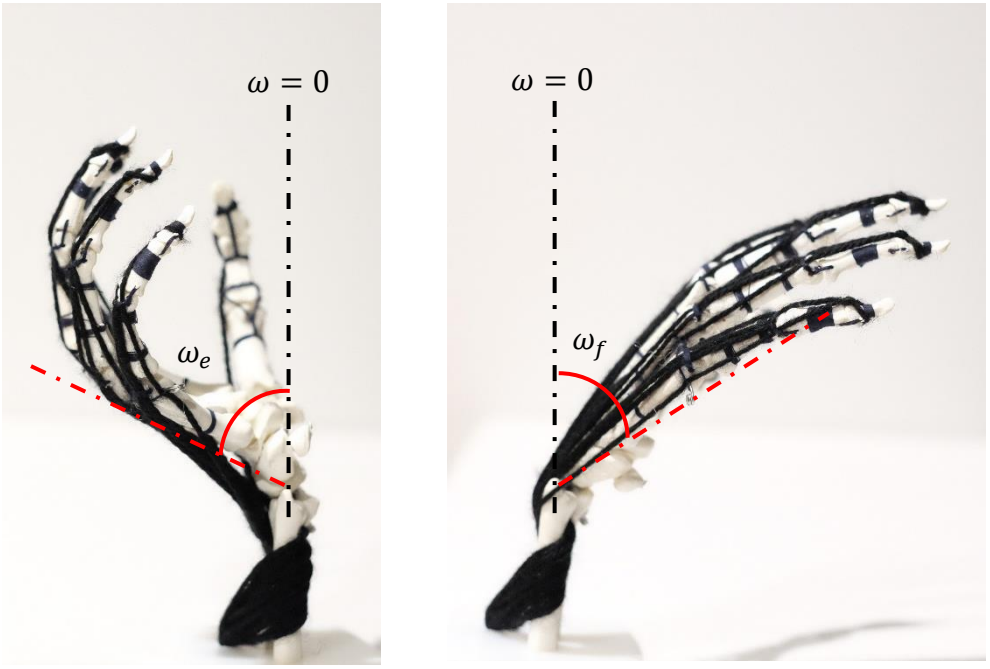

Figure 23: Tendon excursion in the FDP of each finger induced by wrist movement.

The angles ω_f and ω_e represent whether the wrist is in flexion or extension respectively. $\omega = 0$ is located vertically upward from the forearm bones and is measured from the pivot point of the wrist to the metacarpal creating the largest angle from the equilibrium point. Take the artificial FDP flexor tendon of each digit as an example. We can write a set of tendon displacements with respect to the wrist angle. Let, ω_f represent wrist flexion for any $\omega > 0$. We can write

$$\omega_f = \{d_{Fi}\ d_{Fm}\ d_{Fr}\ d_{Fl}\ d_{Ft}\} \tag{12}$$

Where, d is the displacement of the tendon in mm and the subscripts *i*, *m*, *r*, *l* and *t* are the index, middle, ring, little and thumb digits respectively. The subscript, F, represents the flexor tendon and in the case of the thumb, $d_{Ft} = \{\, d_{Ft1}\ \ d_{Ft2}\}$.

Where, $d_{Ft1}\ and\ d_{Ft2}$ mimic the APL and FPL (shown previously in figure 21) tendons respectively. By recording the displacements of the flexor tendons during wrist movement the effect of tendon excursion can be quantified. On average, the FDP tendon in each finger displaced by 11.6mm between the wrist angles ω_f^{max} and ω_e^{max}.

This excursion accounts for over half the amount of the FDP tendons complete movement. In the case of the thumb, the excursion was more prominent. This is particularly limiting to total hand function when considering the vital nature of the thumb in all hand grasping tasks. In either case, the amount of excursion-induced movement from the wrist on these tendons is too large to ignore. The source of displacement for each tendon stems from the servomotor actuating it, therefore, solutions can be found by adjusting the servomotor to account for the unwanted excursion. A servomotor correction factor can be implemented to adjust for the changing wrist angle. The correction factor is characterised by the angle that the servomotor actuating a digit is changed to meet equilibrium during wrist movement where $\omega \neq 0$. Using the relationship of tendon displacement e, with servomotor actuation we can write:

$$e = \left(\frac{\pi R}{180}\right) \times \varphi_i \tag{13}$$

Where, R is the servo horn radius and φ_i is the angle of the servo horn. By so doing, the servomotor angles for each digit can be plotted against the wrist angle, ω at any given time.

The excursion correction angles displayed in figure 24 shows how servomotor angles change with respect to wrist position.

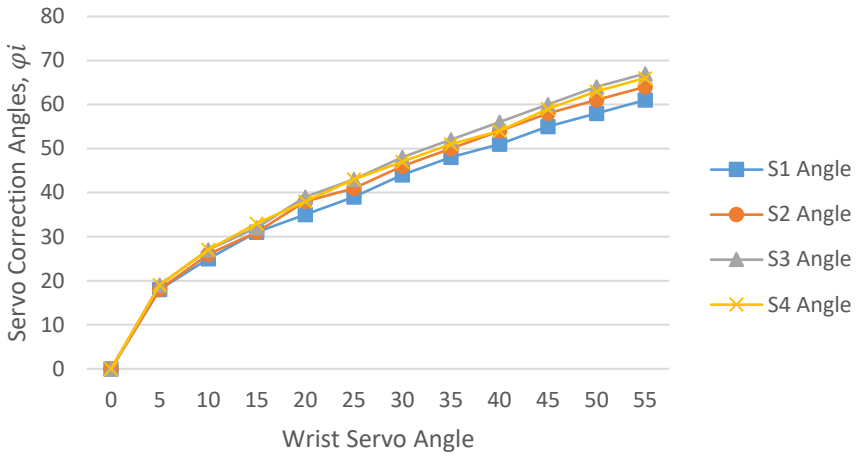

Figure 24: Servomotor correction angles for wrist movement induced tendon excursion in the fingers.

Including these types of correction tables into the control schemes of all electromechanical hands is trivial but important for hands incorporating fully articulated tendon driven wrists.

3.6 Defining Grasps

As described in section 3.5 the movement of the artificial hand is controlled by a set of artificial tendons. These tendons create tensile forces which, induce rotations about the joints of the digits. Tendon arrangements are listed below in Table 3.

Table 3: Tendon arrangement for finger actuation.

Digit	Tendon label *i*	Digit movement
Thumb	1 and 6	Tendon 1 is for flexion and extension Tendon 6 is for opposition and reposition
Index finger	2	Flexion and extension
Middle finger	3	Flexion and extension
Ring finger	4	Flexion and extension
Little finger	5	Flexion and extension

Establishing the tendon arrangement allows the calculation of tendon extension. Tendon extension is a measure of the displacement of the tendon as a function of the joint angles of the finger. The joint angles for each phalanx are shown in figure 25.

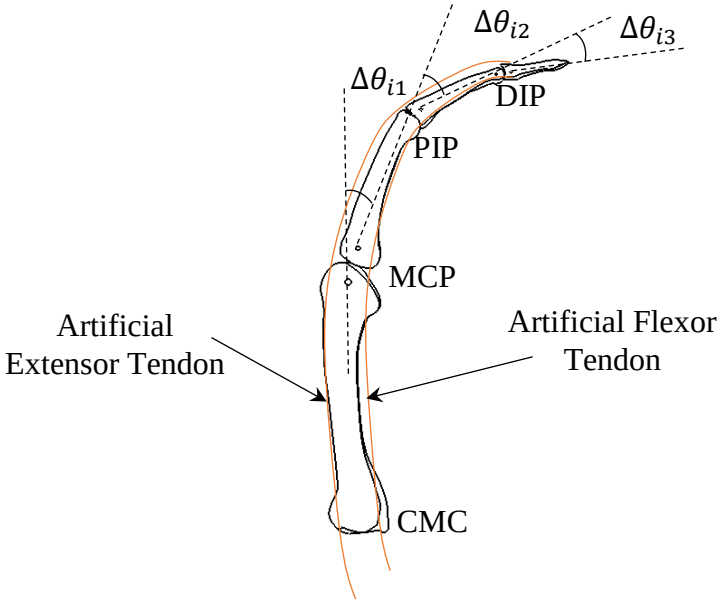

Figure 25: Prosthetic finger tendon network and the associated joint angles.

For simple tendon networks composed of 3 pulleys in a digit, the tendon extension, e_i, is a linear function of the change of the joint angles $\Delta\theta_{i1}, \Delta\theta_{i2}\ and\ \Delta\theta_{i3}$. Therefore, tendon extension can be expressed as

$$e_i = \sum_j r_{ij}\Delta\theta_{ij} \tag{14}$$

Where, r_{ij}, is the radius of the pulley at the j-th joint (j = 1, 2, 3 for $\forall i$ where $i = 1,2,\ldots,5$ and j = 1 for i = 6).

The force induced on the tendons by these extensions can be modelled to calculate fingertip forces and thus grasp strength. (Explanation of the fingertip force due to tendon tension is described in the appendix section A7). The tendons are connected to various servos to actuate digit movement. The prosthetic hand has six servomotors, one for each finger and two for the thumb. A grasp type in this context is defined as

$$\boldsymbol{\phi} = [\varphi_1\ \varphi_2\ \varphi_3\ \varphi_4\ \varphi_5\ \varphi_6\ c]^T \tag{15}$$

Where, $c = \begin{cases} 1, & \text{for force closure grasping} \\ 0, & \text{for form closure grasping} \end{cases}$

When φ_i $(\forall i)$ equals the pre-set maximum servomotor angle, φ_i^{max} the digit is in complete flexion. Otherwise, it is in complete extension (that is $\varphi_i = 0\ or\ \varphi_i^{min}$).

A physical representation of equation (13) is shown in the working principle of finger actuation. The working principle of finger actuation is displayed below in figure 26.

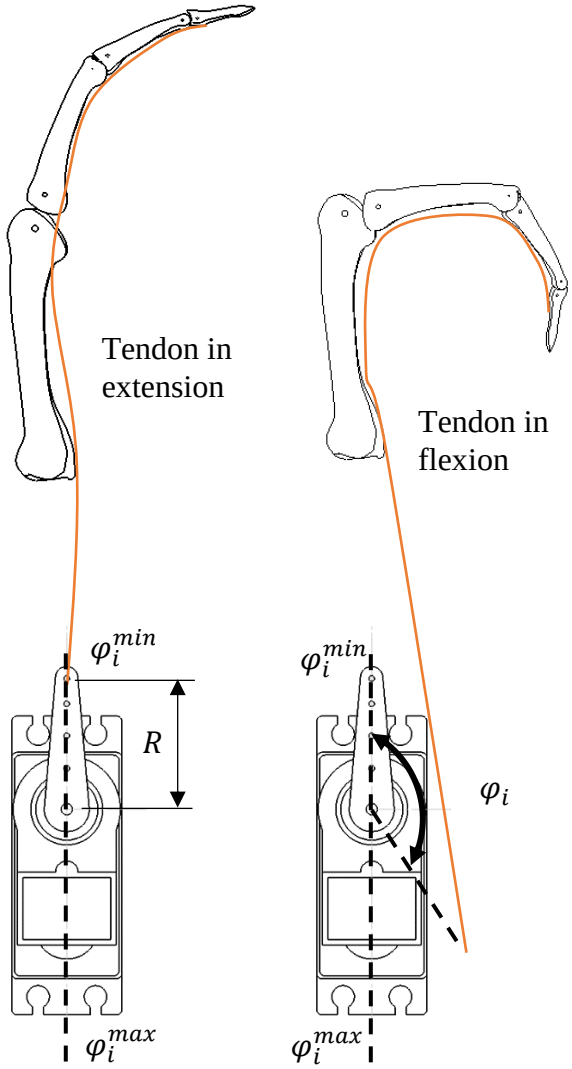

Figure 26: Digit extension and flexion due to the servomotor angle.

3.6.1 Resulting Grasps

Figure 27 shows some common grasp types and their definitions according to the rules established in the previous section: The first four grasps are chosen by their suitability to hold objects that are common in everyday environments. They are the: Palmar pinch, tripod grasp, power grasp sphere (3 finger) and power grasp.

Palmar pinch grasp

$\boldsymbol{\phi}= [\varphi_1\ \varphi_2\ \varphi_3^{max}\ \varphi_4^{max}\ \varphi_5^{max}\ \varphi_6\ 1]^T$

Tripod grasp

$\boldsymbol{\phi}= [\varphi_1\ \varphi_2\ \varphi_3\ \varphi_4^{max}\ \varphi_5^{max}\ \varphi_6\ 1]^T$

Power grasp sphere (3 Finger) grasp

$\boldsymbol{\phi}= [\varphi_1\ \varphi_2\ \varphi_3\ \varphi_4^{max}\ \varphi_5^{max}\ \varphi_6\ 0]^T$

Power sphere grasp

$\boldsymbol{\phi}= [\varphi_1\ \varphi_2\ \varphi_3\ \varphi_4\ \varphi_5\ \varphi_6\ 0]^T$

Figure 27: Various grasp types performed by the prosthetic hand and their definitions.

In the case of objects where one of its dimensions are much larger than the other a tip pinch grasp or a power grasp is appropriate (Figure 28).

Tip pinch grasp

$\boldsymbol{\phi} = [\varphi_1\ \varphi_2\ \varphi_3^{max}\ \varphi_4^{max}\ \varphi_5^{max}\ \varphi_6\ 1]^T$

Power grasp

$\boldsymbol{\phi} = [\varphi_1\ \varphi_2\ \varphi_3\ \varphi_4\ \varphi_5\ \varphi_6\ 1]^T$

Figure 28: Tip pinch grasp and power grasp examples and definitions.

The artificial hand and grasps described here are applied to the control frameworks in chapters 4 and 5.

3.7 Summary

This chapter has approached artificial hand design with the aim of restoring hand function through a biomechanical approach. The key ideas and concepts considered herein acknowledge the physiological and biological characteristics of the human hand that are generally ignored by traditional mechanical engineering and robotics. The quantification of thumb orientation is crucial to hand function because it accounts for more than half of the function of the human hand. Joint stabilization and overcoming tendon excursion are a testament to this biomechanical approach improving the function of artificial hands. Human like dexterity and function increases as biomechanical approaches to mimic the human hand become

popularized. The hypothesis stated at the beginning of the chapter stands, because each concept explored has contributed to improving artificial hand design in one way or another. The following chapter approaches the restoration of hand function through the mimicking of the brain. In particular, the brain function associated with motor movement of the hand. The artificial hand described in this chapter is used as the testbed for investigating the potential of the non-invasive NI's in chapter 4. Chapter 4 is comprised of ideas stemming from the combination of Mātauranga Māori and western science, therefore, the introduction to chapter 4 is followed by an explanation of how each knowledge base is related and complimentary to each other.

Chapter 4

Neural Interfaces for Artificial Hand Control

4.1 Background

As stated, the realisation of the artificial hand developed in chapter 3 is preliminary to and foundational for the development of the Neural Interface (NI) developed in this chapter. This chapter aims to restore hand function by mimicking the human grasping system through the interpretation of non-invasive brain signals. This will be achieved by the implementation of a Support Vector Machine (SVM) for artificial hand control. The hypothesis to be tested is: that by implementing a SVM as the machine learning method for a NI based artificial hand control framework, multiple classifications in real time are feasible. As established in the review of literature, the lack of accuracy, slow response time and sustained control of non-invasive EEG based NI's limit and prevent the technology from entering the market. The main outcome of this chapter is a conventional machine learning based NI approach that improves upon the classification accuracy and response of current NI's. As eluded to and as explained by the overarching research idea there are underlying principles that found and base every approach taken in this work. These principles are rooted firmly in the heritage and history of the Māori people. One such principle is the acknowledgement and understanding of Mauri. Mauri is the underlying principle that encompasses the life force, essence and nature of all living things. The following section describes the preservation of mauri through raranga. The tikanga of raranga is described and its foundational relationship with NI development is stated.

4.1.1 Mātauranga Māori: Raranga

Raranga is the art of weaving used in practical and communicative applications. The importance of raranga to Māori is foundationally important as Māori revere human life and, therefore, priority is given to the preservation and protection of life (Te Kanawa 2018). Raranga is the vessel vital in fulfilling these basic needs of human wellbeing through providing sustenance, clothing and shelter (Nopera 2018). Therefore, tikanga (custom, ethic, protocol and practice) was observed throughout the process of raranga, to preserve the mauri of raranga, to maintain balance, harmony and wellbeing. The tikanga of raranga is the foundation of the approach presented in this chapter. Preliminary to raranga is the preservation of mauri through recognition of Papatūānuku. Papatūānuku is the land, which gives birth to all things. By recognising the land, we understand the significance of our actions on the environment. The initial preservation of mauri through tikanga is accomplished through whakataukī (proverbial sayings), waiata (songs) and karakia (ritual prayers). The following whakataukī describes the holistic approach required for raranga.

Hutia te rito	Pull out the centre shoot
O te harakeke	of the flax bush
Kei whea, te kōmako e kō?	Where will the bellbird alight to sing?
Kī mai ki ahau	If I was asked
He aha te mea nui	What is the greatest thing
O tenei ao?	in this world?
Māku e kī atu	I would be compelled to reply,
He tāngata, he tāngata, he tāngata.	It is people! It is people! It is people!

The whakataukī emphasises the importance of people in the cycle of life, it recognises the reliance of humans on nature and states the guardianship or responsibility of humans towards the natural environment.

4.1.1.1 Ngā Tikanga Whakahaere: Principle Stages of Process

Mēnā ka tika te aho tapu, ka oti pai te kaupapa

Only if the vision is correct, will the work be successfully completed.

Raranga begins with te aho tapu (vision). The vision encompasses the desires of the weaver and the purpose of undertaking raranga. Once the vision is established karakia and waiata begin the processes of Hauhake (harvesting), Whakarite (preparation), Raranga (process of weaving) and Whakatutuki (completion/return).

4.1.1.2 Hauhake

Hauhake is determined by many factors. Hauhake considers the type of plant required, the properties of the plant, its location and its proper handling. These considerations are subject to the seasons, cycles of weather, distance from the equator and soil types. Each consideration prepares and sets a foundation for the proceeding steps of Whakarite and Raranga. The processes of Hauhake are foundational and analogous to the approaches used within this work. NI design considers the location, handling and type of signals required. In essence, just as plants contain and store information through its physical characteristics so do the physiological signals emitted from the brain. The information carried relates to the condition of the signal, its history, its acquisition location and how it has been handled. Hauhake is directly related to the acquisition of physiological signals from the human body. Mauri is preserved in hauhake through the taking of branches that ensure the well-being and survival the plant. So it is with brain signal acquisition, the head is sacred and needs to be treated in such a way that preserves the dignity and Mauri of the person. For this reason, no invasive methods are used, the sanctity of the head is maintained and the Mauri of the person is respected in a way where the acquiring of brain signals is returned to them through the restoration of hand function.

4.1.1.3 Whakarite

Whakarite is preparing the material for working. Preparation includes toetoe (the splitting), hāpine (the scraping), koropupū (the boiling) and whakamaroke (the drying). Each process contributes to the final product and is integral in the overall process of raranga. Each step is specific in its function and cannot be overlooked. Whakarite is analogous to the pre-processing of physiological signals.

4.1.1.4 Raranga

Raranga is the working of the material. A pattern of work is established and the material is manipulated according to the pattern. When completed the material is considered to hold the same knowledge of its origin but has the flexibility to change forms. This process is equivalent to machine learning algorithms and the process of establishing patterns.

4.1.1.5 Whakatutuki

Once the woven item has fulfilled its purpose, the mauri of the item is preserved through the principle of Utu (reciprocity) an understanding epitomised in the whakataukī which states: ‘whenua ki te whenua’ (that born of the land shall return to the land). This in essence means that the item and its life force born of Papatūānuku, must be returned back to Papatūānuku, to continue the cycle of life. The tikanga of raranga is a process that is of the same kind to the design of NI’s. The process and ideas in each knowledge base are analogous, however, the underlying principles are considerably different. With the greatest difference being the preservation of mauri. The following section describes the design of a NI that is based on the principles underlying raranga.

4.2 Framework for a SVM Based Non-invasive EEG Neural Interface

The classification accuracy of a SVM to handle EEG signals generated by motor and imagery tasks consists of four components: the EPOC+ EEG signal acquisition device (Emotiv 2019), a computer, the electromechanical hand and the Arduino Uno microcontroller. The components make up the control framework of the SVM based NI (Figure 29).

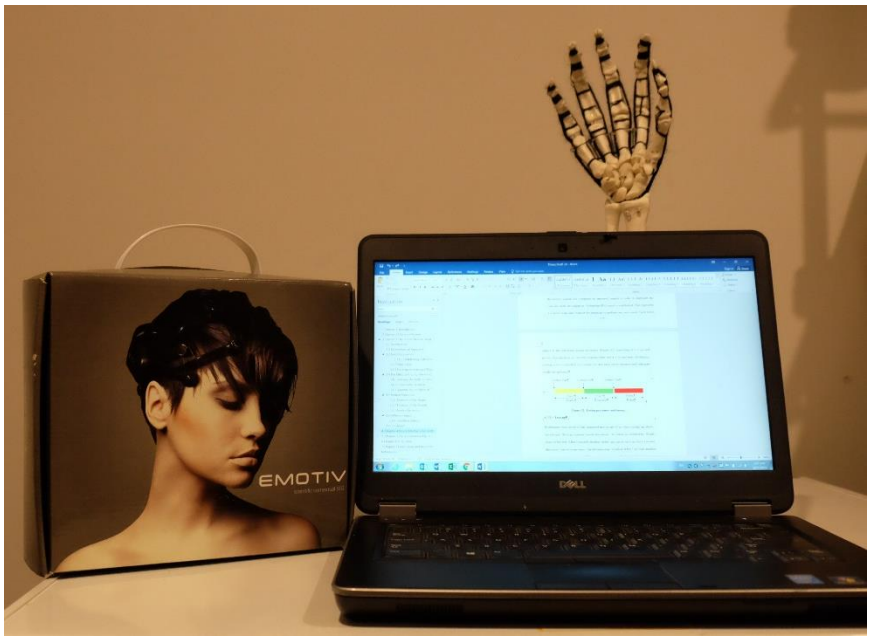

Figure 29: Components of offline experimentation for SVM application of grasping tasks.

These components act as a base for the process flow of the control framework shown below in figure 30.

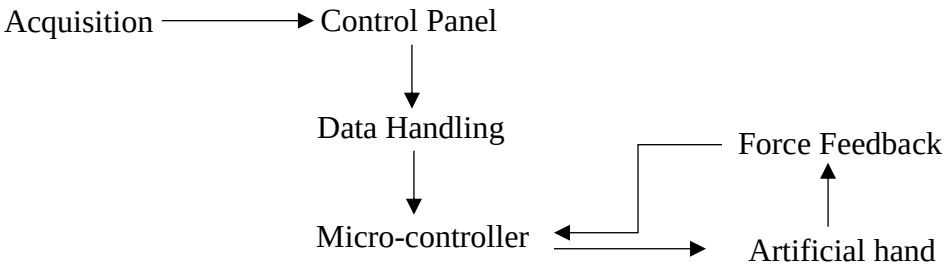

Figure 30: SVM control framework.

The control panel is broken down further (Figure 31) to explain the process of classification including pre-processing.

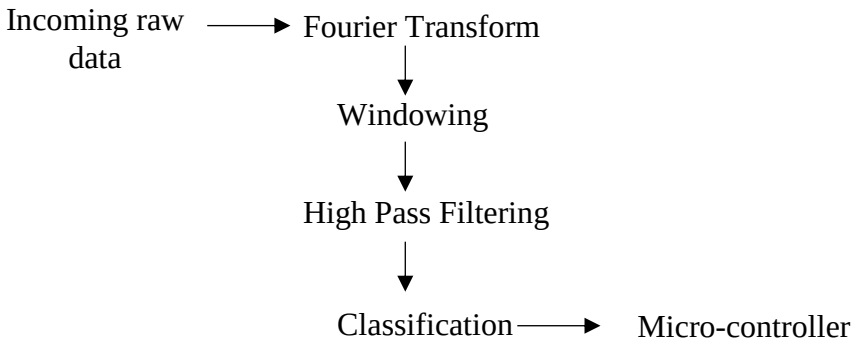

Figure 31: Control panel of the SVM control framework.

The investigation tests the response time and the accuracy of the SVM classification for prosthetic hand grasping applications. There are two considerations that contribute to the restoration of hand function:

1- The speed at which it responds to a user (response).

2- The accuracy with which it classifies user input.

Using the SVM in a NI necessitates the testing of these two considerations. Real time testing ensures the NI can perform with adequate speed and accuracy.

4.2.1 Equipment

The fourteen channel wireless non-invasive EEG acquisition headset EPOC+ by Emotiv allows real time access to raw EEG data. The headset communicates via Bluetooth where the data can be displayed in real time. Good connection quality is required and is dependent upon a number of factors including: sensor preparation, sensor placement, environmental interruption and user proficiency. The data is recorded as .edf and can be converted into .csv format for further offline processing. The Arduino Uno is responsible for the processing and control of the data flow (DFRobot 2019).

4.2.2 Signal Processing

The data handling and communication protocol involves the transformation of data into the frequency domain, windowing and filtering in real time. The Hanning window used in testing is defined as

$$w_n = \frac{1}{2}\left(1 - cos\left(\frac{2\pi n}{N-1}\right)\right) \tag{16}$$

Where N represents the samples of a discrete-time symmetrical function w_n, where, $0 \leq n \leq N-1$. The advantage of using a Hanning window is low aliasing and the prevention of power leakage, however, this comes at the expense of spatial resolution. The nature of the data means a DC offset is present in the signal and requires removal. The removal of the offset introduces unwanted low frequency noise in the signal. This noise is eliminated by a high pass filter.

The EEG signal x_n $(n = 1, 2, \dots, N)$ is applied to the Fourier transform with the window function such that

$$X_k = \sum_{n=1}^{N} x_n \,.\, w_n . e^{-jw_k n} \tag{17}$$

Where,

w_n, is the window function,

X_n, is the value of the signal at time, n,

$w_k = \frac{2\pi}{N} k$, where,k is the frequency $k = 1, 2, \dots, N$,

X_k, is the amount of frequency,k present in the sample, and

$j = \sqrt{-1}$.

The culmination of these signal pre-processing techniques prepares the data for analysis in the SVM. The data is manipulated and prepared to fit the requirements of the SVM. (Code supplied, appendix A8)

4.2.3 Classification

The basic principle of a SVM is that a separating hyperplane can be determined to differentiate between two distinct classes of data (Cortes and Vapnik 1995). Therefore, an approach consisting of two classes separated by a hyperplane is established.

The hyperplane is defined using two labelled training sets of m signals:

$$S_\alpha = \{(x_i, 1) | x_i \epsilon R^d\}, i = 1,2, \dots, m \tag{18}$$

$$S_\beta = \{(x_i, -1) | x_i \epsilon R^d\}, i = 1,2, \dots, m \quad (19)$$

Where (x_i, y_i) is a training set with, $\forall i$ and $x_i \in R^d$ and $y_i \in \{1, -1\}$

The set of training signals $S_{\alpha,\beta}$ can be defined as

$$S_{\alpha,\beta} = \left\{x_i, y_i | x_i \in R^d, \begin{Bmatrix} y_i \in 1 \; if \; x_i \in S_\alpha \\ y_i \in -1 \; if \; x_i \in S_\beta \end{Bmatrix}\right\}, \forall m \quad (20)$$

For linearly separable data, a hyperplane is optimised to separate the data with the largest possible margin (The optimisation of this margin is given in the appendix section A9). In cases where classifications are non-linear the data is mapped onto a higher dimensional signal space using

$$\phi: x_i \in R^d \rightarrow \phi(x_i) \in R^{d'}, (d' > d) \quad (21)$$

Therefore, training can be expressed as the maximisation of

$$L_D = \sum_{i=1}^{m} \lambda_i - \frac{1}{2} \sum_{i,j=1}^{m} \lambda_i . \lambda_j . y_i . y_j . x_i . x_j \quad (22)$$

Where, λ, are Lagrange multipliers found by solving the quadratic optimization problem (presented in the appendix, section A9). By introducing a kernel function we can extend the classification to non-linearly separable classifications. The kernel computes the inner product of two mapped signals by

$$K(x_i, x_j) = \varphi(x_i)\varphi(x_j) = x_i . x_j \quad (23)$$

Where, $K(x_i, x_j)$ is the Gaussian kernel function.

The Gaussian kernel function is defined as

$$K(x_i, x_j) = exp\left(\frac{-\|x_i - x_j\|^2}{2\sigma^2}\right) \quad (24)$$

Combining equations (24) and (22) through (23) we now establish training of the classifier as the maximisation of

$$L_D = \sum_{i=1}^{m} \lambda_i - \frac{1}{2} \sum_{i,j=1}^{m} \lambda_i . \lambda_j . y_i . y_j . K(x_i, x_j) \quad (25)$$

Under the conditions where, $\lambda_i \geq 0, \forall i$ and $\sum_{i=1}^{m} \lambda_i y_i = 0. \, 0 \leq \lambda_i \leq C \;\; \forall i,$ where C is the penalty weight. Finally, the classification outcome of a signal x is calculated by a decision function expressed as

$$f_{\alpha,\beta}(x) = \sum_{i=1}^{m} \lambda_i y_i \, K(x_i, x) + b \quad (26)$$

Where, b, is a bias. The signal, x, is classified as the same class if $f_{\alpha,\beta}(x) > 0$ otherwise it belongs to the other class. In the case of multiple classifications it is possible to establish a number of separating hyperplanes.

4.3 Experimental Procedure

There are three tests designed to investigate the response and accuracy of the SVM. Each test focusses on classifications in isolation and in combination. In some cases the trained signals are compared to untrained signals in order to highlight the outcome of the investigation. A baseline EEG signal is established. This represents a relaxed brain state without the intention to perform any movement. Each test is

subject to the following testing procedure (Figure 32) consisting of a 2 second period of preparation, a 5 second response time and a 3 second time of relaxing. Each period is controlled by a verbal cue and each test is repeated until adequate results are gathered.

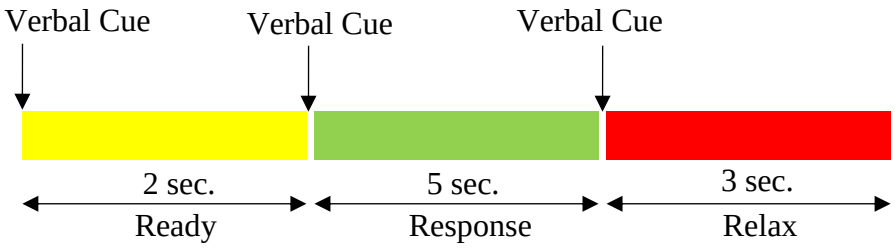

Figure 32: Testing procedure and timing.

4.3.1 Testing

Preliminary tests involved the imagined movement of an object going up, down, left or right. These are termed "mental directions". A verbal cue initiated the 'Ready' phase of the test. After 2 seconds another verbal cue was given to produce a mental direction. Correct or incorrect classification was recorded. After 5 seconds another verbal cue is given to relax. The testing is repeated for each mental direction. Following the preliminary testing, the classification and response were tested by "Isolation and Combined Testing of Grasps for Classification Accuracy"(section 4.3.1.1) and "Combined Testing of Grasps for Response with and without Training"(section 4.3.1.2). The following sections are descriptive of what these tests entailed.

4.3.1.1 Isolation and Combined Testing of the SVM's Accuracy

The testing procedure is repeated, however, this time it is done with the following grasps: power grasp, key grasp, pinch grasp and ball grasp (Figure 33).

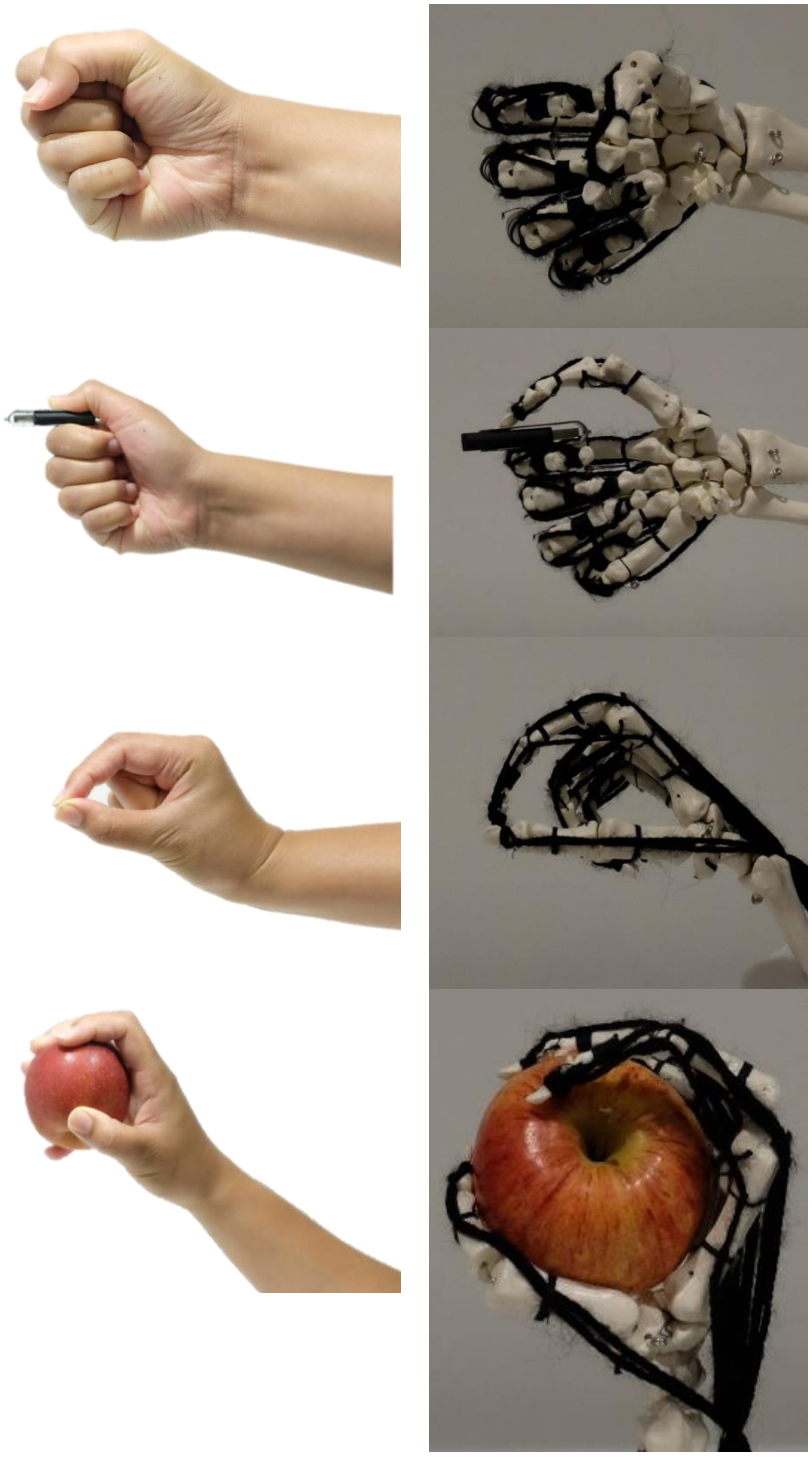

Figure 33: The four grasps to be trained in the SVM.

The results are recorded in isolation and in combination for every test. The definitions of isolation and combination are given below.

- Isolation means that only the relaxed signal and the chosen signal are considered in the classification (binary classification).
- Combined means that the classification considers all involved signals. In this case, any number of signals between one and four.

Combined testing is accomplished by sequentially adding signals and recording the classification accuracy as the number of signals to classify increase. The verbal cues indicate what grasp is to be produced.

4.3.1.2 Combined Testing of Grasps for Response of the SVM with and without Training

The response of the SVM is tested. The time taken from the verbal cue to perform a mental command to the time the SVM recognises the command is recorded for both trained and untrained grasping signals. The difference between trained and untrained grasping signals are described:

1- Trained signals are taught to the SVM with enough trials to make the SVM confident in successfully classifying a signal consistently.
2- Untrained signals are taught to the SVM with one single trial.

This test is performed under the same testing procedure as the previous tests, however, rather than recording accuracy, the response time is recorded. This is accomplished by sequentially adding signals and recording how long it takes for the SVM to respond to the verbal cue given. The increase in response is measured as the number of signals to classify are increased. (This test is repeated for trained and untrained signals.)

4.4 Results

The results focus on the response time and the accuracy of the SVM based NI. The response of the NI is the time taken from the given verbal cue to the first movement of the artificial hand to perform a grasp. This is the least amount of time needed to start actuating the artificial hand and is, therefore, a sensible definition for response time. The accuracy of the NI is how precise the classification is in interpreting user intent.

4.4.1 Response

The comparison of response times between the trained and untrained signals are indicated by the blue and orange lines of figure 34.

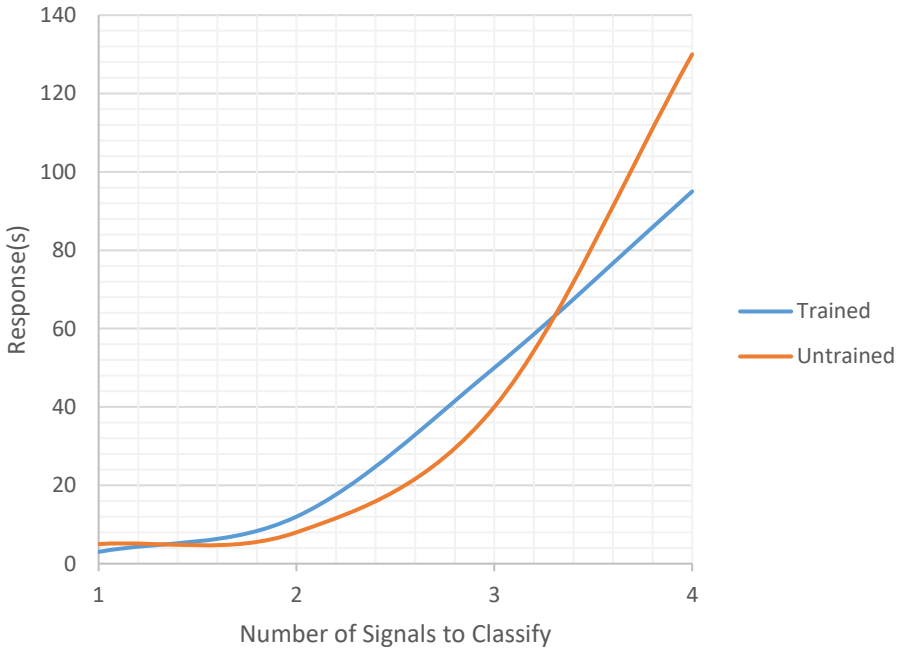

Figure 34: Classification response times for trained and untrained signals.

In the case of classification between the first signal and the baseline signal the SVM would differentiate between the two signals and respond within 5 seconds. The difference in response time as the number of signals increase is due to the loss of

confidence of the SVM to correctly classify signals. It is interesting to note the dramatic effect training has on the response time as the number of signals classified increased. The relationship was linear indicating that the effect of training each signal is consistently effective for up to four classifications. On the other hand untrained signals produced an exponential growth in time as the number of classifications increased. This result suggests that with training, a better response time for each signal would increase the likelihood of it being useful in application. However, response times that are too long are not feasible in application. Therefore, with respect to reasonable timing, the limit of the SVM is two classifications in real time with the possibility of a third (this would involve extensive training). These results are enlightening and show the extent to which the SVM can respond with multiple classifications.

4.4.2 Accuracy

The classification accuracy measures how well the SVM predicts what signal is being given. Preliminary testing produced promising results when considering the ‘mental directions’. Testing the grasps in isolation produced a considerable drop in classification accuracy. Figure 35 demonstrates the effectiveness of the SVM in classifying grasping tasks (in combination and isolation) and mental directions.

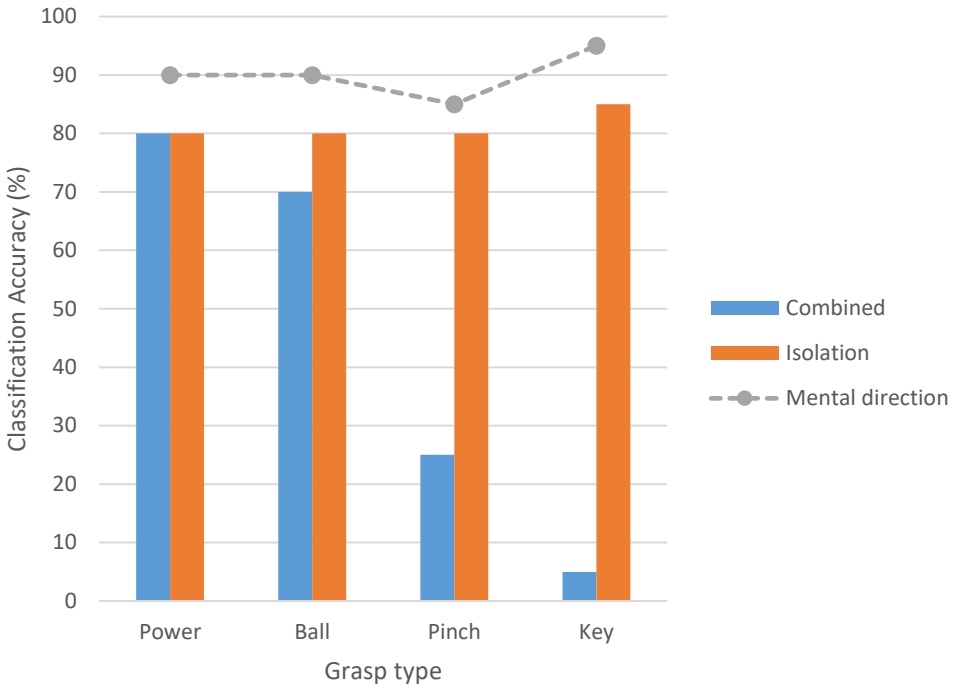

Figure 35: Classification reliability of mental directions, isolated grasp intention and combined grasp intention.

The difference in the isolation classification (established in section 4.3.1.1) and the mental direction classification (established in 4.3.1) shows a consistently less accurate outcome (as expected). It is clear from the results that classifying 'mental directions' and thoughts/intents to act ('combined' and 'isolation') are substantially different as shown by the difference between the grey line and the bar graphs of figure 35. The results suggest that multiple classifications are possible in in real time (this is without consideration to the response time) but are accompanied by serious limitations. As the number of grasp types increased the systems' ability to accurately classify dramatically decreased. This is shown by the 'combined' results which show a drastic decrease in accuracy as the number of signals increased. The SVM performed adequately having to differentiate between the baseline, power and ball grasps. When more than this was added, the system became slow and would not perform well. This outcome suggests the most effective number of outputs from

the SVM is two with a possibility of three based on the requirement of extensive training. Testing reinforced the strengths of using a SVM in such conditions and proved that the SVM based NI is credible to use in artificial hand control.

These results show that multiple classifications in real time are credible, but severely limited because of this there is little benefit to going beyond binary classifications for NI applications in the current technological climate. This claim is discussed more completely in chapter 6. The potential of implementing a SVM as the machine learning method for a NI is exciting because of its ability to classify multiple movements in real time. However, its effectiveness is limited. Additional and/or alternate approaches are required to improve NI's beyond what they are currently capable of. The most intriguing approach to solving this issue is to have the grasp classification responsibility moved to autonomous vision. This would allow the SVM to accurately interpret user intent for open and close classifications.

4.4.3 Relevance

The response and accuracy of the SVM based NI is enlightening, however, as observed from the many attempts in literature to interpret the non-invasive EEG signal it is important to know how it compares with other approaches. By comparing the SVM approach with other machine learning methods we can substantiate the significance of the results and justify the use of SVM's for the control of artificial hands. Three other machine learning methods are chosen to compare against the SVM:

1- Generalized Linear Model based Regression (GLM),

2- A Gaussian Process Regression Model (GPRM), and

3- Binary Decision Tree based regression (BDTR).

A publicly available Grasp and Lift EEG dataset by Luciw, Ewa et al. (2014) is used to test what machine learning method best interprets hand movement from EEG data. The purpose of this analysis is to determine which method performs the best in determining hand movement. The expected output for each model is binary where hand movement or lack of hand movement is determined. The data set contained Electromyography (EMG) signals which, confirms whether hand movement has occurred or not. Figure 36 shows the response of the SVM. The red line is actual hand movement (determined by the EMG data) and the blue line is the approximated hand movement (determined by EEG data).

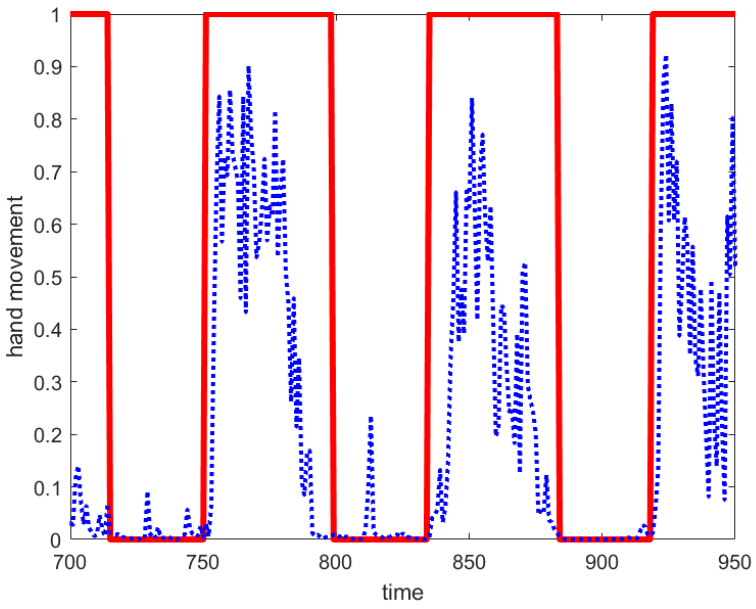

Figure 36: The SVM based interpretation of hand movement through EEG (blue) and EMG (red) data. (Horizontal axis is in seconds).

The analysis was performed for each machine learning method. By calculating the area under the curve, all machine learning methods received a rank. The results are clearly seen in figure 37 where the area under the curve is plotted against the machine learning method for each participant.

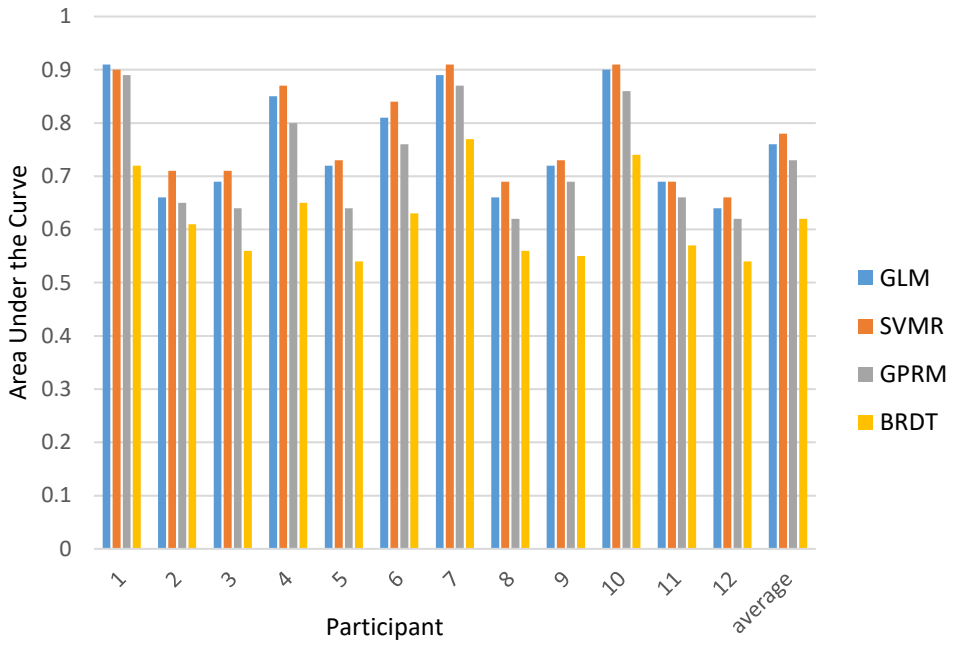

Figure 37: Average area under the curve of all sessions for each participant.

According to the analysis, both the GLM and SVM based machine learning methods show the best approximation of hand movement. The results shown here indicate that SVM based regression performed the best with a score of 0.78. This justifies and reinforces the suitability of SVM based NI's for artificial hand control. For clarity, the Artificial Neural Network (ANN) is omitted from the analysis and subsequent investigations. This decision and approach is backed by many researchers who conclude and provide evidence that deep learning methods (based on ANN's) do not show convincing results that they outperform current approaches (Alomari, Samaha et al. 2013, Elstob and Secco 2016, Lotte, Bougrain et al. 2018).

4.5 Summary

This chapter has dealt with the development of a SVM based EEG NI. The approach taken meets the aim of the chapter to interpret brain signals and restore hand function through a non-invasive EEG based NI. The reliability and response of the SVM based NI is elucidating, showing the strengths and limitations of its application. The SVM is justified as an adequate machine learning method for binary artificial hand control. The hypothesis stated at the beginning of the chapter stands, to a degree. The SVM performed multiple classifications in real time, however, it does so under certain conditions and limitations. The main limitations are:

1- The loss in classification accuracy as the number of signals to classify increases, and
2- The considerable increase in response time as the number of classes to classify increases.

These limitations provide understanding as to why the progress of such systems are limited and justify this works claim that there is little reward for using machine learning based NI's beyond binary (open/close) tasks. For these reasons, chapter 5 investigates and explains the option of improving the SVM based NI by the addition of sensors and autonomous robotic principles.

Chapter 5

The Autonomous Neural Interface

5.1 Background

The previous chapter provided insight to the limitations of SVM approaches towards NI's for artificial hand control and explained why additional approaches are required in the development of NI based control frameworks. Put simply, machine learning based approaches perform best when applied to binary applications in the real world. The aim of this chapter is to explore the potential of combining autonomous machine vision with the non-invasive NI of chapter 4. This aim is achieved by creating a perception of the artificial hands surroundings and applying a control framework for it to work within that environment. The hypothesis to be tested is: That by observing the environment the artificial hand is subject to, its grasping function and response can be improved considerably.

Some key issues with machine learning based NI in general is that they are not accurate and have slow responses in real time. An autonomous approach in conjunction with machine learning based NI's has the potential to restore hand function in a new and inspired way that is responsive and accurate. This idea must not be confused with vision based grasping in automation lines for factory machines. The two ideas are significantly different due to the level of human interaction required for a prosthetic hand to be controlled. Automation lines are set and require little to no human involvement whereas, this research requires a constant human input requiring the system to adapt and change to human produced input. This chapter advances the state of the art by integrating autonomous robotic principles

with a non-invasive NI. The artificial hand of chapter 3 is used to verify the applicability of the autonomous framework. The framework of the autonomous approach is underpinned by Mātauranga Maori, therefore, the chapter begins with an explanation of the underlying principles supporting this approach.

5.1.1 Mātauranga Māori: Waikato Awa

Waikato taniwha rau, he piko he taniwha, he piko he taniwha

Waikato of a hundred chiefs, at every bend a taniwha (chief)

Flowing through a healthy portion of the north island of Aotearoa is the Waikato awa (Waikato river) (Council 2019). The awa is considered a taonga (treasure), tupuna (ancestor) and the mauri of the Tainui and Ngāti Tūwharetoa tribes. In times past, my own ancestors used the river in its entirety, with the awa providing and sustaining spiritual and material needs. Its rere (flow) provides life, food, cleansing and healing. By observing the flow and temperature of the awa my ancestors could determine the health and condition of it. By observing the state and movement of the river, different conditions became expected. Each condition implied different living conditions. For example, weather cycles determined the availability of fish and, therefore, the type of tools for food preparation.

The simple tikanga principles of kitea (observation), whakamahere (planning) and whakahaere (management) determined the condition of the tāngata (people). In some instances, the awa was influenced by the tāngata for their benefit. In the same way my ancestors employed these principles I have approached the design of an autonomous NI to control an artificial hand. The principles of kitea, whakamahere and whakahaere are conveyed in English as perception, planning and control throughout the chapter. The rere or flow of the river is used to describe the mimicry of innervation. The main outcome of this chapter is the development of an autonomous NI framework that is responsive and accurate.

5.2 The Autonomous Framework

The working principle of autonomous robotic systems is based on the control, planning and perception of the system. At the heart of this framework is the SVM based NI described in chapter 4. In order to integrate the SVM based NI with autonomous principles, the classification of the NI will be reduced to a binary user input (open/close). The artificial hand (Figure 38) is embedded with sensors to acquire information from the environment. The acquired information is used to perform grasping tasks. The position of the camera and sensor are justified by the co-ordinate system chosen later in this chapter. The perception is built around the chosen co-ordinate frame. It is acknowledged that the camera position may affect the grasping of objects but for this research it fulfils its purpose adequately.

Figure 38: The autonomous hand testbed with webcam (Logitech 2019) and infra-red sensor (Components 2019).

From the limited literature available of autonomous artificial hands there is one particular approach presented by Dosen and Popovic (2011) that is worthy of note. The reason why this approach is pinpointed is because it does not limit itself to a database of known objects like the other approaches mentioned in chapter 2. With this in mind it stands to reason that with sufficient work the approach can potentially work in any environment. In order to convey the autonomous framework presented herein the perception, planning and control of the framework needs describing. This section will describe the framework and its working principles. Sensor information builds a perception that determines how objects in the environment are to be grasped. When the input signal from the user (open/close) is received, the control of the prosthetic hand issues corresponding command signals to drive the prosthetic hand. With this approach, the hand can adapt to the geometry and size of an object before grasping and interaction occurs. By using information from vison-based sensors the process to recognise and classify objects is simplified. Figure 39 shows the control, planning and perception of the autonomous hand framework.

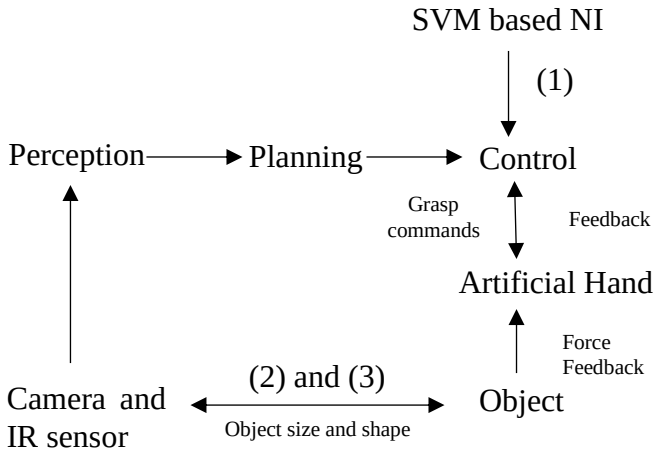

Figure 39: The autonomous hand framework.

There are three signals constituting the information flow of the autonomous framework as indicated by (1), (2) and (3) in figure 39:

1- Binary classification by the SVM based NI to control whether the hand is to perform a grasp or not (Established in chapter 4).
2- The object distance signal determined by the infrared sensor.
3- The object recognition signal determined by the webcam.

These signals and their interactions with the artificial hand are shown in figure 40.

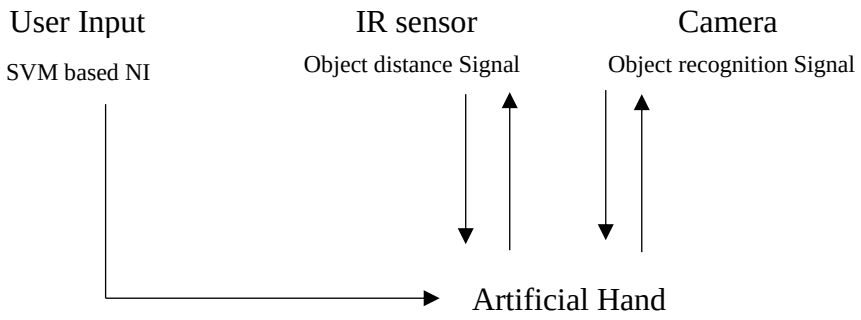

Figure 40: Information flow of the autonomous hand framework.

The SVM based NI is combined with the autonomous framework and is responsible for the binary classification required to either close or open the hand. The object distance signal is a determination of the distance between the hand and the object. The object recognition signal provides the micro-controller with information relating to object geometry and size. This approach mimics the human process of grasping an object in a way that is human-like. Implementation of the autonomous hand framework involves six sets of hardware: a signal acquisition device, a webcam, an infrared sensor, microprocessors, a computer and the artificial hand. The following sections describe the approach taken by explaining the perception, planning and control (as shown previously in figure 39) of the autonomous hand framework.

5.2.1 Perception

The object characteristics extracted from the object image and its distance from the camera make up the perception of the system. The grasping region of the object and the orientation of the prosthetic hand relative to the object for grasp execution is determined by the information gathered by the webcam and infrared sensor. The webcam installed in the palm of the prosthetic hand captures the image which, determines the size and shape of the object. The infrared sensor calculates the distance between the object and the artificial hand. Two parameters are used to define the information extracted from the image captured by the webcam: The minimum dimension, d and the aspect ratio, r. The minimum dimension is the smallest dimension of the bounding rectangle and the aspect ratio is a ratio of the maximum dimension to the minimum dimension of the bounding rectangle. These two parameters characterize the object size and shape. The requirement of the bounding rectangle is that it must be quick to process information so as not to prolong the response of the control framework. This is accomplished by reducing the non-essential object measurement accuracy of the webcam. Therefore, speed is prioritised at the expense of object measurement accuracy. As an example the size and shape characteristics of four objects are extracted. The objects chosen include: a cube, a cell phone, a tennis ball and a servomotor. The cube and cell phone are depicted with their bounding rectangles in figure 41 while the tennis ball and servomotor are shown in figure 42.

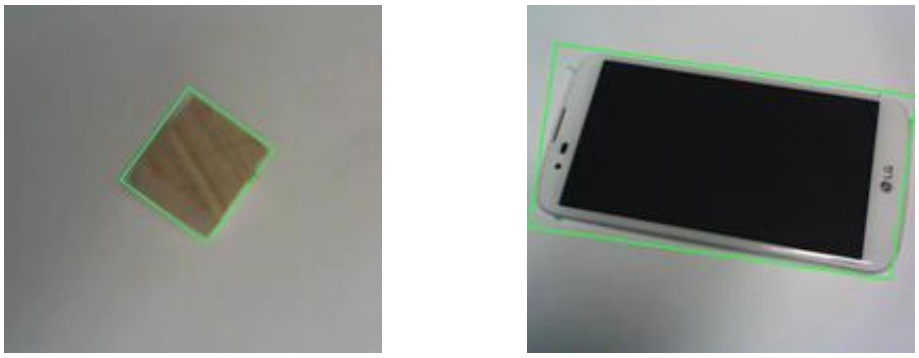

Figure 41: Object characteristics with different shape and different aspect ratio.

The aspect ratio of a small cube is 1 while that of a cell phone is 1.93. The minimum dimension of the cube is 28 mm. The minimum dimension of the cell phone is 75 mm.

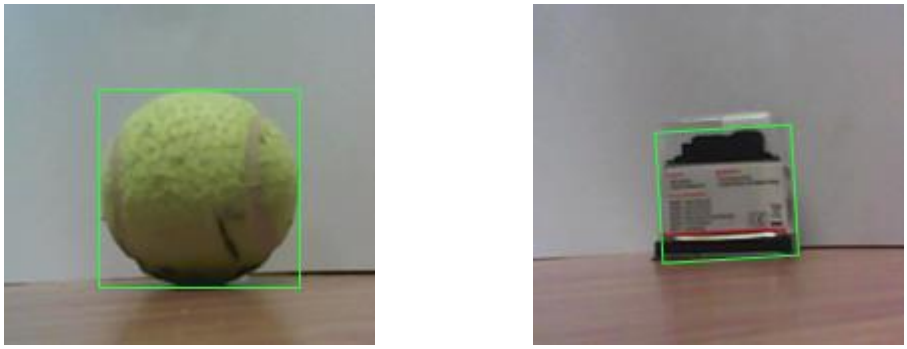

Figure 42: Object characteristics with different shape but the same aspect ratio.

The tennis ball (sphere) has a diameter of 62mm and a servomotor has the dimensions 58mm×44mm×40mm. These two objects have different shapes while their aspect ratios are the same. (The algorithm developed for capturing and extracting the object characteristics is given in the appendix section A10). The dimensions of the grasping rectangle captured by the webcam are measured in pixels while the object size is expressed in metric form. In order to calculate a dimension *h* of the grasping region in the object, a term pixel per metric, *K*, is used.

The dimension is calculated by the following relationship.

$$h = \frac{n}{K} \tag{27}$$

Where, *n* is the dimension measured in number of pixels and *K* is the pixel per metric. (Full explanation of this relationship is given in the appendix section A11). After establishing the function of the webcam and infrared sensor they need to be defined within the coordinate frame of the artificial hand. A coordinate system is established on the webcam of the prosthetic hand as shown in figure 43. The x-axis $\vec{x}_h$ is in the horizontal axis and the y-axis $\vec{y}_h$ is the vertical axis. The z axis $\vec{z}_h$ is determined by the cross product of the x-axis and the y-axis $\vec{z}_h = \vec{x}_h \times \vec{y}_h$. This coordinate system is chosen as a reference coordinate system for the establishment of orientation for an object-grasping region. In this specific instance, the coordinate system of the hand is designed to be the same as that of the webcam.

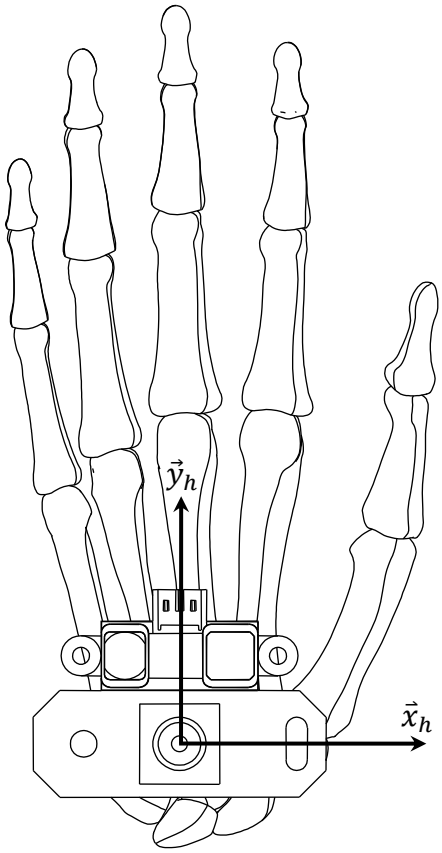

Figure 43: Webcam and IR sensor orientation.

The x-axis $\vec{x}_{object}$and y-axis $\vec{y}_{object}$ of the object coordinate system is defined by the principal axes of the rectangle enveloping the grasping region. The principal axis parallel to the longer side of the rectangle is chosen as the x-axis $\vec{x}_{obj}$.The orientation of the object grasping rectangle is described by the angle, α, between the axes $\vec{x}_{obj}$ and $\vec{x}_h$. The grasping rectangle envelops the projection of the grasping region on a plane through the object and perpendicular to the shooting direction of the webcam. Its dimensions and orientation are estimated from the image captured by the webcam. As an example, figure 44 shows the perception of an object to be grasped. Take a bottle as an example, the bottle is at a distance, *u*, from the artificial hand. The rectangle enveloping the bottle is the grasping region. The rectangle is extracted from the image captured by the webcam. The minimum dimension, *d*, and aspect ratio, *r*, are computed to characterize the geometry and

size of the bottle. The object coordinate system $\vec{x}_{obj} - \vec{y}_{obj} - \vec{z}_{obj}$ is defined by the principal axes of the grasping rectangle with the origin set at a distance, u, along the common $\vec{z}_{obj}$ and $\vec{z}_h$ axes. The angle, α, is the angle between the coordinate system of the hand relative to the object.

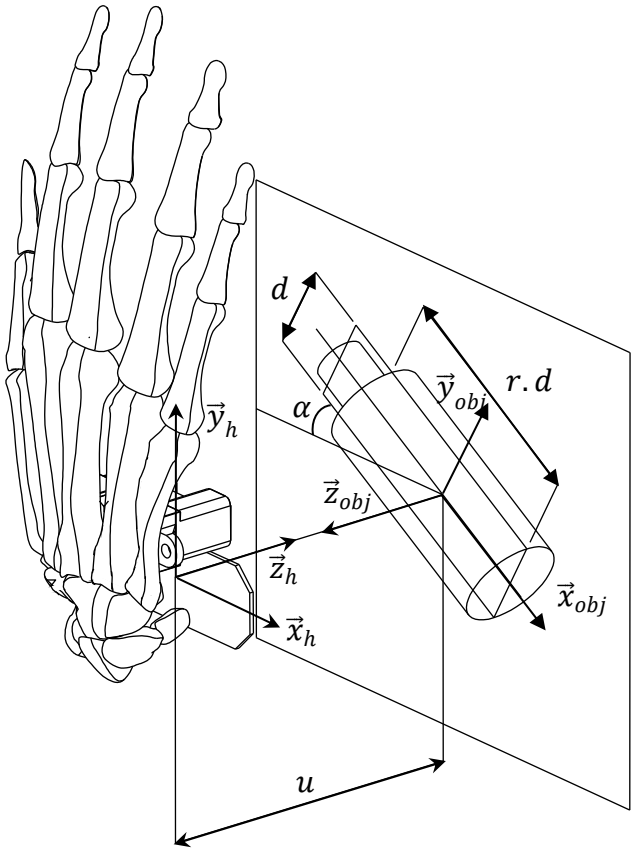

Figure 44: The perception of an object to be grasped displaying the relationship between their coordinate frames.

The establishment of these reference frames and parameters provide a base on which planning and control rely. Through the use of the minimum dimension and the aspect ratio, objects can be classified and be prepared to grasp in a more human like way.

5.2.2 Planning

After characterizing the object through perception, planning begins. During the planning process the grasp type is determined based on the object perception (developed in the previous section) by a grasp mapping,ψ . The grasping region is expressed in terms of a fraction of hand length l as shown in figure 45 with the maximum object size, d_{max}, being $0.8l$. The minimum dimension of an object, d, is expressed as a fraction of hand length.

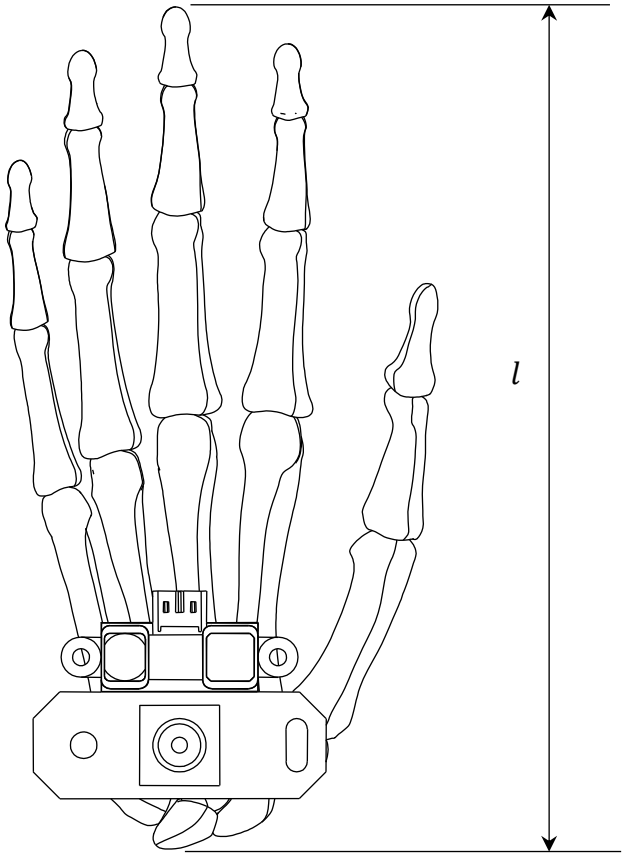

Figure 45: The characteristic hand length.

As a result, the single dimension of an object is categorized into six sets, namely: very small (*VS*), small (*S*), medium (*M*), large (*L*) and very large. Table 4 displays these categories and defines the six sets expressed in terms of hand length *l*.

Table 4: The categorization of the minimum dimension.

Hand length	Minimum dimension categories
$0 \sim \frac{1}{4} \cdot d_{\max}$	Very small ($VS = \{d \mid 0 \le d \le \frac{1}{4} \cdot d_{\max}\}$)
$\frac{1}{4} \cdot d_{\max} \sim \frac{1}{2} \cdot d_{\max}$	Small ($S = \{d \mid \frac{1}{4} \cdot d_{\max} \le d \le \frac{1}{2} \cdot d_{\max}\}$)
$\frac{1}{2} \cdot d_{\max} \sim \frac{3}{4} \cdot d_{\max}$	Medium ($M = \{d \mid \frac{1}{2} \cdot d_{\max} \le d \le \frac{3}{4} \cdot d_{\max}\}$)
$\frac{3}{4} \cdot d_{\max} \sim d_{\max}$	Large ($L = \{d \mid \frac{3}{4} \cdot d_{\max} \le d \le d_{\max}\}$)
Above $d_{\max}$	Very large ($VL = \{d \mid d \le d_{\max}\}$)

A grasping rectangle set $\boldsymbol{O}$ containing all the grasping rectangles of objects that can be grasped is defined by

$$\boldsymbol{O} = \{(d, r, \alpha) | 0 < d \le d_{max}, r \ge 1, \alpha \le 90^0\} \tag{28}$$

Let

$$\boldsymbol{G} = \{\boldsymbol{\phi}^k = [\varphi_1^k \ \varphi_2^k \ \varphi_3^k \ \varphi_4^k \ \varphi_5^k \ \varphi_6^k \ \ c]^T | k = 1,2, \dots, n_g, \varphi_i^k \in [0, \varphi_i^{max}]\} \tag{29}$$

be a finite set of n_g grasp types available from the prosthetic hand and let $\boldsymbol{\phi}_0^k$ be a grasp type with the initial values of φ_i^k. The grasp mapping ψ is defined as $\psi: \boldsymbol{O} \rightarrow \boldsymbol{G}$ such that $\boldsymbol{\phi}_0^k = \psi(o), \forall \boldsymbol{\phi}_0^k \in \boldsymbol{G}$ and $o \in \boldsymbol{O}$. Hence, for any grasping rectangle, $o \in \boldsymbol{O}$, there exists a grasp type $\boldsymbol{\phi}_0^k \in \boldsymbol{G}$ with the initial values of φ_i^k.

The implementation of a grasp mapping requires the adoption of a grasp taxonomy, which defines commonly used human grasp types (Feix, Pawlik et al. 2011, Feix, Romero et al. 2016). A grasping rectangle $o \in \boldsymbol{O}$ can be associated with a grasp type $\boldsymbol{\phi_0^k} \in \boldsymbol{G}$. As a result, six grasp types are chosen and defined:

1- Tip Pinch grasp

2- Palmar Pinch Grasp

3- Power grasp

4- Tripod

5- Power sphere

6- Power grasp sphere (3 fingers)

These grasp types cover all grasping rectangles within the grasping capability of the artificial hand. (Each grasp is defined in chapter 3.6). All grasping rectangles ($\forall o \in \boldsymbol{O}$) are categorized and the grasp mapping, ψ, associates each category with a specific grasp type. The landscape of grasp mapping, ψ, (with orientation $\alpha = 0^o$) is shown in figure 46.

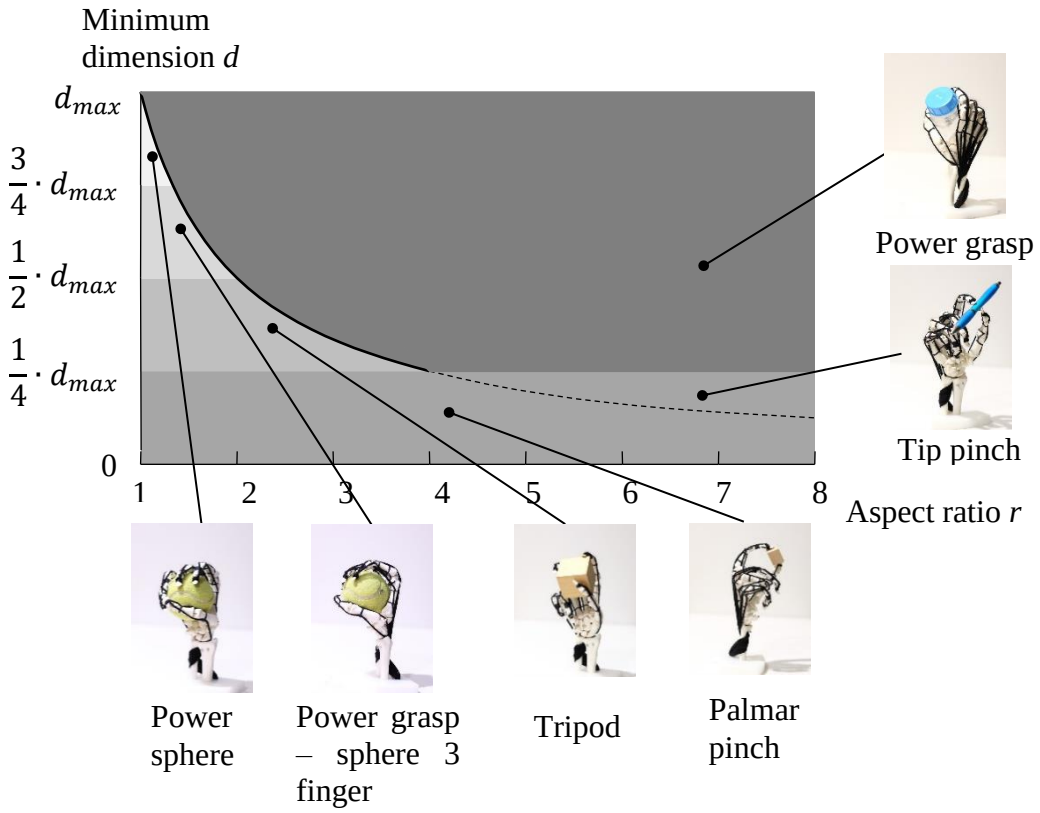

Figure 46: The landscape of grasp mapping. (Aspect ratio is represented on the horizontal axis)

The grasping rectangles for the power sphere, power grasp sphere (3 finger), tripod and palmar pinch all lie within the grasping region of the artificial hand. On the other hand, the tip pinch and the power grasp lie partially without the grasping region. The boundary separating these two groups is given by, $d \cdot r = d_{max}$. There are two conditions where the orientation, α, is either considered critical or non-critical for grasping success. The first is for objects where (d, r) are values such that $d_{upper} \geq d \geq d_{lower}$ and $r \leq \frac{d_{max}}{d_{lower}}$. In this case both dimensions of the grasping region are less than $d_{max} \cdot l$. Therefore, the orientation is not critical for the grasp task. However, the second condition, for objects where (d, r) are values such that $d_{upper} \geq d \geq d_{lower}$ and $\geq \frac{d_{max}}{d_{lower}}$ one of the dimensions of the grasping region is larger than $d_{max} \cdot l$. Therefore, the grasp task can only be performed with an appropriate orientation.

The orientation of the grasping rectangle may also affect the grasping task depending upon the aspect ratio, *r*, of the object to be grasped. Figure 47 depicts the effect of the orientation of an object on the grasping task. In this case one of the dimensions of the grasping rectangle is greater than $d_{max} \cdot l$.

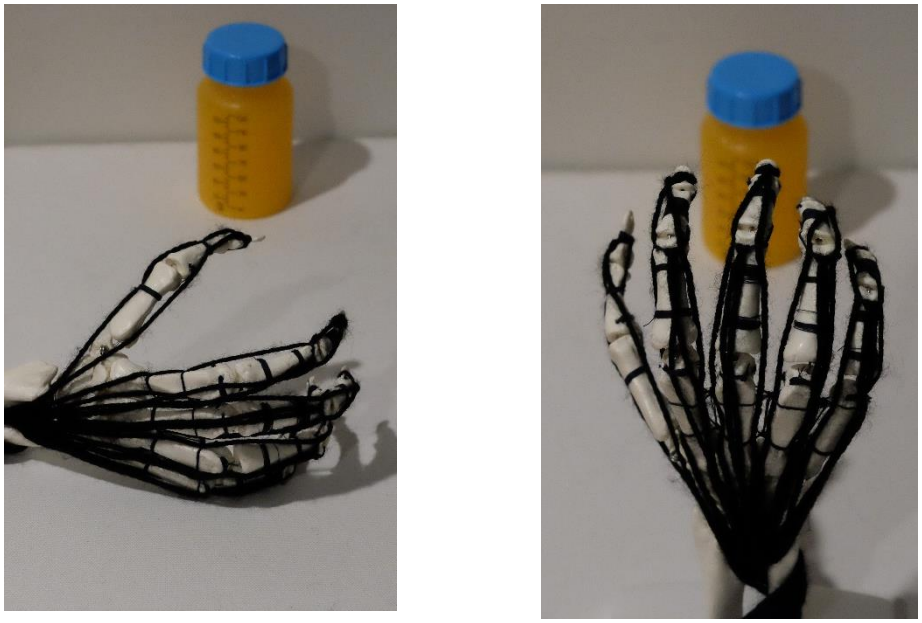

Figure 47: Effect of hand orientation with respect to the grasping of a small bottle.

The prosthetic hand cannot grasp the object as oriented on the right hand side of figure 47. However, by amending the orientation of the hand it can grasp the object (shown on the left hand side) since the acute angle, α, is 0^o. It is important to note that there is a small range of acceptable values for, α, where the object can still be grasped successfully. The landscape of the grasp mapping can be displayed graphically in three dimensions as shown in figure 48 where the orientation, α, is included in the landscape of grasp mapping. The prosthetic hand does not respond if the minimum dimension, *d*, aspect ratio, *r*, and orientation, α, of the grasping rectangle (d, r, α) is within the dashed line region. The landscape of grasp mapping determines the perception of the system.

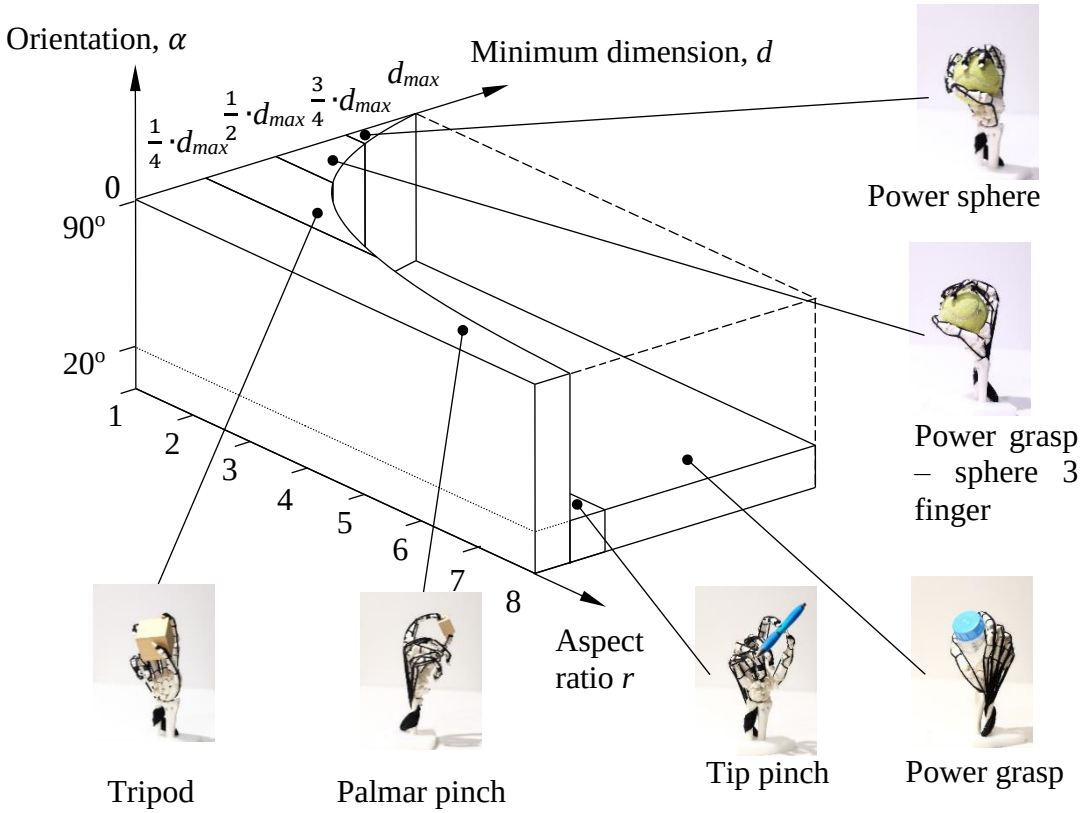

Figure 48: A landscape of grasp mapping with the inclusion of orientation.

5.2.2.1 Pre-shaping

The development of a landscape for grasp mapping solves the preliminary challenge for autonomous grasping systems. However, the high number of DoF of artificial hands creates multiple grasping positions for the same object. For instance, if a cylindrical broom handle-like object required grasping there are at least three possible grasps suitable to hold it: a medium wrap grasp, an index finger extension grasp and an adducted thumb grasp as shown in figure 49. These options require different hand orientations and digit positions. In addition to this each different grasp requires a different approach and, therefore, preparation position from the hand. This idea is called pre-shaping and it occurs before any object is grasped.

Figure 49: Three possible cylindrical grasps for the same object.

Pre-shaping is important because object approach largely determines the type of grasp chosen. A major function of a prosthetic hand is to securely hold an object. Firmly held objects require the consideration of its orientation. Consider the precise movement of holding a small cube with the dimensions 30×30×30mm. The user, by intuition selects the most suitable approach by controlling hand orientation. The aspect ratio and its minimum dimension determine the geometry and size of the object. Consider the following case (Figure 50) where the distance between the webcam and the cube is 150mm. The minimum dimension and aspect ratio are 30.5mm and 1.18 respectively. Furthermore, the orientation of the region, $\alpha = 0.92^{o}$.

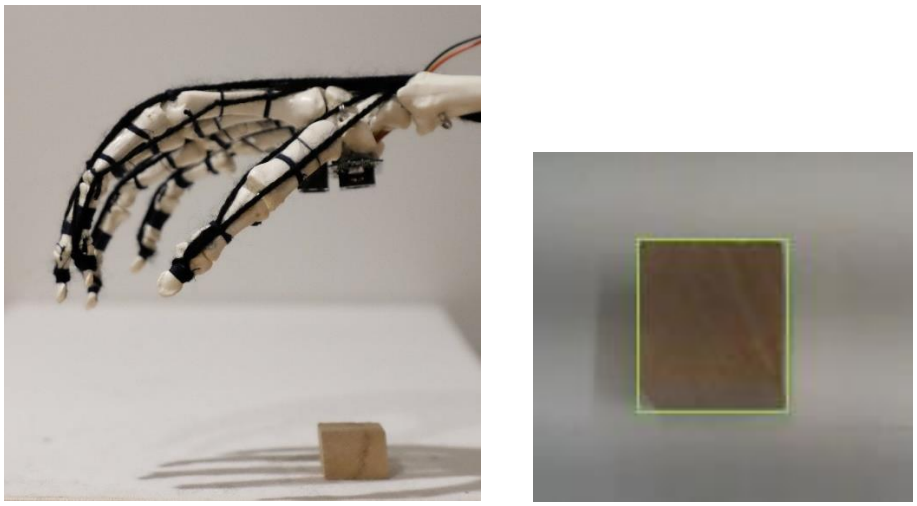

Figure 50: The autonomous hand oriented over the cube to capture an image.

In this implementation, the grasping task is not performed if $\alpha \geq 20^{o}$.The prosthetic hand length, l, is 160mm, therefore, $d_{max} = 128mm$ according to the condition, $d_{max} = 0.8l$. The prosthetic hand is positioned to face the cube (from above), the infrared sensor measures the distance between the hand and the cube and the webcam captures the image. Grasp selection occurs in accordance with the information acquired from the object. Figure 51 shows the pre-shaping of the hand in preparation for the actual grasping of the cube.

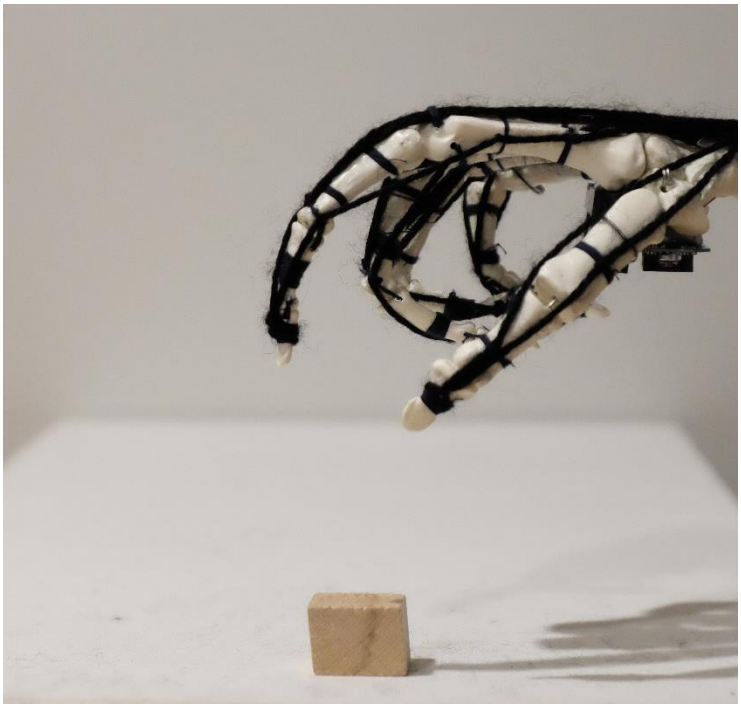

Figure 51: Pre-shaping of the artificial hand.

The artificial hand is moved by the user (Figure 52) into a position where the grasp initiates (makes contact). Once stable the grasp is complete and the cube can be manipulated or moved.

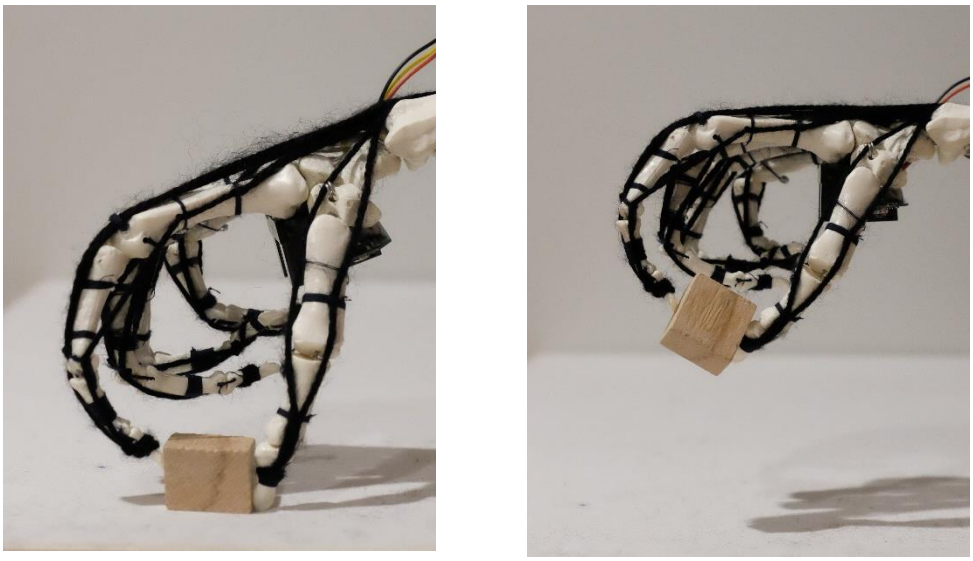

Figure 52: left- Grasp initiation. Right- Grasp execution.

This process is similar for each grasp type and for every object. The implementation of such tasks require control schemes.

5.2.3 Control

The autonomous framework is governed by autonomous principles and user input. A delicate balance between these two control governors is required if the framework is to be successful. The following section describes the user input to the framework and makes vital links between the SVM based NI of chapter 4 with the mimicry of human innervation.

5.2.3.1 User Input

As described and justified in chapter 4 there is little benefit to applying machine learning based NI's beyond binary classification tasks. Therefore, the autonomous framework is designed to receive a binary input from the user deciding whether the artificial hand should close (perform a grasp) or remain open. The user input is literally the implementation of the SVM based NI of chapter 4.

Preliminary to the autonomous framework is the processing of the user input by signal processing and classification. The process flow of user input is described in figure 53.

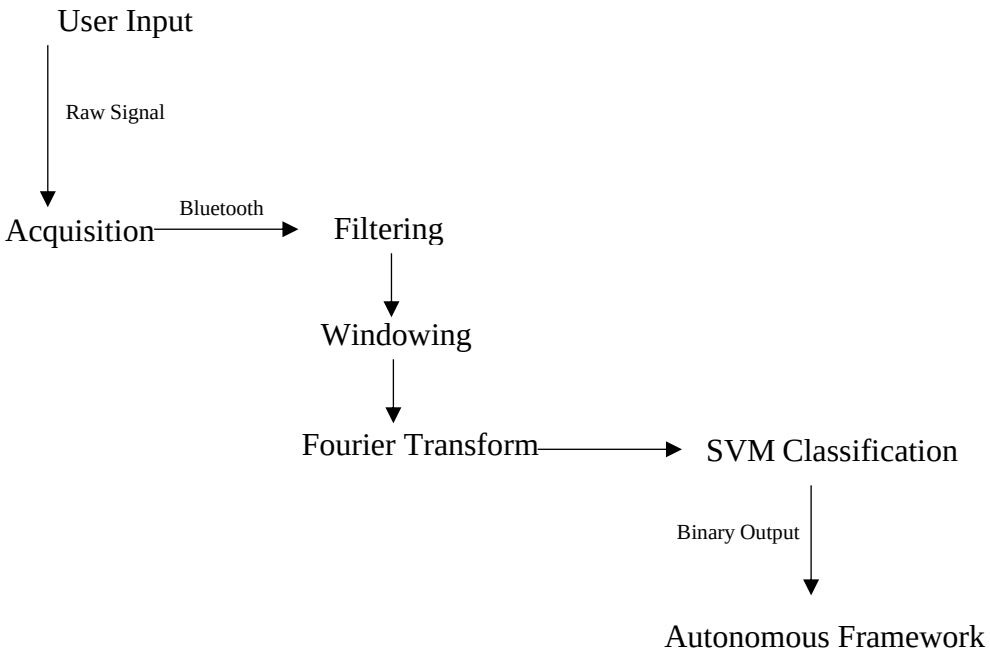

Figure 53: User input process flow preceding its integration with the autonomous framework.

The user input is integrated to the autonomous hand framework and provides the grasp execution signal to control the artificial hand. The framework uses the binary output of the SVM classification as a control signal to decide whether a grasp is to occur or not. By understanding the process flow of the user input, we can use the idea of artificial innervation to improve the control of the framework.

5.2.3.2 The Mimicry of Innervation

In the human body, innervation is the process of supplying muscles with the energy. Action potentials originating at the brain travel through the nervous system, arrive at the muscle boundary and depolarise the muscle cell causing a release of calcium. Calcium release begins chemical reactions that contract the I-band within the

sarcomere of the muscle. The sum of I-band contractions supply muscles with a linear force that activates skeletal movement. As chemical reactions intensify, the intensity of force created at the muscle increases. This process is the dominant mechanism of muscle activation and is required in the human grasping system. The bio-mimicry of innervation begins with establishment of a relationship between muscles and electro-mechanical actuators. From an engineering perspective, all actuators must have a source of power and an input signal. Human muscles also meet this requirement (Figure 54). The source of power for a muscle comes from food (nutrition) ingested into the human body that aids in the chemical process for muscle contraction. The signals muscles receive are action potentials originating at the brain.

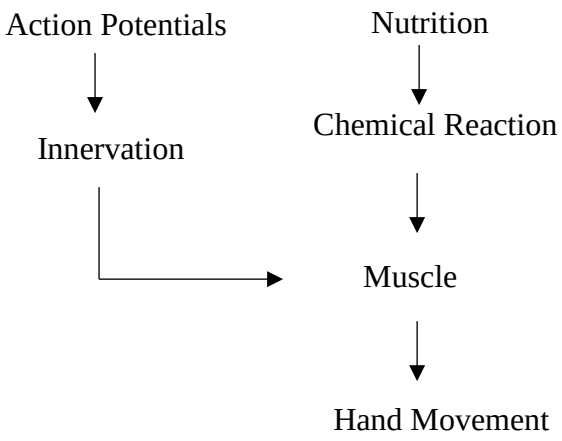

Figure 54: Human actuation system for controlling limbs.

To recreate these conditions for the artificial hand, actuators receive signals from microprocessors and power from batteries (Figure 55). The implementation of artificial innervation bases itself on the principle that there is access to electrical power to execute mechanical movement and that a digital/analog signal representing user intention is acquirable.

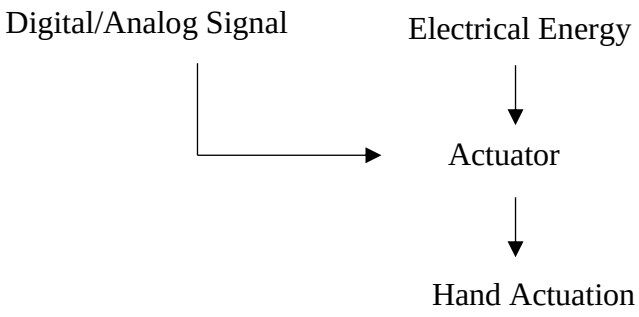

Figure 55: Artificial actuation system for controlling electro-mechanical devices.

With this in mind an approach towards the mimicry of innervation is presented. In the next section the output of the SVM based NI is mapped to the servomotors using the following innervation mapping. The innervation mapping provides a robust solution to artificial hand actuation and is an essential part of the autonomous framework.

5.2.3.3 Innervation Mapping

In order to take advantage of this perspective in mimicking innervation we need to define the point where a specific event within the EEG signal has occurred. To do this we must look at the produced binary output of the SVM in more depth. SVM classifications are made according to its confidence in correctly identifying an event or pattern within a raw signal. When this happens a signal identifying the event is sent to the autonomous framework (making the output binary). The confidence of the SVM, C_{SVM}, is not binary but ranges from $0 \leq C_{SVM} \leq 1$. Where 1 represents complete confidence and 0 represents no confidence.

With this in mind Let, e_1, be an event within the signal and let $\bar{C}$, be the confidence of the SVM at any given time, t. The occurrence of events within that signal can then be defined when:

$$\bar{C} \geq C_T \tag{30}$$

Where, C_T is a threshold ranging between, $0 \leq C_T \leq 1$. C_T is adjusted depending on the user. The recognition of the event, e_1, leads to the initiation of innervation where a signal is provided to a servomotor with the information required to actuate it (artificial innervation). By generalising these conditions let, $e_1, e_2, \dots, e_n$ be the characteristic events unique to different individuals and $C_{T1}, C_{T2}, \dots, C_{Tn}$ are the confidence thresholds for each, e_n. By computing whether the condition $\bar{C} \geq C_T$ holds for any $e_n$we can reliably map the artificial innervation from the SVM to each servomotor for every individual user of the framework.

This idea, although basic, provides a base for artificial hand control frameworks that simplifies and helps match artificial hands to their control framework. This idea works in unison with the perception, planning and object interaction involved in the autonomous framework. The approach taken here is inspired from the mechanisms of muscle innervation.

5.3 Results

The autonomous framework performed effectively with the average classification accuracy performing higher than any machine learning approach investigated in this work. The response time of the classification is the time taken to recognize an object in addition to the time taken for the signal to reach the hand from the user. The

framework mimics the human ability to prepare and execute grasps in a human environment. The correct identification of objects occurred within one second on average and had a classification accuracy of 95%. These results are integrated with the SVM based NI of chapter 4. Five objects are investigated to test the feasibility of the control framework (Table 5).

Table 5: Classification accuracy and response time of the SVM based autonomous framework.

Object	Grasp type	Correct Identification (%)	Response Time(s)
Ball small	Tripod	98	5.2
Cube small	Palmar pinch	95	4.5
Ball large	Power	98	6.6
Cube large	Power	94	4.4
Cell phone	Power	90	4.7

The approach recognised five gestures in real time. When comparing the autonomous framework to the SVM based NI, the results are telling as can be observed in figure 56.

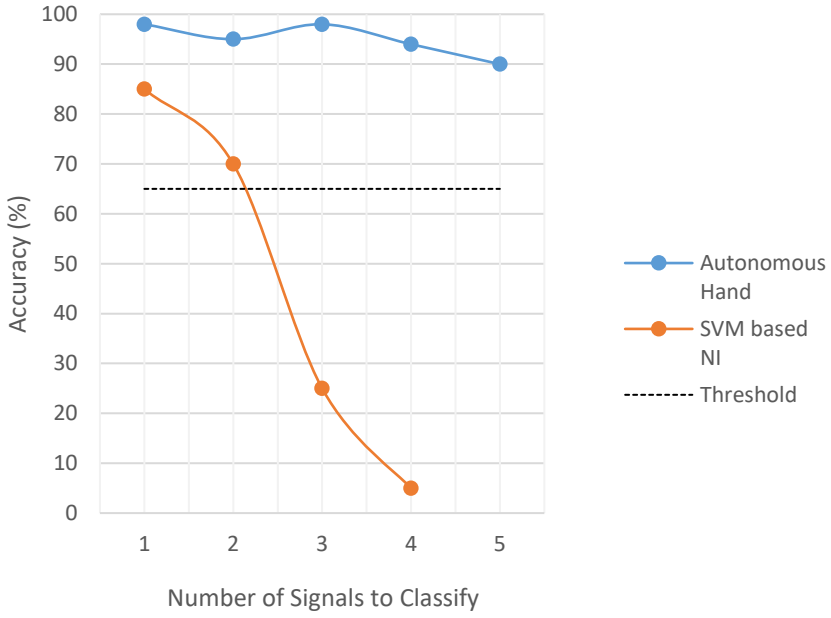

Figure 56: Accuracy of the SVM based NI and the autonomous hand for multiple classifications.

A generous threshold at 65% indicates the point where either of the methods become impractical. The accuracy of the autonomous hand exceeds that of the SVM based NI in every case. This outcome means, multiple classifications are possible in NI technology. This is realised without an increase in response time.

The autonomous framework outperforms the other autonomous hand approaches with an impressive 95% object classification accuracy. In their approaches Fajardo, Ferman et al. (2018) and Ghazaei, Alameer et al. (2017) achieve object classification accuracies of 92% and 85% respectively. In either of these cases their approaches are limited by finite databases of graspable objects. This approach is not limited in that way, therefore, it is more suitable for application in any environment. This outcome is exciting and proves that the potential of such systems can be robust and reliable. The true significance of this result will become apparent as more research is undertaken in the area of autonomous hands.

5.4 Summary

The experimental results prove that the autonomous approach towards restoring hand function is incredibly valuable to the development of NI's for artificial hand control. The accuracy and response of the hand is less reliant on machine learning processes and eliminates redundant non-natural user involvement. The potential to restore hand function is increased by virtue of the improvement of classification accuracy. The hypothesis stated at the beginning of the chapter stands and in many ways has proven that autonomous vision is not only well suited to NI frameworks, but that it is also very human like. An autonomous approach to the development of NI's can increase the reliability of control and overcome the traditional challenges of non-invasive EEG based NI's in a way that does not increase human involvement. The following chapter (chapter 6) delves into the meaningful findings of this work

by discussing the ideas expressed in chapters 3, 4 and 5. It then revisits the overarching research idea of this work and identifies its significance in restoring hand function to amputees.

Chapter 6

Discussion

6.1 Background

The human grasping system consists of many parts that contribute to the ability of humans to grasp objects, express themselves and manipulate processes. The human grasping system consists of three distinct but interconnected areas. The brain, the nervous system and the hand. The approaches presented in the previous chapters (3, 4 and 5) envelop these three areas and define their individual relevance and contribution to mimicking the human grasping system. This chapter aims to discuss the significant findings of this work relating to how hand function restoration can be achieved through mimicking the human grasping system. This chapter will discuss machine learning for NI development, argue the value of machine vision for NI development and revisit the whare kōrero of the work. The enlightening and productive features of each chapter are discussed in order to maintain the clarity of the work. The conclusions are reserved for chapter 7 and will not be included within this chapter.

6.2 SVM based Non-invasive NI for Artificial Hand Control

Chapter 4 described how machine learning is used to develop non-invasive NI's. From investigation it was reinforced that an SVM approach is wise to use in the development of NI technology for artificial hand control. The limitations of the SVM approach will be discussed and the relevance of the results will be put into perspective with respect to the thesis aim. The need for additional approaches is substantiated. The ideas discussed herein are preliminary to the development of NI's going into the future. Binary (open and close) classifications of the SVM based NI proved reliable and responsive in real time. However, in the attempt to classify multiple grasps the feasibility of the approach became questionable. Therefore, we learn that the SVM approach is feasible for application beyond binary classification, up to a point. The SVM based approach produced great results for response and reliability, however, its limitation in classifying multiple signals in real time does not allow reliable control of such systems.

The SVM based NI presented herein has tested the limits of EEG based NI's. In literature, there is value and emphasis placed on the importance of signal acquisition, pre-processing and machine learning. These ideas are substantiated by this work. But, it seems that current research is fixated with the idea that machine learning with sufficient training can provide a comprehensive solution to artificial hand control by non-invasive NI's. To this point in time, there is no substantive evidence to this notion. The lack of non-invasive NI's in the market is evidence of this. Machine learning is key to the processing of information acquired from the brain, however, it is not the be all and end all for non-invasive NI's as so many suggest. Therefore, in the current technological climate there is no benefit to perform classifications beyond binary tasks.

This understanding leads to the realisation of a considerable error in the research field. The increasing availability and reducing cost of non-invasive EEG acquisition systems encourages this type of research, however, the unknowing researcher continues this path of research without knowing it will lead to an inevitable road block. The chances of NI's entering the market through this approach is minimal. This is important to realise and needs addressing. The application of this knowledge to the thesis aim justifies the reasoning that alternate approaches are required to restore hand function in a meaningful way. For this reason the autonomous hand of chapter 5 is realised and discussed later in the chapter. Although in some instances, the SVM was successful there are secondary limitations worthy of discussion. Other limitations worthy of note include:

1- The challenges of training though patterns/mental commands and the associated mental fatigue.
2- Equipment limitations and experimental setup.
3- Environmental and biological noise interference.

These limitations are discussed in the following paragraphs. The unnatural feeling of training and reproducing a thought pattern becomes an ongoing challenge. Like all new processes, adaptation and repetition are the solution to the initial unnatural feelings associated with training thoughts. Another limitation that has a strong link with the reproduction of mental commands is the subsequent mental fatigue. Experimentation involved extensive amounts of training. From the results it is obvious to see that there is a big difference between the trained and untrained results. Therefore, an approach that considers the amount of training against the mental fatigue of the user must be considered.

The calibration and connection changes with the type of EEG acquisition headset being used takes time and can be irritating. Experimental set-up is considerable. Some EEG acquisition headsets simplify acquisition, however, certain drawbacks limit signal quality and ease of use. Physical artefacts and sensor placement were the main contributors to signal loss. Other limitations of signal acquisition are electrode slippage and hair interference. The size and shape of the acquisition headset makes it challenging to move and is uncomfortable

The implementation of machine learning into NI's is human like and requires further statistical validation to confirm its efficacy. The statistical significance will be improved with an increase in the dataset size. There are obvious limits to non-invasive NI's. The main limitation found by this work and reinforced by (Nooh, Yunus et al. 2011) is the poor accuracy and long response time of such systems. Additional approaches to meet the aims of this research are required above and beyond that which is represented in chapter 4. The autonomous hand of chapter 5 responded to this requirement by employing autonomous robotic principles in addition to the SVM based NI to improve response time and classification accuracy.

6.3 The Autonomous NI based Hand

Chapter 5 explored the option of reassigning the responsibility of classification to machine vision. This was required because of the accuracy and response limitations of the SVM based NI developed in chapter 4. Investigations proved that such an approach is more reliable. Of particular importance is the idea that by appropriately assigning classification responsibility we can improve NI's for artificial hand control. This approach clearly outperformed the SVM based NI approach for multiple classifications in real time while reducing the amount of non-natural user interaction. The following section will discuss the prominent learnings from realising an autonomous hand in the real world and explain its relevance towards the aim of this work. The implementation of the artificial hand to the autonomous framework is deliberated upon and the functional design aspects of the biomechanical hand design are discussed.

As established throughout this work the potential of NI's lie in the depth with which it processes and handles information. Machine learning represents the basic and fundamental approach to non-invasive NI's. An autonomous hand extends the non-invasive NI by automating some of the natural human grasping systems function. The autonomous approach extends the idea of NI's by the inclusion of autonomous vision. Chapter 4 justified the need to reduce the load on machine learning methods in order to increase classification accuracy without compromising the response time. The autonomous approach allows multiple grasps while maintaining the response of the NI. This is accomplished without increasing workload and without additional user interaction. An autonomous vision approach, in conjunction with a machine learning based NI, improves object-grasping tasks and, therefore, improves the ability of NI's to restore hand function. Computer vision mimics the human visual

system. Vital information regarding object size and geometry flows through the framework simplifying the process of object grasping.

Interestingly, computer vision minimises human involvement. It may seem counter intuitive to minimise human involvement to improve the restoration of hand function, however, by minimizing the non-natural and redundant human involvement the system is optimized and becomes more human like. A sense of belonging between the user and the artificial limb is created limiting the involvement of the user. This idea is backed by Iris (2014) who labels the non-natural movements as ‘redundant actions’ that negatively impact the autonomous system. Increasing the autonomy of the system is human-like and improves its response to a point where the user is able to express more confidence in it. For example, within the human grasping system it is often forgotten that pre-shaping is performed without realising. Humans are accustomed to becoming so good at things that they are done subconsciously. The idea of the autonomous hand is the same and, therefore, a human like confidence can be rightly expressed in the framework.

Computer vision simplifies the complexity of grasping applications. The current autonomous framework relies on the user orienting the hand and the camera to grasp objects. In most cases this can be a trivial process. Chapter 5 dealt with the grasping of simple objects. However, complex objects require further analysis.

In the case of objects that are more complex, we take the example of a cup (Figure 57). A bird's eye view of the cup reveals a power sphere grasp as the appropriate grasp. On the other hand, a front view of the cup produces a power grasp as the most suited grasp preparation. However, the side image of the cup requires further processing (with minor feature elimination) to recognise the handle as the grasping region.

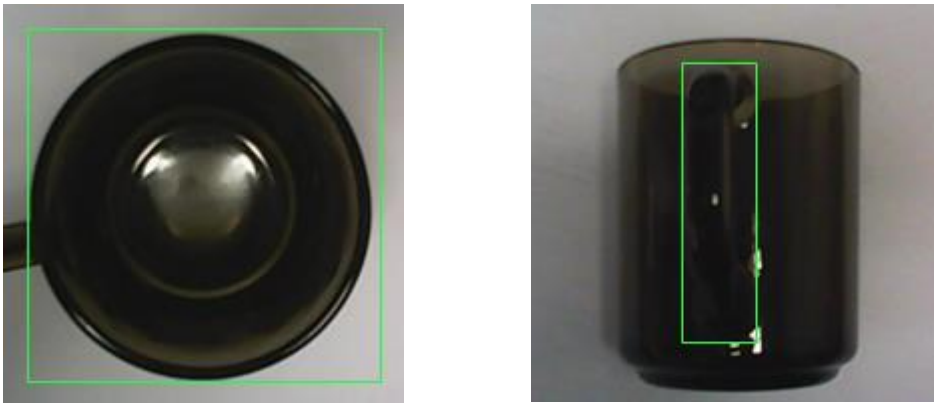

Figure 57: Grasping region of a cup at different viewing angles.

Additionally, the system needs to consider how the hand position affects grasping ability. Figures 58 and 59 illustrate how hand position affects the grasping task. A bottle is presented to the autonomous prosthetic hand.

The prosthetic hand is positioned above the bottle for the webcam to capture the object image. A tripod grasp type is determined and the bottle is grasped.

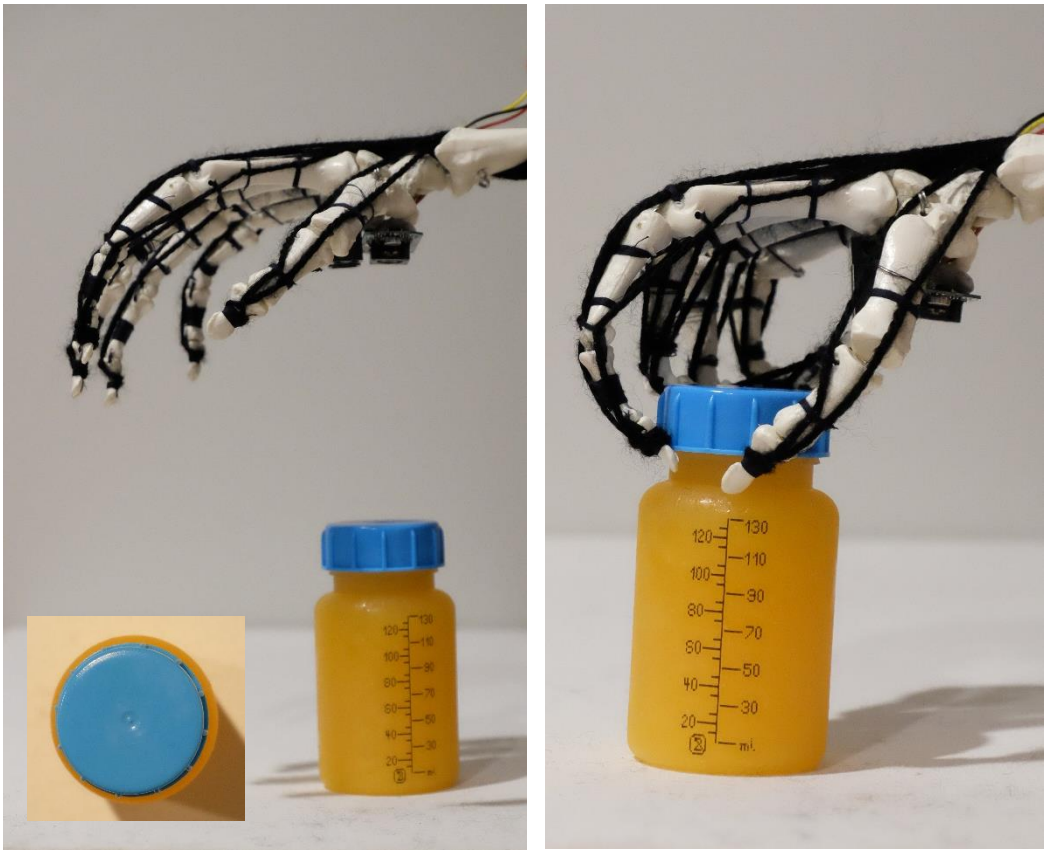

Figure 58: The process of grasping a bottle from its top.

When the prosthetic hand is positioned facing the side of the bottle as shown in figure 59, the side view of the bottle is captured by the webcam. As a result, a power cylinder grip is determined to grasp the bottle.

Figure 59: The process of grasping a bottle from its side.

Figure 60 shows the images captured by the webcam for both angles of approach from the prosthetic hand. The top view of the bottle produces a grasping region with the minimum dimension d = 39.6mm, the aspect ratio r = 1.03 and the pose α = 0.78º. The side view of the bottle produces a minimum dimension d = 40.0mm, the aspect ratio r = 2.75 and a pose of α = 0.02º.

Figure 60: Images captured by the webcam with different angles of approach.

Another example of this is given by the grasping of a mug. Different grasp types are used to grasp the mug from different angles. Depending on the position of the prosthetic hand a different perception is made of the same object. A grasp type of power sphere is employed to grasp the top part of the mug as shown on the left image of figure 61 (this is different from the example above because the minimum dimension between the two objects is different). In the case of the side view (right image, figure 61) the mug is grasped by a power grasp since the view of the mug will look rectangular.

Figure 61: Grasping a mug from two different positions.

Of course, three-dimensional object images can be built using additional cameras or time of flight cameras. A three dimensional perception would increase the information acquisition so that the effect of hand position on grasp type can be less restrictive. However, the computational cost can be an issue as more data needs to be processed with these advanced sensors. Also worthy of discussion is the idea expressed in chapter 5 of the object axis and hand axis not aligning in grasping tasks. Although the orientation of the object relative to the prosthetic hand influences its response, it is not necessary to have both coordinate systems aligned exactly (that is α = 0^o). This is due to the object not being rooted. As a result, the grasp task can be performed if the orientation difference is not too large. For example, when a bottle is placed on a table, its x-axis $\vec{x}_{obj}$ is vertical. When the artificial hand approaches its x-axis $\vec{x}_h$ can vary up to 10^o to the vertical with successful grasping still occurring. As the bottle is grasped, the object coordinate (x-axis $\vec{x}_{obj}$) will align with the prosthetic hand coordinate x-axis $\vec{x}_h$. This is possible due to the object not being fixed and being allowed to move. This can be seen clearly in figure 62.

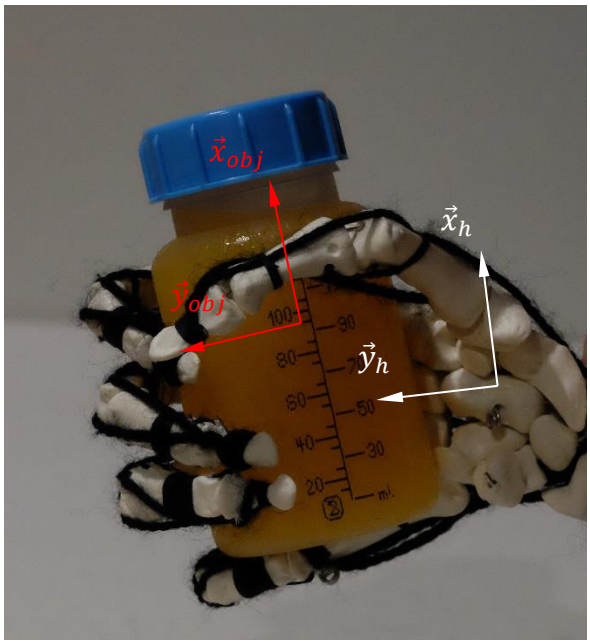

Figure 62: The object approximately aligns with the hand when it is grasped.

Image processing is the main procedure for building the perception. The computation time is usually short when the captured image is simple; especially when the background is pale and light in colour. Dosen and Popovic (2011) state the importance of optimising the image processing in such situations and suggest that colour identification, grayscale thresh holding and pixel brightness are keys to improving image processing in autonomous vision applications. In addition to image processing, the grasping rectangle can be designed to rotate about its centre and then shrink to obtain the smallest possible object area. These two processes (rotation and shrinkage) iterate until the area difference between the object and the rectangle is minimized. Figure 63 shows the grasping area optimization process.

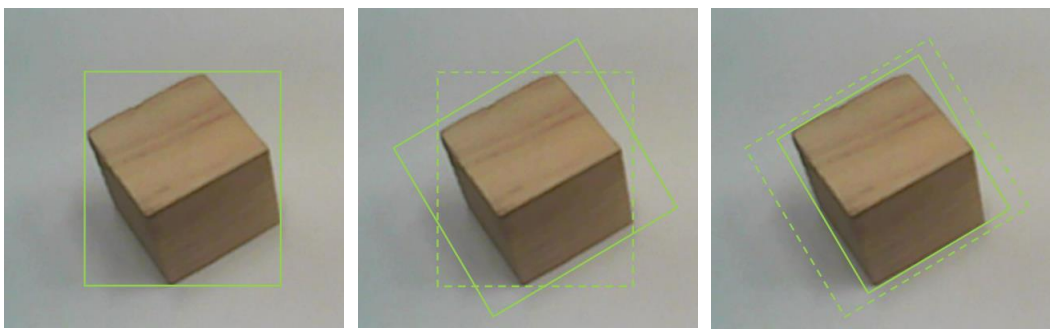

Figure 63: The determination and optimisation of grasping area.

Since a prosthetic hand is an assistive device for an amputee, the response time of the device is critical. In order to shorten the computation time, the rectangle area minimization is not performed when the aspect ratio is less than 2. This is acceptable since the orientation of the grasping region only influences the power grasp and tip pinch grasp types. In addition to improving the system through perception and image processing is the idea expressed by Weiner, Starke et al. (2017) to improve autonomous frameworks by implementing better and more reliable sensors. Other sources suggest time of flight cameras, Infra-red depth sensors and laser pointers as viable methods to improve perception.

Another consideration worthy of discussion is that of amputees controlling the hand. Depending on the case it may not be possible for the amputee to physically control the hand. Therefore, an axis lying through the longitudinal axis of the middle finger aligns objects with the approach of the hand towards the object. This idea requires the determination of object centroid, shape and orientation in real time. All of these parameters are determinable and is, therefore, a matter of implementation. Once the axis are determined for the hand and the object, alignment is possible through actuating and automating the hands approach toward an object by aligning the longitudinal axis of the middle finger with the axis of the object to be grasped. In these cases, an articulated wrist is of paramount importance.

The biomechanical hand is specifically engineered to replicate human hand function and work in compliance with the autonomous framework. This idea is reinforced by Abiri, Borhani et al. (2019) where it says ‘a critical aspect of employing a BCI (Brain Controlled Interface) system is to match the appropriate control signal with the desired application. It is essential to choose the most reliable,

accurate, and convenient paradigm to manipulate a neuro-prosthetic device or implement a specific neuro-rehabilitation program.' This idea is extended to the autonomous framework where appropriate controls are matched to the biomechanical hand of chapter 3. The following section will address the insights gained from matching the artificial hand to the autonomous framework in a way that mimics the human grasping system.

6.3.1 Biomechanical Hand Design Considerations

Chapter 3 described how a biomechanical approach towards hand design can restore hand function for amputees. From investigation it was found that understanding thumb orientation, tendon excursion, joint stabilization and bone geometry improves the function of artificial tendon driven hands. From this we learn more about how mimicking the human hand unlocks function in artificial hands. The following considerations are wise to include in artificial hand design:

1- Bone geometry is foundational to joint and tendon design.
2- Thumb configuration and orientation must be considered. It is critical to hand function.
3- Joint stabilization through artificial ligaments.
4- Tendon excursion planning is critical to the function of tendon driven hands with articulated wrists.
5- The ability of an artificial hand to function in an unmodified human environment can be reduced to the physical property of hand length.

The following paragraphs discuss and justify these considerations and conveys their importance in restoring hand function. The incorporation of human bone geometry into artificial hand design is fundamental to both joint stabilization, tendon networks and bone interaction. Hockings (2018) says that after bone design a great

deal of effort should be placed on the design of tendinous networks. After much deliberation this idea solidified the importance of the interaction between the bones and tendons of the artificial hand. As shown, in chapter 3 the geometrical features of bones accommodate the hand in many functions. By understanding the relationship between bone geometry and hand function, better design outputs for artificial hands can be realised.

Interestingly the effects of bone geometry are often unquantifiable and require a tacit knowledge of the human hand that can only come from interacting with the hand under surgical conditions. The dominant approach of thumb design in most artificial hands is the use of gimbals, ball joints or universal joints (with each employing multiple DoF that come with unwanted joint offsets). These approaches are strikingly different to that of this work. The ideas expressed by Wotherspoon (2016) highlight the unique movement of the thumb due to the metacarpal-carpal interaction of the thumbs CMC joint. This knowledge would have been otherwise unavailable without the personal experience of hand surgery/dissection and rigorous ethical approval. Deducing the best approach towards the design of an artificial thumb came down to realising that the saddle joint is the most effective way to recreate the complex multi-axial movement of the thumb. This design approach helped place the correct emphasis on the importance of thumb orientation.

Thumb orientation should be considered one of the most important design considerations when designing artificial hands. It is explicitly clear that following this design criteria is the most productive source of restoring function in mechanical hand design. The design of the artificial thumb is reinforced and supported by

Gomez, Gondolbeu et al. (2015) who define the roles of thumb ligaments and stress how their interactions provide the correct orientation and motion for thumb function.

An interesting phenomenon occurred within the ligaments of the artificial hand. The ligaments were observed to adapt to the force applied on them from the artificial tendons. This introduced the concept of a changing moment arm in force transferal. The artificial annular and cruciate pulleys placed along the fingers pivot and stretch in the direction of the tendon force. This phenomenon is consistent with Franko, Winters et al. (2011) who claim that the optimisation of force moment arms improves hand function and transferal of forces. In addition to this another interesting occurrence was observed. Due to the simple design of the ligaments it could be seen that as the ligament wound upon itself through each bone of the joint, it would naturally find a resting position to suit the specific bone geometry of the interacting bones. This finding is consistent with Schmidt and Lanz (2004) who suggest that the biological variations of bone length and geometry found in different humans is highly individualised. This approach to some degree accounts for these biological differences. On the contrary to this observation, the positive bone to bone interaction created by the ligament stabilization approach can be negated by the incorrect placement of origin and insertion sites of each ligament. This is a challenging concept when considering the non-quantifiable nature of locating origin and inserts of ligaments.

Further to these observations, the little and ring fingers are naturally smaller and, therefore, capable of a greater grasping force. This phenomenon is rarely accounted for in designs because it is currently normal practice for artificial hand design to repeat the finger design for every digit. Although easier for design realisation, it is

not ‘good practice’. The human hand is capable of precise movements as well as powerful movements. Precise movements are accounted for through the thumb, index and middle fingers while powerful movements are accounted for through the thumb, ring and little fingers. By repeating the design of each finger on the palm in any given hand design there is an imbalance of precise and powerful movements that limit the artificial hands ability to function like the human hand.

The final insight in artificial hand design is tendon excursion. Tendon excursion brutally limits the function of tendon driven hands. As investigated this issue can be solved by servomotor correction factors. Deshpande, Xu et al. (2011) approach wrist design to overcome tendon excursion in a mechanical way that is bulky and unnatural looking. The solution presented here is human-like and easy to use. It is preparatory to works such as Xu and Todorov (2016) and many others who look to incorporate articulated wrist movement into tendon driven artificial hands design.

The design of the biomechanical hand sheds light on good design principles for others to follow up on. The hand represents an integral part of the human grasping system. As the popularity of tendon driven biomechanical hands increases so will their availability. The ideas discussed here are preliminary but are a step in the right direction for artificial hand design. The next section returns to the overarching research idea.

6.4 Overarching Research Idea- Te Ao Māori

The autonomous hand framework combined with a Mātauranga Māori approach does not occur elsewhere and, therefore, constitutes a unique approach towards the restoration of hand function. The main outcome of combining western science with Mātauranga Māori is the added insight and enlightenment that ensue when mauri is maintained and preserved. The holistic approach presented herein encapsulates the idea that there exists an unseen connection between all living things. The maunga, awa and whenua represent three distinct but interconnected processes that are analogous to the human body. Of prominence to this research is the principle of mauri and how it relates to every aspect of the methodology formed herein.

As we receive, we are expected to give back in return with something of greater value. This is the principle of utu (reciprocity) that is formed at the essence of my culture. By taking physiological signals from an individual we must understand that it must be restored and returned (whenua ki te whenua). A koha (gift) of signals emitted from the brain are received from an individual exhibiting hope and trust in the researcher. At a preliminary level, by virtue of utu the koha is returned by restoring hand function which is the aim of this work. On a deeper level mauri is restored to the individual by an increase of independence. Therefore, a gift of increased value is returned to the individual. As a result, the researcher and the individual are lifted. This is a foundational principle in the Māori culture that: as a collective we all rise. The value of this approach is non-quantifiable and difficult to express in English because it is only received through the experiencing of Māori philosophies. By respecting the Mauri of every human being in the design of NI's a restoration of Mauri will occur in the amputee. This restoration of mauri increases the sense of belonging between the amputee and the prosthetic. By so doing, the

aim to restore hand function is met and intensified. This work unconsciously was centred in and based on the premise that when one person is lifted the entirety of people surrounding that person is lifted. If this work is to be successful it needs to be understood unequivocally that: as an individual is empowered so are the people surrounding them. Thus utu must be acknowledged in such systems.

The endowing and enabling power an individual has to improve the lives of others is returned to them through utu. The importance of rising as a collective and not as individuals is taught strikingly by Bristowe (2019). It is a powerful concept that suggests the only way humanity will truly progress is by helping each other and that we must rise as a collective not as individuals. This work is a small example of the truth of that principle. Therefore, the following question and answer that this work is founded on is poignant.

“He aha te mea nui o te ao? He tāngata, he tāngata, he tāngata”

What is the most important thing in this world? It is people, it is people, it is people.

The overarching idea of this work has contributed to and served as the base for realising the aim of this work to restore hand function for amputees. It has also addressed how three separate and distinct processes can work together to produce a better outcome for hand function restoration. This work is underpinned by Mātauranga Māori and is a beginning to more work in this under represented area.

6.5 Summary

The significant findings of this work have been discussed. As NI's mimic the human grasping system more effectively, new information will become known, unlocking the true potential of non-invasive EEG based NI's for artificial hand control applications. Acknowledgement that machine-learning algorithms are not the complete means to an end for NI's is a vital learning from this chapter. A paradigm shift in the development of NI's for prosthetic control must occur. In the current technological climate, there is very little worth in developing machine-learning methods beyond binary decision making for non-invasive EEG. Real development and worth has been found in an autonomous approach toward artificial hand control. The aim to restore hand function through the mimicking of the human grasping system is realised. The mechanical design of many artificial hands are limited and need to acknowledge the importance of critical design areas. The combination of academic approaches and Mātauranga Maori are exciting and can be complimentary with much of both knowledge bases contributing to the overall state-of-the-art.

Chapter 7

Conclusions and Recommendations

It is now possible to answer the research questions posed at the conclusion of the literature review. These questions have been enlightening and fruitful. From these questions the following is concluded in response to the thesis aim. (The research questions are in bold type).

What methods have the greatest potential to improve and restore hand function in NI based grasping systems?

With respect to the most effective method of restoring hand function, there are many approaches yet to be investigated, therefore, one superior overarching method cannot be given. However, the following can be concluded. In response to the knowledge gained by investigating SVM based NI's, there is great potential to improve non-invasive NI's by reassigning the responsibility of object classification to machine vision. The autonomous approach utilizing machine vision has greater potential to restore hand function then machine learning has on its own merits. The classification accuracy of the autonomous approach outperforms most current machine learning approaches and can be used in application. By minimizing unnecessary human involvement the response and reliability of the NI is optimized and the user can experience more confidence in the system. The restoration of confidence proves the value of the approach and implies the research is moving in a positive and constructive direction.

In respect to this understanding, the following principle is relevant in NI progression, that the potential of any NI lies in the depth with which it processes

and handles information. The depth in this case refers to what is done beyond the application of machine learning for NI's in artificial hand control. This concept is valuable because it creates a balance of control between machines and humans that maximises the restoration of hand function.

With regards to the effect of the artificial hand in restoring function for amputees. A naturally operated prosthetic hand can make for a more successful rehabilitation. The design considerations expressed holds keys to producing artificial hands of a higher anthropomorphism that are built to function in an unmodified human environment. By implementing the design considerations herein the aim to restore hand function for amputees is, to a degree, achieved by the application of biomechanical hands to the autonomous approach. Therefore, as biomechanical artificial hands become popularized the ability to restore function for amputees will improve dramatically. There is still lots of room for artificial hand development.

A common notion in literature is that machine learning is the key to NI progression. Contrary to popular belief, this is not the case. The optimisation of SVM based NI's reveals that multiple classifications in real time is possible but challenging. This is significant because it sheds light on the research question: **"Does the non-invasive EEG signal provide sufficient information to control artificial electromechanical hands beyond open and close tasks?"** The answer is yes, but the outcomes are limited. As the number of signals to classify increase the accuracy of the NI decreases dramatically. Four classifications are possible but not credible for use in real world applications due to the long response time and low classification accuracy. Any number of classification between one and four are feasible with extensive training. This knowledge is valuable because it provides a

direction for the development of NI research by saying that additional approaches or methodologies are required to improve NI outcomes. In response to the aim of the thesis, hand function can be restored through machine learning based NI's on its own merit. However it is limited.

What value is there in basing this research in Mātauranga Māori but maintaining a western academic approach?

The combination of knowledge bases represented in this work create a unique value to the research where a holistic approach meets academic structures. There lies an area between the two which is complimentary and beautiful. A relationship that is constructive and edifying. Living in this area for three years has been elucidating. The approaches represented herein belong within the bounds of multiple Māori philosophies. Among these philosophies preserving mauri and observing utu are of great worth. The holistic nature of this work means that beyond restoring hand function we can consider and appreciate the added ability to restore independence and quality of life for amputees. It must be clear that the philosophies spoken of are not hidden to the world, however, they are sacred and treated with care. Therefore, Māori appoint great orators and leaders to guard and share them. In an ever changing world with shifting values and ideals there is need for this type of stability and consistency. Therefore, it is important that more Māori are required to stand in this area between Mātauranga Māori and western academics.

7.1 Recommendations

The work presented herein is based on how hand function can be restored to amputees by mimicking the human grasping system. The grasping system is based on three areas: the brain, the nervous system and the hand. The brain is mimicked through the development of NI's, the nervous system is replicated by data

communication and a biomechanical hand is designed to mimic the human hand. The development and progression of the ideas and concepts of this work are presented in the following section.

Further Development of the Biomechanical hand

The work in developing artificial prosthetic hands is ongoing and ever improving. As biomechanical hand designs become popular it is likely that they will have better design and will naturally increase the chances of restoring hand function for amputees. Further development of biomechanical hands rests in increasing the number of actuators driving the hand, utilizing better materials that mimic the properties of human tissue, incorporating a joint capsule to optimize range of motion and optimizing thumb movement. The development of such hands are led by Hockings (2016) (Deshpande, Xu et al. 2011, Xu and Todorov 2016). As the state of the art is propelled into a bright technological future the design, accessibility and affordability of such hands will increase, thus improving the potential of such hands to restore function.

Further Development of Machine Learning for Neural Interface Based Artificial Hand Control

In consideration of the outcome of the SVM based NI, an additional approach is envisioned through the employment of the Spiking Neural Network (SNN). By implementing a SNN with Finite Automata (FA) theory there is potential to increase the classification accuracy and response of the NI specifically for hand movement.

In order to test this idea the following results were gathered and presented by Kumarasinghe, Owen et al. (2018) at the International Conference of Robotics and Automation with the following outcome shown in table 6.

Table 6: Preliminary results of the SNN/FA approach

	Response (s)	Classification Accuracy (%)
SNN/FA	3.0-10.0	95
SVM	2.0-8.0	85

The SNN/FA approach is a logical progression to the improvement of non-invasive EEG based NI's without machine vision. The SNN/FA framework produces a considerably higher classification accuracy in comparison with the SVM approach. Investigation is required to test the statistical significance of the findings.

Further Development of the Autonomous NI based Hand

The autonomous approach presented herein requires the implementation of minor feature elimination, three dimensional scanning and an increased grasp taxonomy to include more complex grasps. Until this point in time, the autonomous framework classifies all objects into five main grasp types. This overlooks many objects of complex geometry. In most cases, the artificial hand is capable of grasping these objects but fails in so doing due to the lack in strategies to recognise, pre-shape and execute the grasp required. These improvements are realisable in the near future and are exciting in restoring the hand function of amputees.

References

Abiri, R., S. Borhani, E. W. Sellers, Y. Jiang and X. Zhao (2019). "A comprehensive review of EEG-based brain-computer interface paradigms." Journal of Neural Engineering **16**: 1-22.

Agilent Technologies (2018). The Fundamentals of Signal Analysis. A. Technologies**:** 1-68.

Aleksandra, C. (2018). "How is a neuron adapted to perform its function?" Retrieved 06/06/2017, 2017, from https://socratic.org/questions/how-is-a-neuron-adapted-to-perform-its-function.

Alomari, M. H., A. Samaha and K. Alkamha (2013). "Automated Classification of L/R Hand Movement EEG Signals using Advanced Feature Extraction and Machine Learning " International Journal of Advanced Computer Science and Applications. **4**(6): 207-212.

Bashashati, A., M. Fatourechi, R. Ward and G. Birch (2007). "A survey of signal processing algorithms in brain-computer interfaces based on electrical brain signals." Journal of Neural Engineering **4**: 32-57.

Belter, J. T., J. L. Segil, A. M. Dollar and R. F. Weir (2013). "Mechanical design and performance of anthropomorphic prosthetc hands: A review." Journal of Rehabilitation Research and Development **50**(5): 599-618.

Bird, J. J., L. J. Manso, E. P. Ribeiro, A. Ekart and D. R. Faria (2018). "A study on Mental State Classification using EEG-based Brain-Machine Interface." International Conference on Intelligent Systems **1**: 1-6.

Bridges, N. R., M. Meyers, J. Garcia, P. A. Shewokis and K. A. Moxon (2018). "A rodent brain-machine interface paradigm to study the impact of paraplegia on BMI performance." Journal of Neuroscience Methods **306**: 103-114.

Bristowe, C. (2017). Indigenising the Screen, Navigating the Currents of Change, a Vision of Fourth Cinema. Doctor of Philosophy, Waikato.

Bristowe, C. (2019). Personal communication. As a collective, not individuals. M. Owen.

Carpi, F. and D. De Rossi (2014). Non invasive Brain-Machine Interfaces. Italy, University of Pisa.

Carvalho, A. and A. Suleman (2009). Neural Network Controller For An Anthropomorphic Hand Prosthesis. 7th Euromech Solid Mechanics Conference. Lisbon, Portugal.

Cherry, K. (2018). "A Guide to the Anatomy of the Brain." Retrieved 08/02/2019, 2019, from https://www.verywellmind.com/the-anatomy-of-the-brain-2794895.

Cherry, K. (2018). "What you should know about the peripheral nervous system." Retrieved 26/10/2018, 2018, from https://www.verywellmind.com/what-is-the-peripheral-nervous-system-2795465.

Cobos, S., M. Ferre, M. A. Sanchez-Uran, J. Ortego and R. Aracil (2010). "Human hand descriptions and gesture recognition for object manipulation." Computer Methods in Biomechanics and Biomedical Engineering **13**(3): 305-317.

Components, R. (2019). "GP2YOA710K0F." Retrieved 06/06/2019, 2019, from https://nz.rs-online.com/web/p/products/6666577/?grossPrice=Y&cm_mmc=NZ-PLA-DS3A-_-google-_-PLA_NZ_EN_Catch_All-_-Fusion-_-PRODUCT_GROUP&matchtype=&pla-468790558708&gclid=CjwKCAjw0N3nBRBvEiwAHMwvNm0kXyfj7j6sv_hN3CGp4t7VHp2QvfVi_Dl0TteNZ7hM376FJLkA4RoCnTQQAvD_BwE&gclsrc=aw.ds.

Cortes, C. and V. N. Vapnik (1995). "Support Vector Networks." Machine Learning **20**: 273-297.

Council, W. R. (2019). "Environmental Information- Natural Resources." Retrieved 14/05/2018, 2019, from https://www.waikatoregion.govt.nz/environment/natural-resources/water/rivers/waikato-river/about-the-waikato-river/.

Crawford, S. (2009). "Matauranga Maori and western science: The importance of hypotheses, predictions and protocols." Journal of the Royal Society of New Zealand. **39**(4): 163-166.

Cutkosky, M. R. (1989). "On Grasp Choice, Grasp Models, and the Design of Hands for Manufacturing Tasks." IEEE TRANSACTIONS ON ROBOTICS AND AUTOMATION **5**(3): 269-279.

Damasio, H. (1995). Human brain anatomy in computerized images. New York, USA, Oxford University Press.

David, M. (2001). "From psychic energy to the EEG." Perspectives in Biology and Medicine **44**(4): 522-542.

Deshpande, A. D., Z. Xu, M. J. Vande Weghe, B. H. Brown, J. Ko, L. Y. Chang, D. D. Wilkinson, S. M. Bidic and Y. Matsuoka (2011). "Mechanisms of the Anatomically Correct Testbed Hand." IEEE/ASME Transactions on Mechatronics. **18**(1): 238-250.

Devices, M. (2019). "Action Potential." Retrieved 22/06/2015, 2019, from https://www.moleculardevices.com/applications/patch-clamp-electrophysiology/what-action-potential#gref.

DFRobot. (2019). "DFRduino UNO R3." Retrieved 06/06/2019, 2019, from https://www.dfrobot.com/product-838.html?gclid=CjwKCAjw0N3nBRBvEiwAHMwvNrxUqA9m5c_fk9FI

HrH4eoDCMvkyHqKqBH_w9BnKpWGPwhF6C-fIDRoClwEQAvD_BwE.

Dodge, F. A. and R. Rahamimoff (1967). "Co-operative Action of Calcium Ions in Transmitter Release at the Neuromuscular Junction." Journal of Physiology **193**: 419-432.

Dosen, S. and D. B. Popovic (2011). "Transradial Prosthesis: Artificial Vision for Control of Prehension." Artificial Organs **35**(1): 37-48.

Elder, H. and P. Kersten (2015). "Whakawhiti Korero, a method for the development of a cultural assessment tool, Te Waka Kuaka, in Maori traumatic brain injury." Behavioural Neurology: 8.

Elstob, D. and E. L. Secco (2016). "A Low Cost EEG Based BCI Prosthetic Using Motor Imagery." International Journal of Information Technology Convergence and Services **16**(1): 23-36.

Emotiv. (2019). "Emotiv Epoc+." Retrieved 06/06/2019, 2019, from https://www.emotiv.com/epoc/.

Fajardo, J., V. Ferman, A. Munoz, D. Andrade, A. R. Neto and E. Rohmer (2018). User-Prosthesis Interface for Upper Limb Prosthesis Based on Object Classifciation. Latin American Robotics Syposium. Brazil, IEEE.

Feix, T., R. Pawlik, H.-B. Schmiedmayer, J. Romero and D. A. Kragic (2011). "Comprehensive grasp taxonomy." Vienna University of Technology **1**: 1-2.

Feix, T., J. Romero, C. Ek, H.-B. Schmiedmayer and D. Kragic (2013). "A metric for Comparing the Anthropomorphic Motion Capability of Artificial Hands." IEEE TRANSACTIONS ON ROBOTICS **29**(1).

Feix, T., J. Romero, H.-B. Schmiedmayer, A. M. Dollar and D. Kragic (2016). "The Grasp Taxonomy of Human Grasp Types." IEEE Transactions on Human-Machine Systems **46**(1): 66-78.

Ficuciello, F. (2019). "Hand-arm autonomous grasping: Synergistic motions to enhance the learning process." Intelligent Service Robotics **12**: 17-25.

Fitts, R. H. (2008). "The cross-bridge cycle and skeletal muscle fatigue." Journal of Applied Physiology **104**: 551-558.

Franko, O., T. Winters, T. Tirell, E. Hentzen and R. Lieber (2011). "Moment Arms of the Human Digital Flexors." Journal of Biomechanics **44**(10): 1987-1990.

Ghazaei, G., A. Alameer, P. Degenaar, G. Morgan and K. Nazarpour (2017). "Deep learning-based artificial vision for grasp classifcation in myoelectric hands." Journal of Neural Engineering **14**: 1-19.

Gomez, C. L., A. M. Gondolbeu, R. M. Marti, I. P. Renart and M. L. Perez (2015). "The role of the metacarpal ligaments of the thumb in stability and

the development of osteoarthritis lesions: an anatomical study." Acta Orthopaedica Belgica **83**: 449-457.

Guger, C., W. Harkam, C. Hertnaes and G. Pfurtscheller (2001). "Prosthetic Control by an EEG-based Brain-Computer Interface (BCI)." Semantic Scholar: 1-6.

Gustus, G., G. Stillfried, J. Visser, H. Jorntell and P. Van Der Smagt (2012). "Human hand modelling: kinematics, dynamics, applications." Biological Cybernetics **1**: 1-15.

Hall, Z. W. and J. R. Sanes (1993). "Synaptic Structure and Development: The Neuromuscular Junction." Neuron **10**: 99-121.

Hazrati, M. K. and A. Erfanion (2010). "An online EEG-based brain-computer interface for controlling hand grasp using an adaptive probabilistic neural network." Medical Engineering and Physics **32**: 730-739.

Hikuroa, D., K. Morgan, M. Durie, M. Henare and T. Robust (2011). "Integration of Indigenous Knowledge and Science." The International Journal of Science in Society **2**(2): 105-113.

Hockings, N. (2016). Material and Mechanical Emulation of the Human Hand, University of Bath.

Hockings, N. (2018). Personal Communication. Importance of tendinous structures. M. Owen. Brisbane.

Hornshaw, P. (2011). "NeuroSky's Mindwave could offer new insights to developers." Retrieved 25/02, 2015, from http://www.appolicious.com/articles/8321-neuroskys-mindwave-could-offer-new-insights-to-developers.

Hunt, C. C. and S. W. Kuffler (1954). "Motor innervation of skeletal muscle: Multiple innervation of individual muscle fibres and motor unit function." Journal of Physiology(126): 293-303.

Huxley, H. E. (2004). "Fifty years of muscle and the sliding filament hypothesis." European Journal of Biochemistry **271**(8): 1403-1415.

Instruments, N. (2019). Understanding FFTs and Windowing, National Instruments.

Iris, K. (2014). Improving Robotic Prosthetic Hand Performance Through Grasp Preshaping. Master of Sciences, Edinburgh University.

Kotsiantis, S. B., I. D. Zaharakis and P. E. Pintelas (2006). "Machine Learning: a review of classification and combining techniques." Artificial Intelligence **26**: 159-190.

Krotkov, E. and R. Simmons (1996). "Perception, planning and control for autonomous walking wuth the ambler planetary rover." The International Journal of Robotics Research **15**(2): 155-180.

Kumarasinghe, K., M. Owen, D. Taylor, N. Kasabov and C. Au (2018). FaNeuRobot: A Framework for Robotic and Prosthetics Control Using the NeuCube Spiking Neural Network Architecture and Finite Automata Theory. IEEE International Conference on Robotics and Automation. Brisbane, Australia**:** 4465-4472.

Ladd, A. L., W. C.A-P., J. J. Crisco, E. Hagert, J. M. Wolf, S. Z. Glickel and J. Yao (2013). The Thumb Carpometacarpal Joint: Anatomy, Hormones, and Biomechanics. Instructional Course Lecture, National Institutes of Health Public Access. **62:** 165-179.

Lapsley, H., N. Waimarie and R. Black (2002). KIA MAURI TAU. M. H. Commission. Wellington, Mental Health Commission. **1:** 1-212.

Lewis, T. (2019). "Human Brain: Facts, Functions and Anatomy." Retrieved 08/02/2019, from https://www.livescience.com/29365-human-brain.html.

Li, C., H. Zhao and H. Wang (2012). "Research on EEG-Based Control of Prosthetic Hand." Advanced Engineering Forum **2**: 423-426.

Liao, K., R. Xiao, J. Gonzalez and L. Ding (2014). "Decoding Individual Finger Movements from One Hand Using Human EEG Signals." PLOS ONE **9**(1): 1-12.

Logitech. (2019). "HD WEBCAM C525." Retrieved 06/06/2019, 2019, from https://support.logitech.com/en_us/product/hd-webcam-c525.

Lotte, F. (2008). Study of Electroencephalographic Signal Processing and Classification Techniques towards the use of Brain-Computer Interfaces in Virtual reality Applications. Doctorate, Insa De ennes.

Lotte, F., L. Bougrain, A. Cichoki, M. Clerc, M. Congedo, A. Rakotomamonjy and F. Yger (2018). "A review of classification algorithms for EEG-based brain-computer interfaces: a 10 year update." Journal of Neural Engineering. **15**: 1-28.

Luciw, M., J. Ewa and E. Benoni (2014). "Multi-channel EEG recordingsduring 3936 grasp and lift trials with varying weight and friction." Scientific Data **1**: 140047.

Mai, J. K. and G. Paxinal (2012). The Human Nervous System. Sandiego, CA, USA, Elsevier Inc.

Marquard, R. (2012). "Biological Psychology: Parts of the Neuron and Neuronal Transmission." Retrieved 25/02, 2015, from https://benchprep.com/blog/biological-psychology-parts-of-the-neuron-and-neuronal-transmission/

Maurice, L. (2011). "Give Hope - Give a Hand." Retrieved 25/02, 2015, from http://web.stanford.edu/class/engr110/2011/LeBlanc-03a.pdf

McFarland, D. J., A. T. Lefkowicz and J. R. Wolpaw (1997). "Design and operation of an EEG-based brain-computer interface with digital signal

processing technology." Behaviour Research Methods, Instruments, & Computers **29**(3): 337-345.

McMinn, R. M. H. and R. T. Hutchings (1977). A Colour Atlas of Human Anatomy. Holland, Wolfe Medical Publications Ltd.

Muller, K.-R., M. Tangermann, G. Dornhege, M. Krauledat, G. Curio and B. B. (2008). "Machine Learning for real time single-trial EEG-analysis: From brain-computer interfacing to mental state monitoring." Journal of Neuroscience Methods **167**: 82-90.

Newman, J. and H. Moller (2005). "Use of Matauranga and Science to guide a Seabird Harvest: Getting the Best of Both Worlds?" Senri Ethnological Studies **67**: 303-321.

Nicolas-Alonso, L. F. (2012). "Brain Computer Interfaces, a Review." Sensors **12**: 1211-1279.

Nishimoto, A., M. Kawakami, T. Fujiwara, M. Hiramoto, K. Honaga, K. Abe, K. Mizuno, J. Ushiba and M. Liu (2018). "Feasibility of task-specific brain-machine interface training for upper-extremity paralysis in patients with chronic hemiparetic stroke." Journal of Rehabilitation Medicine **50**: 52-58.

Nooh, A. A., J. Yunus and S. M. Daud (2011). "A review of Asynchronous Electroencephalogram-based Brain Computer Interface Systems." International Conference on Biomedical Engineering and Technology. **11**: 55-59.

Nopera, T. (2018). "Personal Communication. Raranga Whakatutuki."

OpenEdition. (2019). "Filtering- The basics." Retrieved 06/06/2017, 2017, from https://blricrex.hypotheses.org/filtering-introduction#Filter%20types%20and%20FIlter%20response

Owen. M (2015). The Development of a Brain Controlled Robotic Prosthetic Hand. Master of Engineering, University of Waikato.

Pattnaik, P. K. and J. Sarraf (2018). "Brain Computer Interface issues on hand movement." Journal of King Saud University **30**: 18-24.

Pendleton, S. C., H. Andersen, X. Du, X. Shen, M. Meghjani, Y. H. Eng, D. Rus and M. Ang (2017). "Perception, Planning, Control, and Coordination for autonomous vehicles." Machines **5**(6): 1-54.

Prassler, E., A. Ritter, C. Schaeffer and P. Fiorini (2000). "A short history of cleaning robots." Autonomous robots **9**: 211-226.

Roberts, S. J., G. Gruber, G. Klosch and O. Filz (1999). "Artifact Processing in Computerized Analysis of Sleep EEG - A Review." Neuropsychobiology **40**: 150-157.

Samuel, A. L. (1967). "Some Studies in Machine Learning Using the Game of Checkers.II-Recent Progress." IBM Journal: 601-617.

Schmidt, H.-M. and U. Lanz (2004). Surgical anatomy of the hand. Stuttgart, Thieme.

Schwartz, A. B., X. T. Cui, D. J. Weber and D. W. Moran (2006). "Brain Controlled Interfaces: Movement Restoration with Neural Prosthetics." Neuron **52**: 205-220.

Srinivasan, L., U. T. Eden, S. K. Mitter and E. N. Brown (2007). "General-purpose Filter Design fo Neural Prosthetic Devices." Journal of Neurophysiology **98**: 2456-2475.

Stewart, A. X., A. Nuthmann and G. Sanguinetti (2014). "Single-trial classification of EEG in a visual object task using ICA and machine learning." Journal of Neuroscience Methods **228**: 1-14.

Straebel, V. and W. Thoben (2014). "Alvin Lucier's Music for Solo Performer: Experimental music beyond sonification." Organised Sound **19**(1).

Szymik. B (2011). Neuron Anatomy. Arizona, Arizona State University.

Taghva, A., D. Song, E. R. Hampson, S. A. Deadwyler and T. W. Berger (2012). "Determination of Relevant Neuron-Neuron Connections for Neural Prosthetics Using Time-delayed Mutual Information: Tutorial and Preliminary Results." World Neurosurgery **78**(6): 618-630.

Te Kanawa, K. (2018). Personal Communication. Te Aho Tapu. M. Owen. Ngaruawahia.

Teplan, M. (2002). "Fundamentals of EEG Measurement." Measurement Science Review **2**(2): 1-11.

Uriguen, J. A. and B. Garcia-Zapirain (2015). "EEG artifact removal- State-of-the-art and guidelines." Journal of Neural Engineering: 1-43.

Varone, M. (2019). "What is Machine learning? A definition." Retrieved 12/02/2019, from https://www.expertsystem.com/machine-learning-definition/.

Vidal, J. J. (1977). "Real-Time Detection of Brain Events in EEG." Proceedings of the IEEE: 633-641.

Weiner, P., J. Starke, F. Hundhausen, J. Beil and T. Asfour (2017). The KIT Prosthetic Hand: Design and Control. 8th International IEEE EMBS Cnference on Neural Engineering. Shanghai.

Westfall, T. C. and D. P. Westfall (2011). Neurotransmission: The Autonomic and Somatic Motor Nervous Systems. The Pharmacological Basis of Therapeutics. L. L. Brunton. New York. **12:** 171-218.

Wotherspoon, P. (2016). Personal Communication on the CMC thumb joint. M. Owen. Hamilton.

Xu, Z. and E. Todorov (2016). Design of a highly biomimetic anthropomorphic robotic hand towards artificial limb regeneration. 2016 IEEE Intrnational Conference on Robotic and Automation. Sweden.

Glossary

(English Translations)

Ao	World
Aotearoa	New Zealand
Arawa	Voyaging canoe
Awa	River
Ingoa	Name
Iwi	People
Otukou	Marae associated with the author.
Hapū	Sub tribe
Hāpine	Scraping
Hauhake	Harvesting
Hikairoa	Sub tribe
Hikurangi	Mountain associated with the author.
Kaikou	Awa associated with the author
Karakia	Prayer
Kitea	Observation
Koha	Gift
Kōrero	Speak
Koropupū	Boiling
Mahi	Work
Māori	The indigenous people of Aotearoa
Marae	Maori gathering place
Mātauranga	Knowledge, education.
Matawaia	Marae associated with the author

Matua	Father
Maunga	Mountain
Mauri	Life force, essence.
Moana	Ocean
Moemoea	Dream
Mōtatou	Mountain associated with the author
Papakai	Marae associated with the author.
Papatūānuku	Earth mother
Pēpeha	Proverbs
Pipiwai	Marae associated with the author.
Raranga	Weaving
Rere	Flow
Tainui	Tribe
Tāngata	Person
Taonga	Treasure
Tikanga	Supportive practice
Toetoe	Splitting
Tongariro	Mountain associated with the author
Tupuna	Ancestor
Tūwharetoa	Tribe of the author
Ūpoko	Head
Waiata	Song
Waiomio	Marae associated with the author
Waka	Canoe
Ngāpuhi	Tribe of the author
Nga Tikanga Whakahaere	Principle stages of process

Ngāti Hine	Sub tribe of the author
Ngati Tuwharetoa	Tribe of the author
Ngātokimatawhaorua	Voyaging canoe
Whaea	Mother
Whakahaere	Management
Whakamahere	Planning
Whakamaroke	Drying
Whakarite	Arrange, assign or put in order
Whakataukī	Proverb
Whakatutuki	Finish, complete.
Whare	House
Whenua	Land

Appendices

A1- Preliminary Investigation

As an example, the following preliminary investigation by Owen. M (2015) was conducted to investigate the limitations non-invasive NI applications employing the mindwave mobile EEG acquisition device by neurosky (Hornshaw 2011). Initially it was theorised that neural oscillations (as eluded to by (Straebel and Thoben 2014)) could provide the necessary information to control an electro-mechanical device. This was not the case. Neural oscillations are interpretations of the current brain state and it is not plausible to expect individuals to control such events. Table 1 explains the relationship between neural oscillations and the mental state of the user.

Table 1

Brainwave Type	Frequency Range	Mental States and Conditions
Delta	0.1Hz to 3Hz	Deep, dreamless sleep, non-REM sleep, unconscious
Theta	4Hz to 7Hz	Intuitive, creative, recall, fantasy, imaginary, dream
Alpha	8Hz to 12Hz	Relaxed, but not drowsy, tranquil, conscious
Beta	12Hz to 30Hz	Formerly SMR, relaxed yet focused, integrated

An additional theory involving the combining of neural oscillations was born. By observing user state during the production of EEG, it is feasible to suggest what neural oscillations relate to a user being in an attentive state. Quantifying the attentive state by the presence of multiple neural oscillations presented a framework for prosthetic control (Figure A). Proprietary algorithms yielded a classification accuracy of 50%. This result is no better than randomly guessing the intent of the user.

Figure A: Real time testing of the Neurosky Mindwave based EEG neural Interface Prototype.

After testing, it was obvious that this early NI attempt possessed multiple restrictions that limited its suitability for success in the replication of the human grasping system. The following challenges limited the accuracy of the NI:

1- Poor spatial resolution

2- Limitations with acquisition: Biological interference

3- Signal analysis and machine learning

4- Preparation time

Overcoming these limitations of EEG based NI's is, therefore, a major subject of many papers and research.

A2- Centroid Calculation

Locating the centroid of the phalanges is required to define the insertion points of the stabilising ligaments of the hand. The following is the calculation of the centroid for the proximal phalange of the index finger. Locating of the centroid is performed in SOLIDWORKS and relates explicitly to section 3.3.1.1.

Mass properties of proximal phalange (index finger)

Locating the Centroid

Configuration: Default
Coordinate system: -- default --

Density = 0.00 grams per cubic millimeter

Mass = 0.11 grams

Volume = 109.32 cubic millimetres

Surface area = 162.91 square millimetres

Centre of mass: (millimetres)
X = 167.09
Y = 340.34
Z = -56.84

Principal axes of inertia and principal moments of inertia: (grams * square millimetres)
Taken at the centre of mass.

Ix = (0.14, 0.98, -0.13)	Px = 0.23
Iy = (-0.62, 0.19, 0.76)	Py = 1.53
Iz = (0.77, -0.02, 0.63)	Pz = 1.63

Moments of inertia: (grams * square millimetres)
Taken at the centre of mass and aligned with the output coordinate system.

Lxx = 1.56	Lxy = 0.18	Lxz = -0.07
Lyx = 0.18	Lyy = 0.28	Lyz = -0.17
Lzx = -0.07	Lzy = -0.17	Lzz = 1.55

Moments of inertia: (grams * square millimetres)
Taken at the output coordinate system.

Ixx = 13277.98	Ixy = 6341.34	Ixz = -1059.15
Iyx = 6341.34	Iyy = 3473.75	Iyz = -2157.37
Izx = -1059.15	Izy = -2157.37	Izz = 16030.86

A3- Collateral Insertions

The collateral insertion positions are a function of the centroid position (determined in section A2), the phalanx length, the head/base of the phalanx and the optimal insertion position found through experimentation. Table 2 shows the horizontal distance from the phalanx ends that locate the horizontal positions of the insertions. Table 3 establishes the phalanx lengths and table 4 shows the optimal positions for collateral insertion. This information reinforces the approach taken in section 3.3.1.1.

Table 2: The percentage of the total length of the each phalanx needed in order to locate the horizontal position of the ligament insertion points.

	Metacarpal %		**Proximal %**		**Intermediate %**		**Distal %**	
	Head	**Base**	**Head**	**Base**	**Head**	**Base**	**Head**	**Base**
Index	10	x	15	18	23	23	x	25
Middle	9	x	19	16	14	11	x	22
Ring	11	x	18	16	14	14	x	21
Little	11	x	14	14	17	17	x	18
Thumb	10	x	23	27	x	x	x	23

Table 3: Phalanx length. Measured in the radial view plane.

	Proximal	Intermediate	Distal
Index	40mm	22mm	16mm
Middle	43mm	36mm	18mm
Ring	44mm	29mm	19mm
Little	35mm	23mm	17mm
Thumb	26mm	x	22mm

Table 4: Optimal insertion position for collateral ligaments. (x-axis)

	Proximal		Intermediate		Distal	
	Head	Base	Head	Base	Head	Base
Index	6mm	7mm	5mm	5mm	x	4mm
Middle	8mm	7mm	5mm	4mm	x	4mm
Ring	8mm	7mm	4mm	4mm	x	4mm
Little	5mm	5mm	4mm	4mm	x	3mm
Thumb	6mm	7mm	x	x	x	5mm

The following tables 5-10 are representative of the ideal horizontal position for the collateral ligament insertion points for the index finger. 1 indicates successful joint movement. 2 indicates a limited range of motion and 3 indicates a severe limit to the range of motion. These tables are used to calculate the ideal insertion points for the index finger. A similar approach was conducted for each digit of the hand.

Table 5

3mm

	Proximal Base	Intermediate Base	Distal Base
1	3	2	1
2	3	1	1
3	3	2	1
4	3	2	1
5	3	2	1
6	3	2	1
7	3	2	1
8	3	1	1
9	3	2	1
10	3	2	1
11	3	2	1
12	3	2	1
13	3	2	1
14	3	1	1
15	3	2	1
16	3	2	1
17	3	3	1
18	3	2	1
19	3	2	1
20	3	2	1

Table 6

4mm

	Proximal Base	Intermediate Base	Distal Base
1	2	1	1
2	3	1	1
3	2	1	1
4	3	1	1
5	2	1	1
6	2	1	1
7	2	1	1
8	3	1	1
9	3	1	1
10	2	1	1
11	3	1	1
12	2	1	1
13	3	1	1
14	2	1	1
15	2	1	1
16	2	1	1
17	3	1	1
18	2	1	1
19	1	1	1
20	3	2	1

Table 7

5mm

	Proximal Base	Intermediate Base	Distal Base
1	2	1	1
2	2	1	1
3	2	1	1
4	2	1	1
5	2	1	1
6	2	1	1
7	2	1	1
8	2	1	1
9	2	1	1
10	2	1	1
11	2	1	1
12	2	1	1
13	2	1	1
14	2	1	1
15	2	1	1
16	2	1	1
17	2	1	1
18	2	1	1
19	2	1	1
20	3	2	1

Table 8

6mm

	Proximal Base	Intermediate Base	Distal Base
1	1	1	2
2	1	1	2
3	1	1	2
4	1	1	2
5	1	1	2
6	1	1	2
7	1	1	2
8	1	1	2
9	1	1	2
10	1	1	2
11	1	1	2
12	1	1	2
13	1	1	2
14	1	1	2
15	1	1	2
16	1	1	2
17	1	1	2
18	1	1	2
19	1	1	2
20	3	2	1

Table 9

7mm

	Proximal Base	Intermediate Base	Distal Base
1	1	2	3
2	1	2	3
3	1	2	3
4	1	2	3
5	1	2	3
6	1	2	3
7	1	2	3
8	1	2	3
9	1	2	3
10	1	1	3
11	1	1	3
12	1	2	3
13	1	2	3
14	1	2	3
15	1	2	3
16	1	2	3
17	1	1	3
18	1	1	3
19	1	1	3
20	3	2	1

Table 10

8mm

	Proximal Base	Intermediate Base	Distal Base
1	1	3	3
2	1	3	3
3	1	3	3
4	1	3	3
5	1	3	3
6	1	3	3
7	1	3	3
8	1	3	3
9	1	3	3
10	1	3	3
11	1	3	3
12	1	3	3
13	1	3	3
14	1	3	3
15	1	3	3
16	1	3	3
17	1	3	3
18	1	3	3
19	1	3	3
20	3	2	1

A4- Physical Workspace of the Artificial Hand

The artificial hand model is designed in SOLIDWORKS by separate parts. Each part is added and mated in an assembly. The mates and relationships of each part mimic the joints and ranges of motion of the artificial hand. Manual measurements of the maximum fingertip trajectories are recorded iteratively with movement governed by the kinematic equations. An offset distance is used and can be remedied by translating the hand by a vector equivalent to the position of the MCP joint of the middle finger. Results from the investigation are given in tables 11-15.

Table 11

Index		
x	y	z
62	115	252
62	110	253
62	107	253
62	106	254
62	106	254
79	100	252
96	100	246
112	99	234
124	99	220
133	98	203
133	97	159
117	96	134
108	96	127
108	96	127
108	95	127
108	94	128
108	90	128
121	92	139
130	95	153
136	99	172
135	104	193
125	109	218
105	113	238
62	116	252

Table 12

Middle		
x	y	z
62	75	266
62	75	266
73	75	266
94	75	260
111	75	250
124	75	237
134	75	224
143	75	198
129	75	143
104	75	124

Table 13

Ring		
x	y	z
62	52	255
62	47	255
62	44	255
62	39	254
62	39	254
80	39	252
101	41	243
115	43	233
129	45	216
137	49	197
138	54	169
133	57	151
110	62	124
110	62	124
110	60	124
110	58	124
110	56	126
126	56	139
136	55	160
139	55	179
131	54	212
115	53	234
104	53	243
62	52	255

Table 14

Little		
x	y	z
62	36	226
62	32	226
62	26	225
62	15	223
62	15	223
81	16	220
101	19	201
111	21	200
119	25	188
124	32	166
123	37	150
120	40	140
100	47	117
100	47	117
100	45	116
100	41	116
100	36	115
116	36	132
124	36	155
123	36	175
113	36	200
95	36	216
79	36	223
62	36	226

Table 15

Thumb		
x	y	z
123	166	112
123	160	124
123	156	130
123	149	138
123	142	144
123	135	150
123	124	156
123	124	156
122	116	155
120	107	154
117	101	152
114	94	149
112	91	148
112	91	148
114	85	146
116	75	143
115	64	139
106	45	134
99	37	131
89	31	129
86	29	129
86	29	129
91	26	129
99	24	129
118	21	125
134	24	119
143	28	114

Continued		
x	y	z
143	28	114
143	38	129
143	43	135
143	52	142
143	59	146
143	64	148
143	67	150
143	67	150
148	76	145
150	78	144
155	92	137
157	98	135
158	107	130
158	115	126
156	129	119
152	142	112
139	164	107
120	180	98
107	187	90
107	187	90
107	187	95
107	185	104
107	181	117
107	176	128
107	168	140
107	159	151

A5- MATLAB Code for Mana Motuhake Hand Model

The code established here is related to the physical model of the artificial hand designed within this work. Section 3.4.1. of the thesis relies on the working of this code to establish the quantification of thumb orientation on hand function. The code is adapted to fit the framework provided by (Feix, Romero et al. 2013).

```
function [data values lbls handlength] = ManaMotuhake

handlength = 20;


I1 = 3.7; %index
I2 = 2.1;
I3 = 1.1;
x1 = 2.89;
y1 = 3.59;
z1 = 2.96;
T1 = 4.0; %thumb
T2 = 2.7;
x2 = 4;
y2 =1;
z2 = 7.18;
M1 = 4.1;%middle
M2 = 2.6;
M3 = 2.1;
x3 = 1.29;
y3 = 3.59;
z3 = 2.96;
R1 = 4.1;%ring
R2 = 2.6;
R3 = 1.9;
x4 = 0;
y4 = 3.59;
z4 = 2.9;
L1 = 2.9;%little
L2 = 1.9;
L3 = 1.6;
x5 = -1.3;
y5 = 3.59;
z5 = 2.96;
delta =  - [x3 y3 z3];
dofs= [4 4 4 4 4];

DH = [0 0 0  deg2rad(90)       0 deg2rad(45); ...
      0 0 I1 deg2rad(-90)      0 deg2rad(45); ...       %index
      0 0 I2 deg2rad(0)       0 deg2rad(37.4); ...
      0 0 I3 deg2rad(0)       0 deg2rad(33.1); ...
      0 0 0 deg2rad(90)       0 deg2rad(0);...       %thumb
      0 0 T1 deg2rad(0)       0 deg2rad(0);...
      0 0 T1 deg2rad(0)       0 deg2rad(50);...
      0 0 T2 deg2rad(0)       0 deg2rad(28.9); ...
      0 0 0  deg2rad(90)       0 deg2rad(45); ...          %middle
      0 0 M1 deg2rad(-90)      0 deg2rad(45); ...
      0 0 M2 deg2rad(0)       0 deg2rad(37.4); ...
      0 0 M3 deg2rad(0)       0 deg2rad(33.1); ...
```

```
      0 0 0  deg2rad(90)       0 deg2rad(45); ...          %ring
      0 0 R1 deg2rad(-90)       0 deg2rad(45); ...
      0 0 R2 deg2rad(0)       0 deg2rad(35); ...
      0 0 R3 deg2rad(0)       0 deg2rad(30); ...
      0 0 0  deg2rad(90)       0 deg2rad(45); ...          %little
      0 0 L1 deg2rad(-90)       0 deg2rad(45); ...
      0 0 L2 deg2rad(0)       0 deg2rad(35); ...
      0 0 L3 deg2rad(0)       0 deg2rad(30)]; ...

base = [x1 y1 z1 degtorad(90)  degtorad(0) degtorad(90); ...
        x2 y2 z2 degtorad(-90) degtorad(0) degtorad(110); ...
        x3 y3 z3 degtorad(90)  degtorad(0) degtorad(90); ...
        x4 y4 z4 degtorad(90)  degtorad(0) degtorad(90); ...
        x5 y5 z5 degtorad(90)  degtorad(0) degtorad(90)];
%creating fingers
num_fing = 1;
inc = 1;
names = {'Index' 'Thumb' 'Middle'  'Ring' 'Little'};
for i = 1:size(DH,1)
  links(inc) = Link(DH(i,:));
    if (inc == dofs(num_fing))
       temp = SerialLink(links(1:inc));
       mat                                                    =
transl(base(num_fing,1:3))*trotz(base(num_fing,6))*troty(base(num_
fing,5))*trotx(base(num_fing,4));
       temp.base = transl(delta)*mat;
       temp.tool = trotz(-pi/2)*troty(-pi/2);
       temp.name = names{num_fing};
       finger{num_fing} = temp;
       num_fing = num_fing +1;
       inc = 0;
       clear links;
    end
inc = inc + 1;
end
data.finger = finger;
data.dof = dofs;
openingangle = 43;
vals = deg2rad(-openingangle:0.1:0)';
n = length(vals);
offset = linspace(0,deg2rad(openingangle/10),n)';
values = [vals vals zeros(n,2) vals vals vals zeros(n,1) vals vals
zeros(n,2)   vals   vals-offset   zeros(n,2)   vals   vals-2*offset
zeros(n,2)];

lbls = ones(n,1);
```

A6- Thumb Orientation Optimisation Results

The effect of thumb orientation is computed in MATLAB where the model explained and defined in section A5 is applied at differing thumb face normal values. The results here (Table 16) are related to figure 18 within the thesis.

Table 16: Testing of thumb orientation effect

Thumb face normal	Degree	AI
-25	10	0.32721
-15	20	0.40889
-5	30	0.57229
0	35	0.60001
5	40	0.71323
15	50	0.81695
25	60	0.90953
35	70	0.98953
45	80	0.99953
55	90	0.93953
65	100	0.88814
75	110	0.80132
85	120	0.65388
95	130	0.57232
105	140	0.40892
115	150	0.31263
125	160	0.24544
135	170	0.24544
145	180	0.24544
155	190	0.24
165	200	0.24544

The difference between the thumb normal face angle and the degree is -35. The difference is due to the use of the simulation angle being at a 35 degree offset from the actual hand. The AI column is explained in the body of work.

A7- Fingertip Force Due to Tendon Tension

This appendix defines the fingertip force of the fingers of the artificial hand due to the extensions expressed in section 3.6. By calculating the fingertip force it is possible to determine the grasping force of the hand and, therefore, a force feedback control can be used to control the artificial hand when delicate or robust grasping is required for different objects.

Let T_i be the tension on the tendon i, we can write

$$T_i = \frac{\tau_i^m}{R}$$

Where, τ_i^m is the servo torque for tendon i and R is the servo horn radius. Equating the work done yields the torque τ_i acting on the fingertip:

$$T_i \cdot e_i = \tau_i \cdot \sum_j \Delta\theta_{ij}$$

The fingertip force f_i is given by

$$f_i = \frac{T_i \cdot e_i}{\sum_j \Delta\theta_{ij}} \cdot \frac{1}{l_i}$$

Where, l_i is the perpendicular distance between the fingertip force f_i and the MCP joint. e_i is the tendon extension. The subscripts i and j represent the tendons and joints respectively. A force sensor is used to measure the fingertip force f_i and the servomotor stops turning when f_i reaches a set threshold value. Figure B shows the relationship between fingertip force and tendon tension.

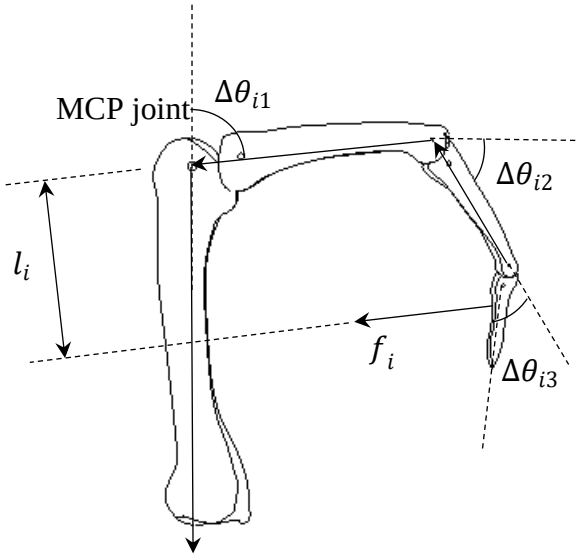

Figure B: Digit of the artificial hand showing the fingertip force with respect to the phalanx length and joint angles.

A8- Signal Pre-Processing

Signal pre-processing is at the heart of NI technology. Pre-processing requires filtering, windowing and conversion to the frequency domain through the FFT. The information and code provided here serves as the backbone for section 4.2. The following code Imports the raw Emotiv EEG data into matlab

```
% Import raw CSV file
input_data = csvread('EPOC+datafile.csv',1,0); % This excludes the first row
eegcols = 3:16; % EEG Columns.
eeg.raw = input_data(:, eegcols);
```

The DC offset requires removal before the FFT can be performed

```
% median value removal
med = median(eeg.raw,2); % calculate median of each sample
eeg.raw = eeg.raw - repmat(med, 1, 14); % remove it
% limit slew rate
for j=2:size(eeg.raw,1)
del = eeg.raw(j,:) - eeg.raw(j-1,:);
del = min(del, ones(1,14)*15);
del = max(del, -ones(1,14)*15);
eeg.raw(j,:) = eeg.raw(j-1,:) + del;
end
% High pass filter
a = 0.06; % HPF filter coeffs
b = 0.94;
preVal = zeros(1,14);
eeg.filt = zeros(size(eeg.raw));
for j=2:size(eeg.raw,1)
preVal = a * eeg.raw(j,:) + b * preVal;
eeg.firfilt(j,:) = eeg.raw(j,:) - preVal;
end
```

Following the importing and DC offset removal the following code performs the FFT

```
% Variables
fftlength = 1024; % Set FFT length
stepsize = 32; % Set step size
samples = fftlength:stepsize:length(eeg.raw); % create an index array
c = 1:fftlength;
channel = 1; % AF3
%Specify hanning window
hanning = [1:fftlength]';
hanning_in = 2* pi() * (hanning - (fftlength+1)/2)/(fftlength+1);
```

```
%rescaled x-axis to match sample length?
hanning = (sin(hanning_in)./hanning_in).^2; % sinc^2?
hanning = repmat(hanning, 1, size(eeg.raw,2)); % match to number of channels
f=[128/fftlength:128/fftlength:128]; % frequency index for the spectral array
for kk = 1:length(samples)
k = samples(kk);
% step through every quarter second starting at first possible sample
spectrum = fft(eeg.iirfilt(k-fftlength+1:k,:) .* hanning)/fftlength; % apply window
to HP filtered data
spectrum = 2 * (sqrt(spectrum .* conj(spectrum))); % get magnitude
```

A display of the FFT result can be viewed with the following code.

```
%plotting the data
subplot(211)
% time domain
plot(c,eeg.iirfilt(k-fftlength+1:k, channel));
title('Amplitude of Channels');
xlabel('Samples');
ylabel('Amplitude');
xlim([0 fftlength]);
%IIR fft
subplot(212)
plot(f,spectrum(:, channel));
%add graph details.
title('Amplitude Spectrum of Channels');
xlabel('Frequency (Hz)');
ylabel('|Y(f)|');
xlim([0 50]);
% ylim([0 80]);
pause(0.5);
end
```

All coding is based on table 17 which is in reference to the Epoc+ headset and the

10-20 international system of electrode locations.

Table 17: International 10-20 system applied to the EEG headset.

Channel	Column
3	AF3
4	F7
5	F3
6	FC5
7	T7
8	P7
9	O1
10	O2
11	P8
12	T8
13	FC6
14	F4
15	F8
16	AF4

A9- Optimising the Margin for Linearly Separable Training Sets and Application of the Lagrangian for the SVM Classifier.

This appendix explains the underlying theory behind the application of the SVM for classification. The first section describes the optimisation of the SVM hyperplane by determining the maximum margin between two sets of training data. The second section shows how the Lagrangian is applied to optimise the SVM hyperplane in higher dimensional space.

Section 1

As established in chapter 4.2.3 a set of labelled training patterns $(x_i, y_i), \dots, (x_m, y_m)$ are linearly separable if a vector w and a scalar b exist that satisfy

$$w.x_i + b \geq 1 \; if \; y_i = 1$$

$$w.x_i + b \leq -1 \; if \; y_i = -1$$

Where $y_i \in (1, -1)$ then we get

$$y_i(w.x_i + b) \geq 1, \forall i$$

The optimal hyperplane

$$w_0.x + b_0 = 0$$

Separates the data with the largest possible margin. Let r be the distance of the margin where it in minimized by

$$r_{(w,b)}^{min} = \frac{w.x}{|w|}$$

Where, x:y=1 and maximized by

$$r_{(w,b)}^{max} = \frac{w.x}{|w|}$$

Where, x:y=-1. By maximising the difference between these equations the following is yielded

$$r_{(w_0,b_0)} = \frac{2}{|w|} = \frac{2}{\sqrt{w_0.w_0}}$$

This means the optimal hyperplane minimizes $w.w$ subject to

$$y_i(w.x_i + b) \geq 1, \forall i$$

Therefore, the construction of the optimal hyperplane is a quadratic problem.

Section 2

To do this we use the Lagrangian

$$L_{(w,b,\lambda)} = \frac{1}{2}w.w - \sum_{i=1}^{m} \lambda_i[y_i(x_i w + b) - 1]$$

Also subject to

$$y_i(w.x_i + b) \geq 1$$

Where, $\lambda = \lambda_1, \ldots, \lambda_m, \forall \lambda_i > 0$. The solution to the optimisation is determined by the saddle point of this Lagrangian where the minimum is found with respect to w and b.

For $w = w_0$

$$\frac{\partial L}{\partial w}(w, b, \lambda) = w_0 - \sum_{i=1}^{m} \lambda_i y_i x_i = 0$$

For $b = b_0$

$$\frac{\partial L}{\partial b}(w, b, \lambda) = \sum_{\alpha_i} y_i \lambda_i = 0$$

By deriving $\frac{\partial L}{\partial w}(w, b, \lambda)$ we get

$$w_0 = \sum_{i=1}^{m} \lambda_i y_i x_i$$

Note that the only training vectors that contribute here are x_i with $\lambda > 0$. By combining this and $\sum_{\alpha_i} y_i \lambda_i = 0$ into the Lagrangian we get

$$W(\lambda) = \sum_{i=1}^{m} \lambda_i - \frac{1}{2} w_0 . w_0$$

$$= \sum_{i=1}^{m} \lambda_i - \frac{1}{2} \sum_{i,j-1}^{m} \lambda_i . \lambda_j . y_i . y_j . x_i . x_j$$

This specific equation is used in section 4.2.3. We have now established its origin. Maximising this subject to

$$w_0 - \sum_{i=1}^{m} \lambda_i y_i x_i = 0$$

Where $\lambda \geq 0$ we optimise the hyperplane for separating the labelled training patterns.

A10- Image Processing

Below is the image processing sequence for obtaining object size and geometry. The processing is performed in LABVIEW and is relevant to the image processing presented in the perception section of chapter 5.

1- Load the color image into the buffer.

2- Apply color plane extraction to extract the HSL saturation plane so that the color image is converted into a grayscale image.

3- Pre-process the image by thresholding. A range of pixel values is defined as threshold. Any pixel value outside the range becomes zero and any pixel value inside the range becomes one.

Thresholding results in a binary image.

4- Run 20 iterations of Advanced Morphology Operator to remove speckle-noise showing up in the binary image.

5- Use Fast Fourier Transform Filter to compute backgrounds in order to correct light drifts. This allows straight edges to be easily seen.

6- Detect the edge by Canny Edge Detection algorithm.

7- Use Advanced Morphology Operator to fill inside of loop of edges detected. EG:

8- Apply Image Equalization to enhance the contrast.

9- Detect the shape.

10- Draw a rectangle to envelope the detected shape.

11- Minimize the rectangle area by rotating the rectangle.

12- Measure the dimensions and the orientation of the rectangle.

13- Return the original image by Image Buffer.

The images of major process sequences are shown in Figure C.

(a) Original image

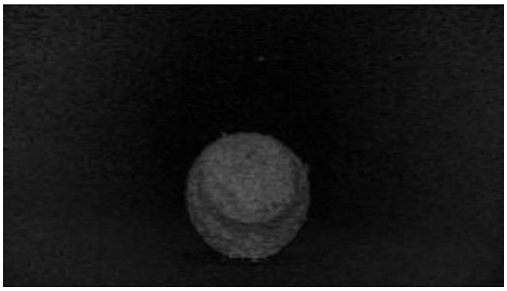

(b) After colour plane extraction

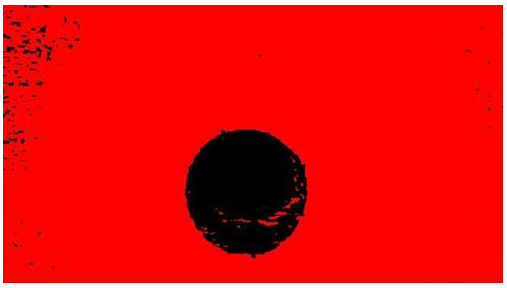

(c) After thresholding

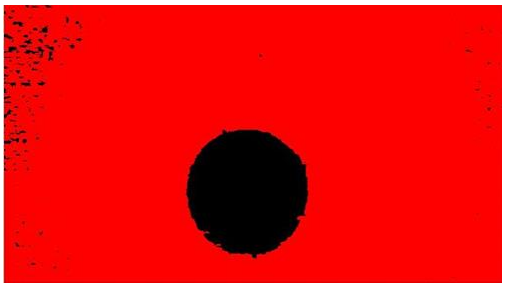

(d) After 1st iteration of speckle-noise removal

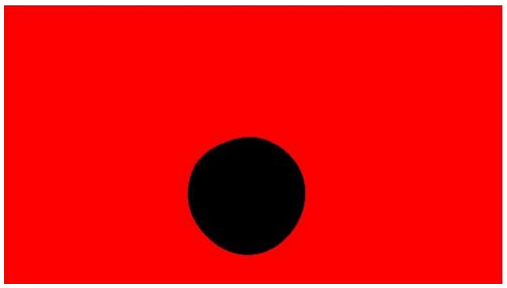

(e) After FFT filtering

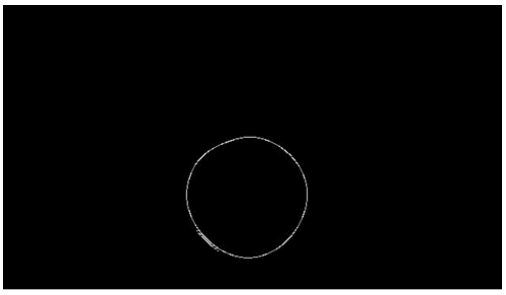

(f) After edge detection

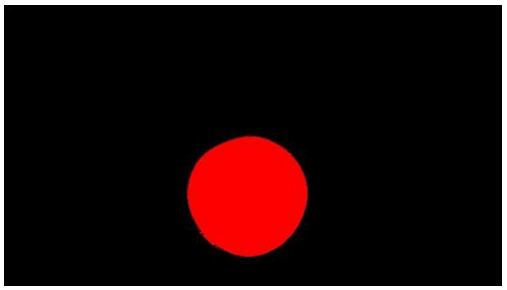

(g) After filling up the area

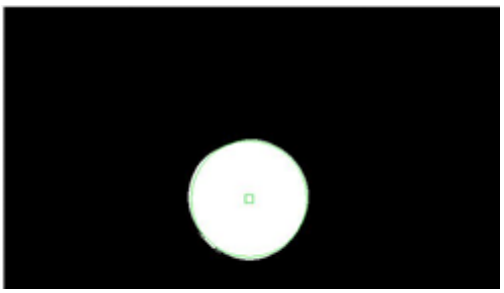

(h) After image equalization

Figure C: Image processing

The size of an image in a picture is expressed in terms of number of pixels. This number is a function of the object size and the distance between the object and the webcam

A11- Optical Schematics

The autonomous hand employs a webcam for its framework. The optical schematics of the autonomous hand are shown below. Figure D shows the optical schematics of object and image. The pixel per metric, *K*, is a function of the webcam pixel size *c*, object distance *u* from the webcam and the webcam focal length *f*. The Logitech C525 webcam has an image size of 480×640, a pixel size of 5.52×5.82 μm and a focal length of 39.5mm. Since the pixel sizes are not equal in the horizontal and vertical directions, the final dimension is obtained by Pythagoras' Theorem using the horizontal and vertical directions to compute.

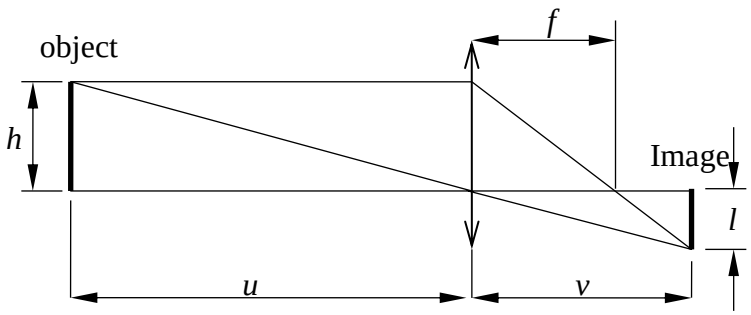

Figure D: Optical schematics of object and image

Let *h* and *l* be the object height and image height respectively. *u* and *v* are the object and image distance, then

$$\frac{h}{u} = \frac{l}{v}$$

or

$$\frac{h}{u} = \frac{nc}{v}$$

where *c* is pixel size while *n* is the number of pixels of the image

Since the relation among object distance *u*, image distance *v* and focal length *f* of a webcam is given as

$$\frac{1}{u}+\frac{1}{v}=\frac{1}{f}$$

Where *f* is the focal length of the webcam. Hence,

$$\frac{h}{u}=nc\left(\frac{1}{f}-\frac{1}{u}\right)$$

or

$$\frac{n}{h}=\frac{1}{c\left(\frac{u}{f}-1\right)}$$

Hence, pixels per metric $K=\frac{1}{c\left(\frac{u}{f}-1\right)}$.

I certify that this thesis is my own work, that any copying or paraphrasing of the words or ideas of others in any way or form to the best of my knowledge is properly acknowledged through referencing.